Temporal changes in ecological status in Vestfjorden, inner Oslofjord, Norway

Gerald L. Decelles III

Institute of Geosciences

The Faculty of Mathematical and Natural Sciences

UNIVERSITY OF OSLO

06/2019

Temporal changes in ecological status in Vestfjorden, inner Oslofjord, Norway

Gerald L. Decelles III

Master Thesis

Environmental geology – environmental stratigraphy

60 credits

Institute of Geosciences

The Faculty of Mathematical and Natural Sciences

UNIVERSITY OF OSLO

06/2019

2019

Temporal changes in ecological status in Vestfjorden, inner Oslofjord, Norway

Gerald L. Decelles III

http://www.duo.uio.no/

Trykk: Reprosentralen, Universitetet i Oslo

Abstract

The inner Oslofjord has undergone many changes in ecological quality throughout time. The Vestfjorden Avløpsselskap (VEAS) wastewater treatment plant has been involved in these changes with a generally positive effect. Given current analytical tools (CTD, total organic carbon (TOC), trace metals (TM), foraminifera, current meters), assessment of the impact (ecologically) that VEAS is having on the benthic zone surrounding the discharge pipes was conducted in fall 2017. This study found an incongruity in ecological quality between benthic areas north and south of the discharge area. Based on sample collected in 2018, the work of this thesis looked to confirm this discrepancy, add temporal markers to tie data collected at this site with data from the rest of the inner Oslofjord, assess the efficacy of foraminifera as indicators of ecological status, and search for a possible mechanism for discrepancy by studying current and circulation regimes in the area near the VEAS discharge. While unable to confirm the data values found in TM analysis in 2017 or the impact of currents in the area on the discharge regime, radiometric dating of a new core placed the changes seen in the area around VEAS in temporal context with what has happened to the inner Oslofjord as a whole. Additionally, discrepancies between values from different cores taken from the "same" location have led to better understanding of random and systemic methodological errors in analysis of samples specifically TOC and trace metals. Finally, foraminifera analysis along with dating of the core supports other research on the effectiveness of these organisms as indicators of ecological quality.

Acknowledgements

Firstly, I would like to express my gratitude to my supervisors Elisabeth Alve and Silvia Hess for enthusiastically and willingly sharing their knowledge with me over the course of this master's study. Both were always available to me, constantly taking time out of their own work to answer my questions and were supportive throughout my time at UiO. I would like to thank Mufak Said Naroz and Magnus Kristoffersen of the UiO Geosciences Department for their technical support in the laboratory. I am also grateful to the crew on FF Trygve Braarud, particularly the captain Sindre Holm and Jan Sundøy for their assistance and insight over several cruises. Special thanks also to Stefan Rothe for taking the time to work with me on QGIS and expand my understanding of GIS applications, you are a great teacher. Thanks to Aivo Lepland and NGU for use of the Oslofjord bathymetry data. Thanks also to Anouk Tosca Klootwijk for helpful input and assistance. My gratitude to SIS for giving me the time to pursue this goal.

I must also recognize the members of the BIO 4301 class, specifically Alia, Ask, Brita, Even, Gordon, Katharine, Lars, Malin, Martine, Newt, Ragnild, Ulrik, Victor and others who made my time at UiO a much more enjoyable experience. I hope we keep in touch.

Thank you to my proofreaders Chris and Andrew for taking the time to make this thesis better.

A very special thankyou to my partner Nina for her help and for supporting me during this long process. Without you I would not have made it to the end.

Finally, I must recognize my mother, who passed away suddenly at the start of this process. I have needed the strength and wisdom she bestowed in me many times during these last two years. I hope that she would be proud.

Table of Contents

Table of Figures

1 Introduction

Norway has a strong connection to the sea that dates to the first settlers of the country. Those moving into Norway after the last ice age made their way along the coast where living was easier due to the milder conditions brought by the warming Gulf Stream and access to the bounty of food the sea provided (Libæk et al., 1999). Now, as then, a majority of Norwegians live in close proximity to the sea, with eighty percent of Norway's population living within 10km of the coast (Sætre, 2007). This is not by chance, Norway's coastline is immense, covering 24,000km or more than half the distance around the equator (Sætre, 2007). This reliance on the coast, make it more important now than ever, that it is a resource that is protected and nurtured for future generations.

Regional, national and global programs exist to monitor and remediate coastal areas in an effort to return "human-impacted" areas back to "reference" conditions (European Union, 2000; OSPAR Commission, 2000). Reference conditions (conditions defined as biological quality elements that would exist at high status) for areas within the European Union (EU) were originally slated to be met by 2015 but have now been adjusted to 2021 (Alve et al., 2009). Many communities are struggling not only to meet the criteria (as defined by the European Water Framework Directive – WFD), but also on how to define the status of "reference-conditions" (Alve et al., 2009). Information about reference water quality has been difficult to come by due to limited longitudinal study data (Alve et al., 2009). The inner Oslofjord (shown in inset of figure 2.1) is an important coastal area to the approximately 500,000 people who live in the greater Oslo area. There have been several studies to find the reference conditions in the inner Oslofjord including Alve et al. (2009) and Dolven et al. (2013), which used microfossils in sediment cores taken from the bottom of the fjord to see differences in benthic foraminifera and how different foraminifera respond under different water conditions. Additionally, Lepland et al. (2010) used heavy metal analysis and chronostratigraphy to analyse the concentrations of Cu, Cd and Hg and correlate that with chronological emission peaks from industry and pollution from Oslo.

Due to their short reproductive cycle, wide distribution, high species diversity, high number, and hard exoskeleton (test), benthic foraminifera are excellent bioindicators of environmental change (Coccioni, 2000). Benthic foraminifera provide the ability to study and reconstruct

environmental conditions both past and present (dependent upon sedimentation rates) as well as help in the establishment of "reference" conditions for specific bodies of water (Alve, 2000). Correlation between benthic foraminifera and other environmental indicators (primarily dissolved oxygen) have shown to be significant resulting in the use of foraminifera for classifying ecological quality status (EcoQS) (Dolven et al., 2013). Benthic foraminifera have since been accepted as a basis for determining reference conditions of Norwegian water bodies by Norway's *Miljødirektoratet* in 2013 (Klassifisering, 2015). Table 1 shows some of the parameters (both biological and chemical) and boundaries for establishing EcoQS. Remediation is required to bring the water body back to reference conditions by the WFD (European Union, 2000). This process involves first, the determination of the biological quality of a water body and whether or not it is at or near reference conditions. This is followed by a determination of the physio-chemical/hydromorphological properties of the water body which act as supplemental criteria for determination of the final EcoQS. If these supplemental criteria are not of good or high status, then the overall EcoQS will be downgraded (European Commission and Directorate-General for the Environment, 2003).

***Table 1**: Environmental quality classification tools and indicators. Note that 2018 ranges show quality indicator boundaries based upon foraminifera (* = $H'log_{2\_f}$ and ES_{100_f}) along with the Norwegian Quality Index (NQI) as proposed for foraminifera (**) by Alve et al. (2019) As taken from (Alve et al., 2019; Bakke et al., 2010; Direktoratsgruppen, 2018; Dolven et al., 2013; Miljødirektoratet, 2015b).*

	Environmental quality indicators - 2018 ranges				
Criteria	**High**	**Good**	**Moderate**	**Poor**	**Bad**
Cu (mg/kg)	0.0-20	84		84-147	>147
Cd (mg/kg)	0.0-0.2	0.2-2.5	2.5-16	16-157	>157
Zn (mg/kg)	0-90	90-139	139-750	750-6690	>6690
Pb (mg/kg)	0.0-25	25-150	150-1480	1480-2000	2000-2500
TOC_{63}	0-20	20-27	27-34	34-41	41-200
$H'log_{2\_f}$	*5.0-3.4	*3.4-2.4	*2.4-1.8	*1.8-1.2	*1.2-0
ES_{100_f}	*35-18	*18-13	*13-11	*11-9	*9-0
$NQI_{\_f}^{**}$	1.0-0.54	0.54-0.45	0.45-0.31	0.31-0.13	0.13-0

For the inner Oslofjord, ecological conditions have changed dramatically over time. General improvements to water quality have come only in recent decades after the industrialization of the Oslo area that began in earnest in the second half of the 19th century (Alve et al., 2009; Baalsrud and Magnusson, 2002). In order to combat poor surface water quality in the inner Oslofjord, proximal municipalities have established wastewater treatment plants including the VEAS

(Vestfjorden Avløpsselskap) wastewater treatment plant shown in figure 2.1 (Arnesen, 2001). VEAS, located at Slemmestad, is one of the three major wastewater treatment plants in the inner Oslofjord. From the 1980's onward, the water conditions in the inner Oslofjord have been steadily improving with the reduction of emissions of materials into the water that diminish environmental quality (Arnesen, 2001).

Recent studies (conducted by UiO students in the Environmental Stratigraphy class in 2017) have focused on the area around the discharge for VEAS and have discovered spatial anomalies in ecological status conditions between areas north and south of the discharge tubes. This past research was on sediments (60m depth) near the discharge pipes belonging to VEAS lying at approximately 59.79 N, 10.51 E in the inner Oslofjord east of the town of Bjerkås (see figure 2.1). These anomalies suggest some other force at work impacting ecological status in this area, possibly related to circulation patterns or discharge regimes, but since these findings were based upon a single core they have lacked replication along with the spatial and temporal data necessary to conclusively establish reference/current conditions and to link this data to other parts of the Oslofjord.

The purpose of this thesis is to fill in the gaps in spatial and temporal data from the previous study. By collecting additional sediment cores/surface samples both at and around the previous location north of the discharge area along with biological, geochemical, radiometric, and long term (30 days) current analyses, this thesis aims to determine; (1) can the difference in ecological status observed previously (2017) be confirmed and to what extent?, (2) are temporal changes in geochemical status consistent with previous studies throughout the Oslofjord and does methodology impact the efficacy of these analyses?, (3) is VEAS having an observable impact on the environment in the area of their wastewater discharge?, (4) does the biological analysis (foraminifera) conform with recent work to utilize this species as a biological indicator of ecological status in Norwegian waters?, (5) are water circulation patterns in the area impacting distribution of discharge and if so to what extent?

2 Study area

2.1 Inner Oslofjord

The Oslofjord extends north from the Skagerrak, encompassing several deep (200 – 400m) basins in the outer Oslofjord to the Drøbak sill (19m) that separates the outer and inner Oslofjord areas (figure 2.1) (Oug et al., 2015). The inner Oslofjord extends for nearly 40 km north of the sill and consists of two main basins, the Bunnefjord and the Vestfjord, each with a maximum depth of c. 160m (Dolven et al., 2013). The underlying bedrock lithology of the inner Oslofjord is dominated by Early Paleozoic metasedimentary rocks with selective erosion occurring (Lepland et al., 2010). This selective erosion of NE – SW striking metasediments has resulted in a series of NE – SW trending ridges and depressions in the seabed that are visible on bathymetric mapping of the region (Lepland et al., 2010). In addition to the erosional features, the bedrock of this area has been marked by the Oslo rift creating many faults, dikes and fractures that run almost perpendicular to the erosional features mentioned above (Lepland et al., 2010).

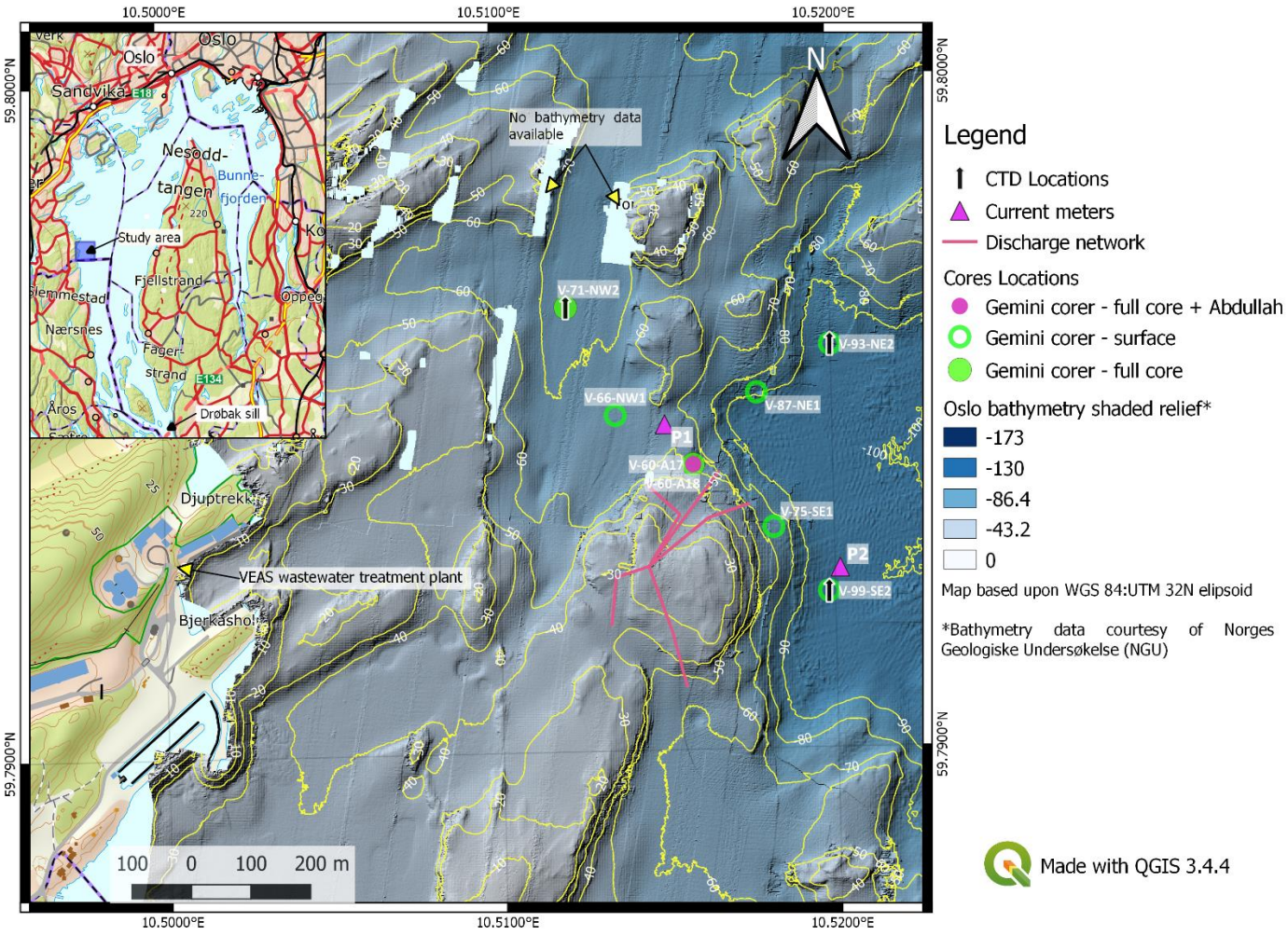

Figure 2.1 *Map of study area depicting location relative to Oslo and the Drøbak sill (inset map), along with general bathymetry of the study area (main map) courtesy of data provided by Norges Geologiske Undersøkelse (2018) and sampling locations (table 2 for exact coordinates) in relation to the VEAS discharge pipe network.*

The shallow sill (approximately 20m depth) and island populated channels allows for limited deep water renewals between the inner and outer Oslofjord or the Skagerrak (Dolven et al., 2013). Some tidally induced flushing does occur, reflecting mostly in the Vestfjord basin and growing weaker as you move north of the Drøbak sill (Staalstrøm and Røed, 2016). In addition, there is limited freshwater intrusion in the inner Oslofjord compared to that of the outer resulting in reverse estuarine circulation in the spring and summer (Dolven et al., 2013).

Water chemistry in the Oslofjord is monitored by *Fagrådet for vann og avløpsteknisk samarbeid i indre Oslofjord* at a number of sampling sites throughout the Oslofjord (figure 2.2) and released to the public through annual reports, cruise reports, and other means (Fagrådet for vann og avløpsteknisk samarbeid i indre Oslofjord, 2019). The sampling site in closest proximity to the

area of study with concurrent data is Dk1, though the sampling depth is at 80m (compared to 60m for the primary site of this study) (Fagrådet, 2017). Historical data for this location (dissolved oxygen in ml/L) is shown in blue in figure 2.2 and matches data taken from CTD's during core sampling in May 2018 (figure 2.3). These measurements place water chemistry measurements for the study site in the Vestfjord basin with the pycnocline, halocline, and thermocline occurring between 10 – 25m depth during the time of sample (figure 2.3) and match cruise data conducted by Norconsult for *Fagrådet* on 15th of May 2018 (figure 2.3).

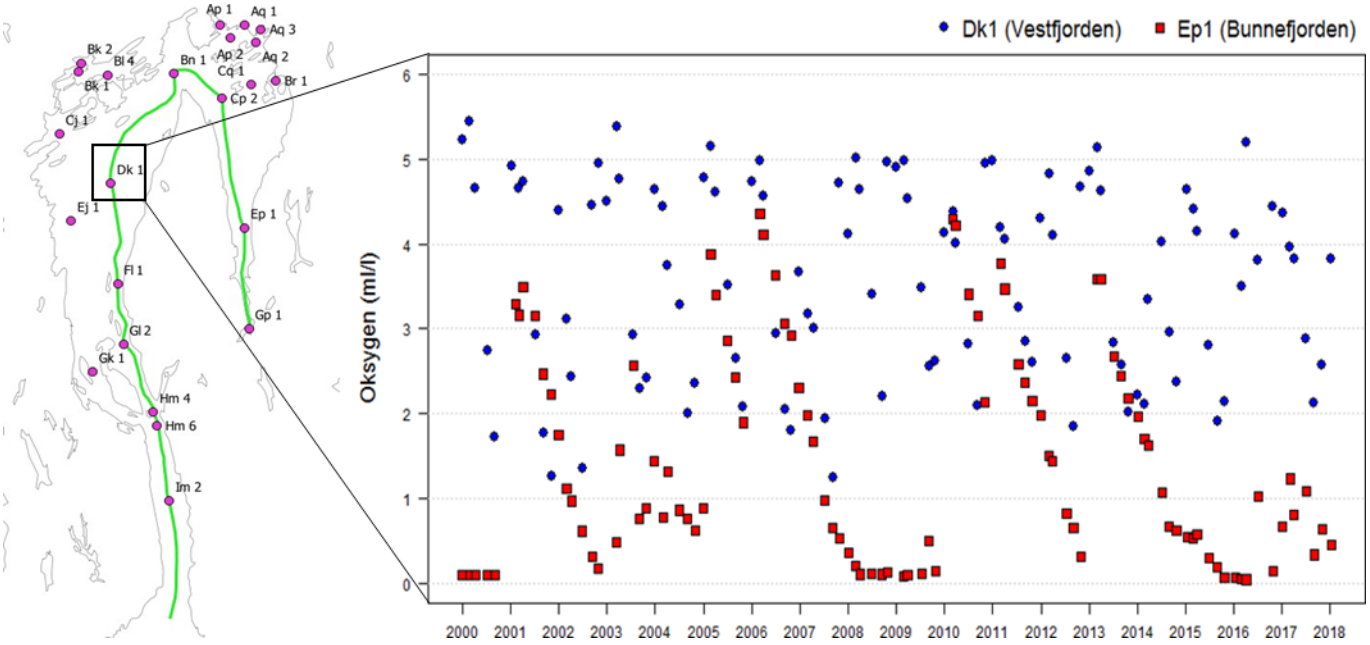

Figure 2.2 *Map locations of sites sampled for Fagrådet (left) along with historical data for dissolved oxygen concentrations for site Dk1 (in blue – 90m depth) and Ep1 (in red – 80m depth in Bekkelage basin) from Fagrådet's year report (2017).*

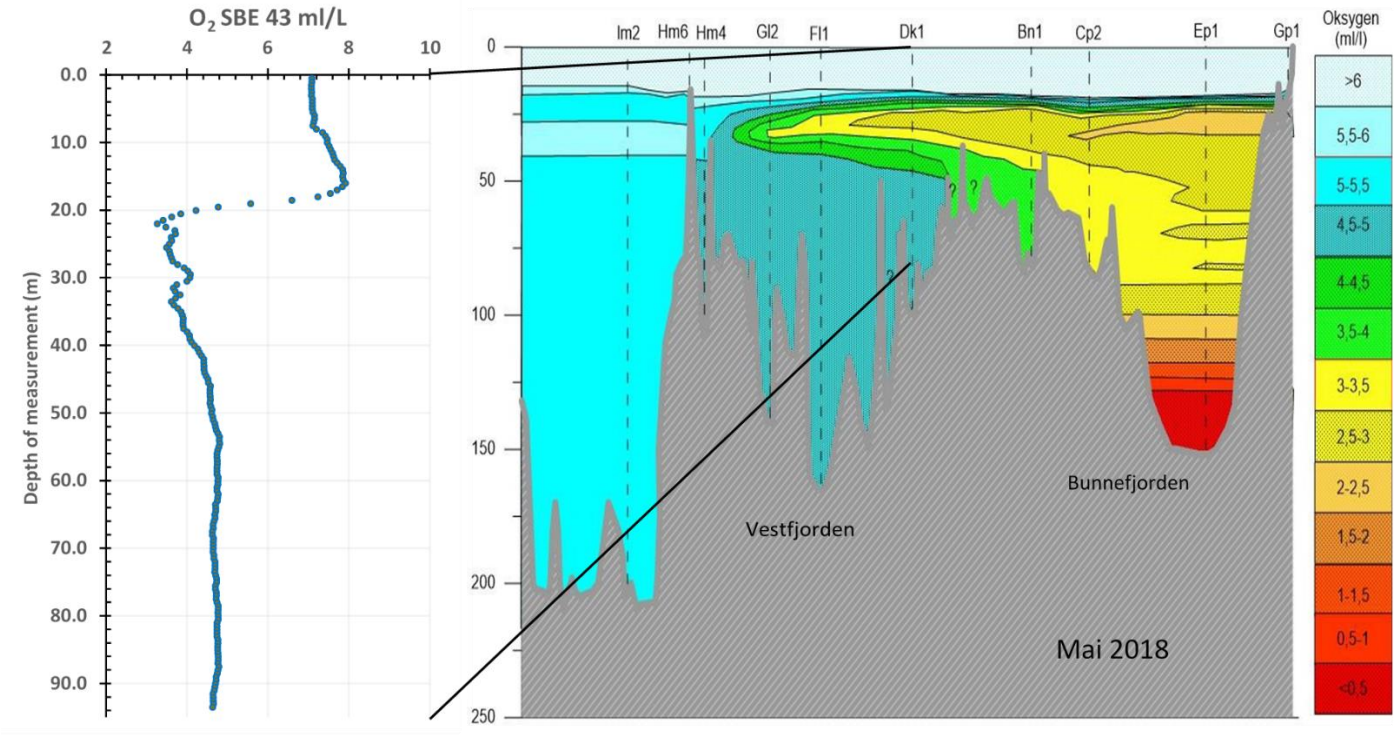

Figure 2.3 *CTD measurement graph for oxygen (left) from study area site V-93-NE2 taken on 3 May 2018 with comparison graph (right) from Norconsult cruise for Fagrådet taken on 15 May (Norconsult, 2018).*

Bottom sedimentation reflects both glacial and modern deposition forming a patchwork of sediment thicknesses present throughout the inner Oslofjord (Lepland et al., 2010). Basins and other depressions tend to have the thickest sedimentation which can be in excess of 100m (Bunnefjord) in some locations (Lepland et al., 2010). In contrast, ridges and other topographical high locations can have a relatively thin (<2 m) layer or can be completely bare of sedimentation (Lepland et al., 2010) as shown in Figure 2.4. Sediment succession begins with glacial diamictite and moves upward with Holocene mud and may be interspersed with glacial till deposits (Lepland et al., 2010). The Holocene mud sequence is usually loose and is rich in organic material reflecting modern sediment regimes in the inner Oslofjord (Lepland et al., 2010).

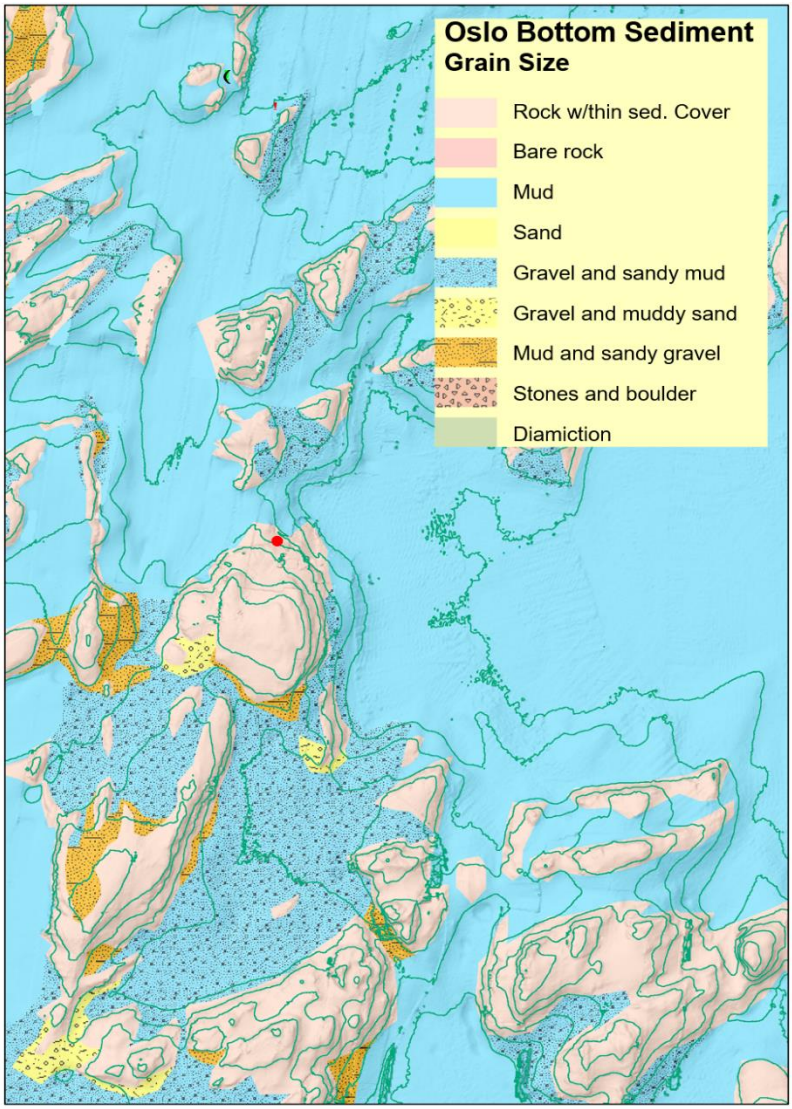

Figure 2.4 *Bottom sediment map of VEAS site with bottom contours (green lines) from Norges Geologiske Undersøkelse (NGU) (2015). Red dot shows approximate location of previous V-60-A17 survey sampling location.*

2.2 Fjord mixing and currents

Historic study of fjords and their circulation regimes has taken place for over one hundred years with the fundamental aspects of circulation understood by the early twentieth century (Syvitski et al., 1987). Farmer and Freeland (1983) as mentioned in (Syvitski et al., 1987) note five sources of energy responsible for mixing water masses in fjords; wind, tidal interactions, double diffusion instabilities, surface cooling/ice formation, and kinetic energy associated with fronts. Figure 2.5 shows a simplified overview of the fjord circulation processes discussed below.

Fjords usually contain one or more sills, such as the one located at Drøbak in the Oslofjord, and these features define many of the physical and biochemical characteristics of the fjord. Water stored in fjord basins protected by a sill can be almost stagnant, with well stratified temperature and density profiles due to limited exchange between basin and marine water (Syvitski et al., 1987). Thus, events that flush and renew deep water in fjord basins are important to circulation regimes and the overall health of the fjord ecosystem. These events occur when the water outside of the sill is denser than the water inside and sufficient energy is present to lift this denser water over the sill triggering a density current as basin water is replaced (Syvitski et al., 1987). In the Vestfjord of the inner Oslofjord, these renewals occur on average once per year during the spring and winter when prevailing winds trigger renewal events (Dolven et al., 2013; Gade, 1971).

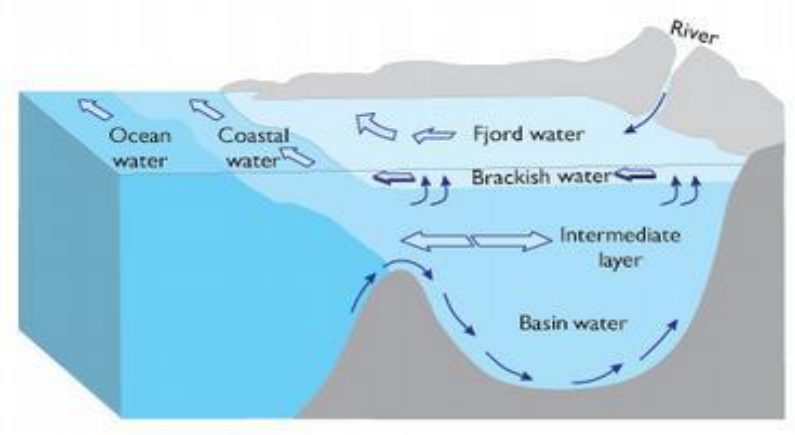

Figure 2.5 *Model of basic fjord circulation processes for reference (Institute of Marine Research, 2014).*

As fjords are a type of estuary, they can experience estuarian circulation as well as the deep water renewal mentioned above (Syvitski et al., 1987). In estuarian circulation, freshwater plumes from rivers and streams flow on the surface of denser saline water driven by the gravity. As the freshwater layer flows over saline or brackish layers shear forces between the layers entrain turbulent eddies of more saline water and establish density currents counter to the freshwater flow (Syvitski et al., 1987). In the Oslofjord system, three sources of freshwater exist in the form of runoff from the inner Oslofjord, brackish water supplied from the Drammensfjord, and river discharges from the outer parts of the fjord (Gade, 1971). As observed by Gade (1971) and mentioned in Dolven et al. (2013) there is little freshwater supply in the inner Oslofjord when compared to the water occurring outside of the Drøbak sill. This sets up a reverse

estuarine circulation regime inside of the inner Oslofjord as less saline water flows over the sill from the outer Oslofjord in the summer months making the final two inputs of freshwater the most important in the circulation regime (Dolven et al., 2013; Gade, 1971).

2.3 History and pollution

The second half of the 19th century saw the industrialization in Oslo area begin in earnest (Baalsrud and Magnusson, 2002). This, along with increases in the population in the early 20th century and the introduction of the water flushing toilet, saw the amount of wastewater discharged into the inner Oslofjord increase (Baalsrud and Magnusson, 2002).
As early as 1900, the problem of wastewater in the fjord was apparent and discussions were begun on how to deal with the problem with the first sewage treatment plant becoming operational in 1910 (Arnesen, 2001). Increases in population in the Oslo area meant that even with additional plants being built in subsequent years, the treatment facilities were not capable of dealing with the pollution. In the mid 1920's Oslo looked to England for a solution through the adoption of a treatment technique developed there called "activated sludge" which was billed by the Oslo Sewerage Authority as the answer to the problem (Arnesen, 2001). Funds were set aside for the building of plants using this technology, but not everyone was convinced that this new technique was necessary. In 1932, the newspaper "Aftenposten" called the condition of the fjord "worse than ever before" and blamed the Sewerage Authority for what was happening to the fjord (Arnesen, 2001). Public opinions on the matter began to shift during the 1930's with the closing of several public bathing areas and the moving of several swimming competitions to areas farther out in the fjord due to the smell and dirty color of the water (Arnesen, 2001).
Alerted to the deteriorating conditions of the fjord, marine scientists started conducting studies on the impact of sewage on the marine environment. In 1945, professor T. Braarud concluded that there was a positive correlation between the wastewater and the phosphorus it contained and the increase in phytoplankton production (Arnesen, 2001). Even so, it took many years for a more complete understanding of the role that nutrients (like phosphorous and nitrogen) play in eutrophication events and how these events impacted the health of the fjord. All the while, discharge to the inner Oslofjord increased in form of organic materials, nutrients and heavy metals that adversely affected the marine environment (Arnesen, 2001).

Following World War II, this pollution also included many toxic chemicals from manufacturing including heavy metals, PAHs, PCBs, and a host of other chemicals from industry and transportation (figure 2.6 for historical reference) (Alve et al., 2009). In the 1960's, research conducted by Norwegian Institute of Water Research (NIVA), painted a more complete picture of the interactions between wastewater, fjord processes, and the overall health of the fjord (Arnesen, 2001). They were able to find the connections between wastewater discharge, phytoplankton blooms (eutrophication events) in the upper layers, and oxygen depletion in the lower layers that is magnified by infrequent deep-water renewal events (Arnesen, 2001).

Figure 2.6 *Images from the industrialized history of Oslo harbor including the grain silo at Vippetangen (left) from Wilse (1935) and the Oslo harbor area near Filipstadkaia (right) circa 1970 (Ørsted, 1970).*

With this new information, regulations were implemented (beginning in the 1970's) to improve the water conditions, and several wastewater treatment plants were built. These were later upgraded to also remove phosphorus and nitrates (after Norway signed the North Sea Declaration in 1987) from the wastewater (Arnesen, 2001; Baalsrud and Magnusson, 2002). To improve the conditions in the inner Oslofjord additional measures such as better control of the industrial pollution, better wastewater treatment, and capping of old sediments with non-polluted post-glacial clay have been tried in the Bekkelaget basin (Hess et al., 2014). In the harbour area, old contaminated sediments are resuspended due to propeller wash from large ships, and bioturbation (Lepland et al., 2010). This leads to a longer time for the pollution to be remediated through burying of newer non-polluted sediments and the overall recovery of the inner Oslofjord to reference state will take longer (Lepland et al., 2010).

In order to combat poor surface water quality in the inner Oslofjord, proximal municipalities (Asker, Bærum and Oslo) established the VEAS (Vestfjorden Avløpsselskap) wastewater treatment plant in 1976 (Arnesen, 2001). VEAS is one of three wastewater treatment plants

(Nordre Follo Renseanlegg and Bekkelaget Renseanlegg are the others) in the inner Oslofjord located at Slemmestad.

2.4 VEAS

Due to deteriorating conditions in the inner Oslofjord and the EU Water Framework Directive (that all marine areas including the inner Oslofjord should be remediated to the way it was before human influences on water quality), steps have been made to improve conditions in the Oslofjord through wastewater treatment (Alve et al., 2009). Perhaps the most important aspect to improving conditions in the inner Oslofjord are the initiatives of municipalities, such as Asker, Bærum, and Oslo in establishing the VEAS facility to combat poor surface water quality in the inner Oslofjord (Arnesen, 2001). Operational in 1982, VEAS uses mechanical, biological and chemical treatment protocols for wastewater. Biological treatment did not begin at the plant in 1982 but was brought online in 1996 as discussed below. It then discharges between 100-110 mill. m^3 of treated wastewater per year into deeper layers of Vestfjorden (Arnesen, 2001; Vestfjorden Avløpsselskap, n.d.).

The plant has 6 process lines that along with chemical precipitation help treat wastewater allowing it to be discharged through one of 5 diffusers in the Oslofjord as shown in figure 2.1 (diffuser map) and figure 2.7 (visualization of the process) (pers.com. Åsne Nannestad, 2018).

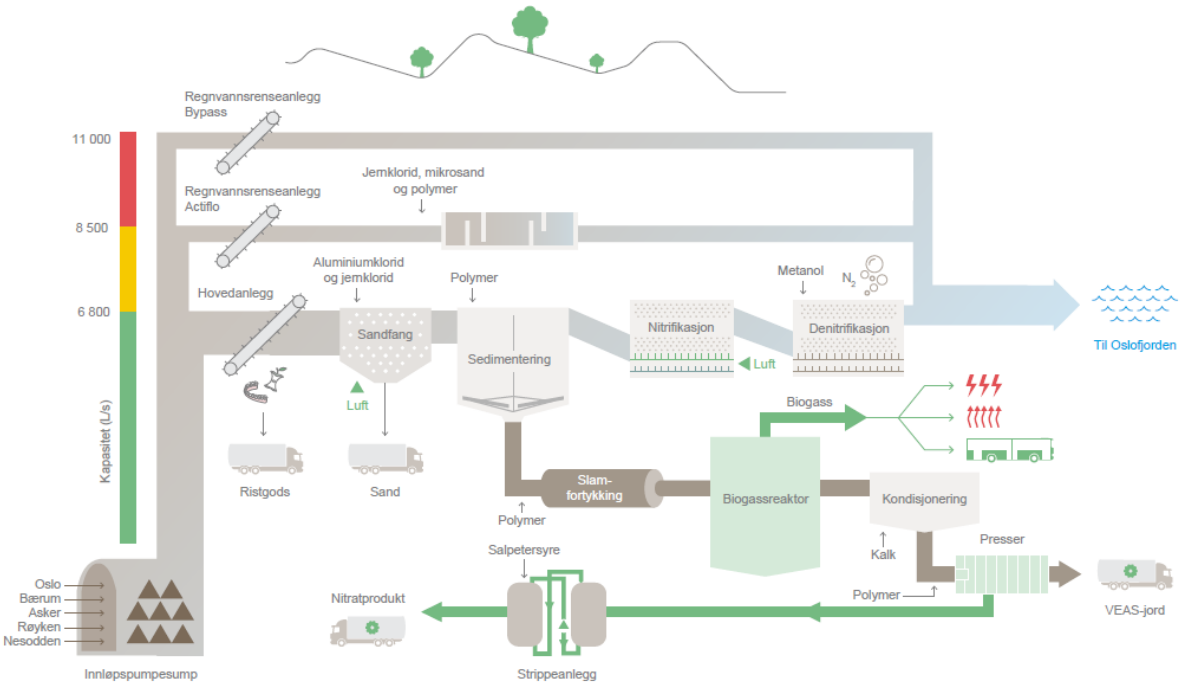

Figure 2.7 *Diagram of VEAS plant operation from input to discharge along with alternative processes such as biogas and compost (Nannestad, 2019a).*

Initially, discharge limits for the wastewater were for chemical oxygen demand (COD) along with biochemical oxygen demand (BOD5) and phosphorous (90% removal), though in 1996 process lines were re-worked and nitrogen was also limited (70%) (pers.com. Åsne Nannestad, 2018). From the 1980's onward, the water conditions in the inner Oslofjord have been steadily improving with the reduction of emissions of phosphorus, nitrates, and ammonia in the water that had previously caused plankton booms (Arnesen, 2001). In 2008, a stormwater line was opened increasing the hydraulic capacity of VEAS. It was designed to reduce overflow situations where by which untreated water was directly discharged at Lysaker (though stormwater treatment does not reduce nitrogen and the overall treatment under storm conditions is less effective than at the main plant) (pers.com. Åsne Nannestad, 2018). Additionally, this treatment requires the use of microsand, some of which is not recoverable and may be discharged to the fjord (pers.com. Åsne Nannestad, 2018). Figure 2.8 shows TOC emissions from the VEAS plant in tonn/year showing the drop-off of an additional eutrophicating contaminate. Plankton blooms have historically been responsible for many deep basins in the inner Oslofjord experiencing oxygen reduced conditions, an example being the Bunnefjord basin which has experienced oxygen reduced conditions at 70 - 150m (Arnesen, 2001; Dolven et al., 2013). Additionally, VEAS has also worked at reducing

contamination of heavy metals (through educational programs aimed at limiting input into the system, also known as “upstream” work) that can also have a negative impact on the quality of the environment as shown in figure 2.9.

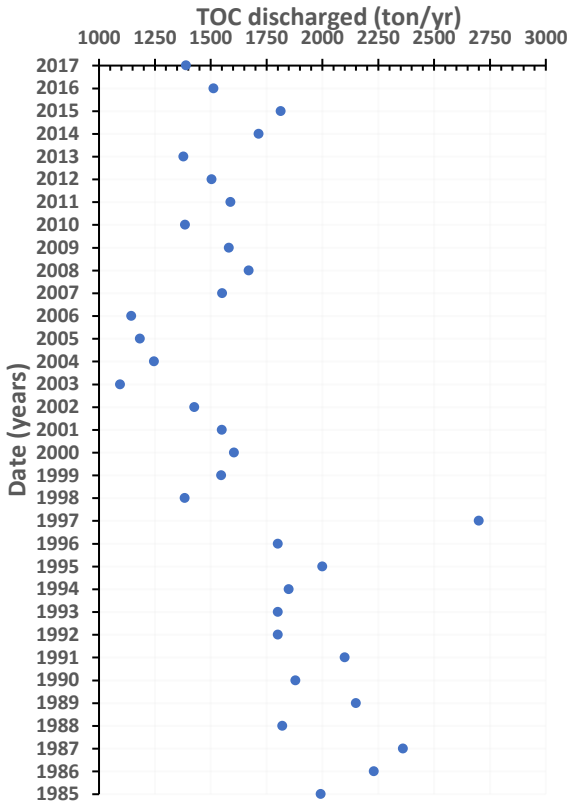

Figure 2.8 *TOC discharged by VEAS from years 1985-2017 in tons per year. Note the overall trend of discharged TOC is decreasing, with the exception of 1997. VEAS is unable to provide a reason for the spike at this particular year (pers.com. Åsne Nannestad, 2018).*

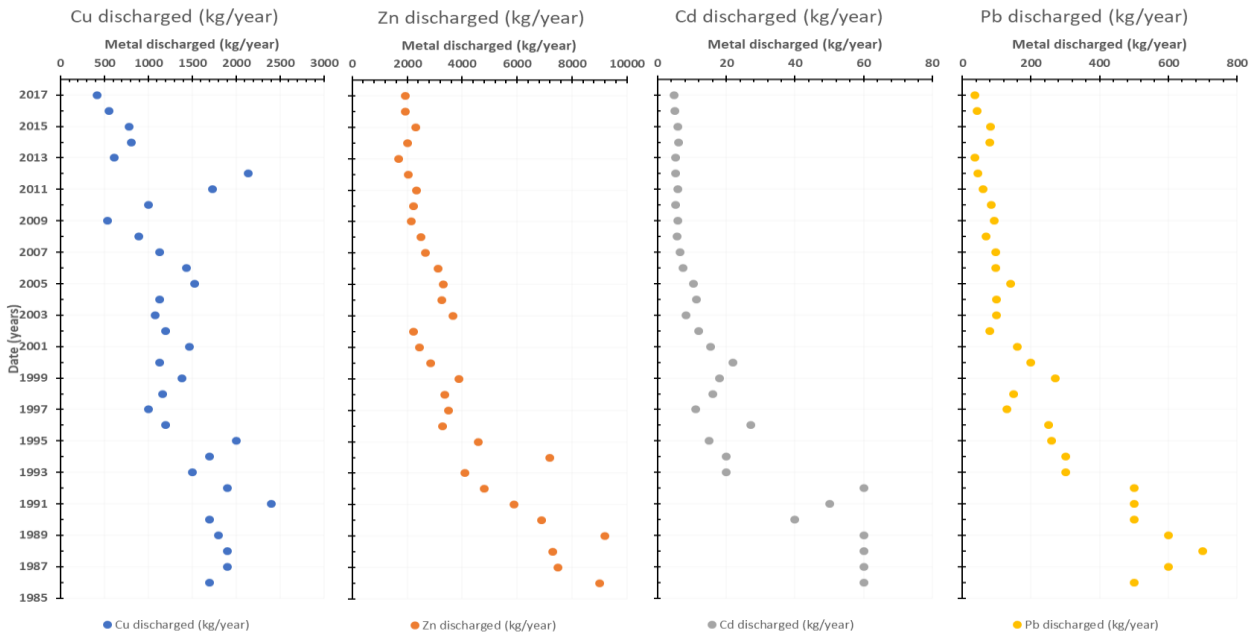

Figure 2.9 *Historical metals discharge data from VEAS for Cu, Zn, Cd and Pb from 1986 to 2017. Note the general trend is towards decreasing discharge. The higher copper values present in 2011 and 2012 are the result of contaminated lab equipment used in testing and should not be thought of as part of the overall trend (pers.com. Åsne Nannestad, 2019b; Vestfjorden Avløpsselskap, 2013).*

3 Materials and methods

3.1 Sample collection and preparations

Sediment cores and surface samples were collected at seven sites in the inner Oslofjord 3rd May 2018 using a Gemini corer (see table 2 for site names, location data, and tests performed). The Gemini corer collects two sediment cores at the same time ensuring replicates come from the same location.

The initial sampling site was a resampling of the V-60-A17 site (sampled by UiO graduate students in 2017) just north of the VEAS discharge tubes at 60m water depth where a sediment core was taken. From here a cross shaped sampling pattern was chosen with two locations to the northwest (NW), northeast (NE) and southeast (SE) of this initial location, each separated by approximated 150m surface distance (figure 2.1). The other sediment core was obtained at location labeled V-71-NW2 approximately 300m NW of the original V-60-A17 location in 71m water depth. The sediment cores were sectioned (1cm sections down to 20cm core depth, 2cm sections from 20cm till the end of core) and frozen for preservation. All other samples were

surface samples only, where the top (0-1cm) of both Gemini cores for a location where sectioned and combined. No sample were taken from the SW as previous work and surficial maps had indicated insufficient sediment thickness for sampling. The sampling pattern was chosen because (1) it would allow for confirmation of the results of the V-60-A17 core from 2017, and (2) it would allow for exploration of discharge transportation and/or locating additional sources of input. Sample containers for sediment were weighed before the cruise with weights noted for use in calculations when samples were weighed again following preparations described below.

Table 2 *Station names, location coordinates, depth, equipment used, samples taken, and date of sampling for study area.*

Station name	LAT.	LON.	Depth (m)	Equipment/sample	Year of sampling
V-66-NW1	59.79498	10.51353	66	Gemini corer/surface	2018
V-87-NE1	59.79528	10.51777	87	Gemini corer/surface	2018
V-93-NE2	59.79598	10.51998	93	Gemini corer/surface + CTD	2018
V-99-SE2	59.79232	10.51982	99	Gemini corer/surface + CTD	2018
V-71-NW2	59.7966	10.51212	71	Gemini corer/full core + CTD	2018
V-75-SE1	59.79328	10.5182	75	Gemini corer/surface	2018
V-60-A17	59.79423	10.51583	60	Gemini corer/full core	2017
V-60-A17	59.79423	10.51583	60	Abdullah/full core	2017
V-60-A18	59.79423	10.51583	60	Gemini corer - full core	2018
P1	59.79483	10.515	62	Current meter	2018
P2	59.79266	10.52016	90	Current meter	2018

Freeze-drying is the starting point for all analysis as it allows for samples to retain all chemical residue (quantitively and qualitatively), allows preservation of biological materials, and allows for calculation of water content (useful for determining porosity, as well as checking for the possible physical disturbance of sediment samples). Upon return from the cruise all samples were placed in a freezer (-25 °C) for approximately 3 days (amount of time needed is only what is required for completely frozen sample) as the first step in the freeze-drying process. Sample container covers were then exchanged with ventilated covers to allow for water vapor removal through the freeze-drying process. The process relies on sublimation occurring through the use of a vacuum chamber and the frozen sample. The vacuum pump on the Christ Alpha 1-4 LDplus freeze dryer (part # 101541), was switched on and warmed up through a designated cycle. Samples were transferred to trays located in the vacuum chamber of this unit and the vacuum

chamber cover was replaced. A blanket was placed over the unit to protect organic material from radiation degradation. Care was taken throughout these processes to ensure that samples remained frozen as this could disrupt future analysis and lead to residual water in the samples. The samples were then processed through the unit until all samples had had water removed. Dried samples were then carefully broken up and homogenized. Samples for TOC and trace metals were pulverized using an agate mortar and pestle to homogenize the samples and to break apart clumping that can occur through the process. Pulverization apparatus were cleaned with ethanol solution (70%) between samples to prevent contamination.

The water content of the samples was calculated and corrected for salt content based upon CTD measurements from the area (salinity 33psu). Knowing the water content down core allows for comparison of similarities between cores and their replicates and was used to confirm cores sent for radiometric dating.

3.2 Sediment radiometric dating

One core (V-60-A18) was sent to the Environmental Radioactivity Research Centre at the University of Liverpool for analysis. The core sections were prepared for analysis as stated in section 3.1. These samples were analyzed based upon direct gamma assay of ^{210}Pb, ^{226}Ra and ^{137}Cs radionuclides (Appleby and Piliposian, 2019). The constant rate of ^{210}Pb supply model (CRS) and the constant initial concentration (CIC) models are then applied (Appleby, 2001). Both ^{210}Pb and ^{226}Ra are naturally occurring radionuclides that find their way into the environment through radioactive decay, ending up in both lake and marine sediments (Appleby, 2001). ^{137}Cs radionuclides are found in the environment through artificial means, mostly through the testing of thermonuclear weapons from 1954 – 1963 and through fallout from the Chernobyl disaster in 1986 (Appleby, 2001). Corrections for the effects of low energy γ-rays on the samples were also applied (Appleby and Piliposian, 2019).

3.3 Total organic carbon (TOC) and nitrogen (TN)

All cores and surface samples were analyzed for TOC and TN. Approximately 1g of pulverized sediment powder was transferred to a labelled centrifuge tube. All apparatus used were cleaned between samples with ethanol solution (70%) to prevent contamination of samples. Inorganic carbon was removed by slowly adding 15mL of 1M Hydrochloric Acid (HCL) to the centrifuge

tube with the sample and placing it on a shaker for at least 3 hours (our samples remained overnight due to time constraints). The acid was then decanted off and the sample residue was rinsed with distilled water, centrifuged, and decanted at least 3 times. This sample residue was then dried overnight at 40 °C, upon which samples were sent to be analyzed using the Elemental Analyzer (UiO Biology Department). TOC and TN were utilized to calculate the carbon nitrogen ratio (C:N) to help determine the origin of carbon input into the ecosystem. TOC_{63} was also calculated based upon data from micropaleontology analysis (% sediment <63µm, Appendix G).

3.4 Metal analyses

Analysis of heavy metals can be used as chronostratigraphic markers and together with other analyses (micropaleontological) to determine the EcoQS (Alve et al., 2009; Lepland et al., 2010). The metal analyses follow Norwegian Standard (NS4770/1994). The following trace metals were analyzed; Cu, Zn, Pb, Cd. Hg was also analyzed, though only semi-qualitatively and as such the results were not a focus of this thesis.

For the metal analysis, 1 gram of freeze-dried sediments were put into labelled Teflon containers with the accuracy of four decimals for each of the sliced intervals. Then, 20 mL of 7M HNO_3 (nitric acid) were added to extract the bioavailable fraction of the metals from organic matter and clay (Lepland et al., 2010). The properly mixed samples were then placed in an autoclave at 120 °C and 1.2 bar for 30 minutes. To separate the dissolved fraction from the sediment, all the extracted fractions were put in a centrifuge for 10 min at 4000 revolutions per minute (rpm). For the samples to be analyzed by the Inductively Plasma Mass-Spectrometry (ICP-MS) (Bruker Aurora Elite), they were diluted 50 times with 1% HNO_3.

3.5 Micropaleontology analysis

Preparation of sediment samples for foraminifera analysis begins with the freeze drying and careful homogenization of sliced core samples. For a representative sample the 0.5, 1.5, 2.5, 3.5, 4.5, 9.5, 14.5, 19.5, 25 and 31cm core depths of the V-60-A18 core were subjected to this analysis. Approximately 3g (mass to two decimal points) of sediment was transferred to labeled (core name, sliced depth) plastic containers. This material was then wet-sieved through a 63 µm sieve to remove mud and other fine particles, with agitation. Once no more mud comes through

the sieve, the sediment is returned to the container while a sieve stack of 63, and 500 µm sieves is prepared. The sediment is then added to the sieve stack and re-agitated and washed to divide the sediment into the predetermined size fractions. Each fraction is then transferred with as little water as possible (care was taken not to pipette off excess water or pour water into the sink as foraminifera tests will be lost and instead excess water was poured back through the appropriate sieve and any material captured carefully transferred back to the box) to a labelled (core name, sliced depth, sieve fraction size) plastic box. The plastic boxes were placed into a drying cabinet at 40°C until all water is evaporated. If necessary, finer fractions were sieved through a dry 500 µm sieve to break apart clumps. Finally, the dry 63-500, and > 500 µm fraction were weighed and transferred to labeled glass vials.

Both fractions were studied under the microscope. From the >500 µm fraction, notes were made of all organisms and other objects of interest (shell fragments, clasts) and put in a specimen slide for each depth. The 63-500 and >500µm fractions were studied in greater detail under the microscope. The glass vials holding the 63-500µm fraction were blended to make sure that the foraminifera taken out were a representative sample. This was done because foraminifera have different shapes and will distribute unevenly throughout the glass vials if not blended, influencing the result. Small amounts of the material were evenly distributed on the picking tray before picking. The picking tray was placed under the microscope and foraminifera were picked and transferred by using a thin wet brush to a faunal slide with glue. On the faunal slide, the foraminifera were sorted by species and counted. Where possible, around 200 foraminifera were picked from each depth. The remaining grains on the picking tray were weighed and transferred to a new labeled glass vial.

Original counting results are presented in Appendix G. The species found were separated by agglutinated and calcareous species and listed in alphabetical order for each depth. For the different samples the sum of foraminifera was calculated. The dry weight of the material before washing, the weight of the different size fractions picked and unpicked were also measured and entered into the data table (Appendix G). The number of foraminifera per gram of the sample and the number of foraminifera per g dry sediment were entered before calculating the percent of agglutinated and calcareous species. In addition, the relative abundance (%) was also calculated and recorded. The total number of species per depth was counted as well as percent of sand at

sample depth based upon the 63-500µm fraction. Samples were additionally analyzed for similarities in the community structure, cluster-analysis and non-metric multidimensional scaling (MDS)-ordinations. The analyses were based on square-root transformed Bray Curtis similarity (Bray and Curtiss, 1957) and the species abundance patterns were overlain on the MDS plots using PRIMER version 6.1.6 (Clark and Gorley, 2006).

Micropaleontological data was also used in PRIMER to calculate the diversity indices Shannon-Weiner (H'_{log2}) (Shannon and Weaver, 1963) and Hurlberts (ES_{100}) (Hurlbert, 1971) for the foraminifera. Shannon-Weiner is the most common index in benthic ecology and incorporates richness and equitability (Kröncke and Reiss, 2010). It is calculated by the formula:

$$H' = -\sum(p_i) \times (\log_2 p_i)$$

where p_i is the proportion of individuals found in species i. Hurlberts diversity index is calculated based upon the expected number of species (ES) for a certain number of individuals (in this case 100) based upon rarefaction and is less dependent than Shannon-Weiner on sample size (Hurlbert, 1971; Kröncke and Reiss, 2010). It is calculated based upon the formula:

$$E(S_n) = \sum_i \left[1 - \frac{\frac{N - N_i}{n}}{\frac{N}{n}} \right]$$

Where n is the number of individuals selected at random from a collection containing N individuals, S species, and N_i individuals in the ith species.

Foraminifera AZTI Marine Biotic Index (Foram-AMBI) was also calculated based upon the work of Alve et al. (2016) for the micropaleontological data. AMBI is based upon the sensitivity of a given organism to a gradient of stress. For Foram-AMBI this stress is the supply of organic material. Species were classified based upon their response/tolerance to this stressor into ecological groups (EG) from 1 to 5 based upon the work of Grall and Glémarec (1997) and Borja et al. (2000) as cited in Alve et al. (2016). The groups follow a gradient as follows; EG 1 – species sensitive to organic matter enrichment, EG 2 – species indifferent to organic matter enrichment, EG 3 – species tolerant of excess organic matter, EG 4 – 2nd order opportunistic species show a positive response to organic matter enrichment, and EG 5 – 1st order opportunistic species that show a clear positive response to excessive organic matter with a higher abundance at higher stress than EG 4. Species % of assigned species was multiplied by an

AMBI factor based upon the EG the species was assigned. For each core depth these values were summed up and dived by 100 giving the overall AMBI value for that depth of the core. The Norwegian Quality Index (NQI) was also calculated for chosen core depths based upon the micropaleontology data. The NQI is a multimeric index that has a diversity component and a sensitivity component (AMBI) (Alve et al., 2019) that has been utilized for macrofauna. Based upon the work of Alve et al. (2019), this index was proposed to be intercalibrated for foraminifera based upon AMBI values and the ES_{100} diversity index. The following formula was used:

$$NQI_{\_f} = 0.5\left(1 - \frac{AMBI_{\_f}}{7}\right) + 0.5\left(\frac{ES_{100\_f}}{35}\right)$$

(the use of $_f$ denotes that these indices represent foraminifera).

Finally, normalized Ecological Quality Ratio (nEQR) was calculated for the chosen core depths based upon the values calculated for H'log2, ES100, and NQI. nEQR is the ratio of observed biological parameters to reference biological parameters and has a scale between 0 and 1 with 0 representing bad status and 1 representing good status. nEQR is first calculated for each index based upon the formula:

$$nEQR = \left(\frac{(index\ value\ -\ classes\ losest\ index\ value)}{(classes\ highest\ index\ value\ -\ classes\ lowest\ index\ value)}\right) \times 0.2 + classes\ nEQR\ base\ value$$

Class base values for nEQR were obtained from Veileder 02:2018 (Direktoratsgruppen for gjennomføringen av vannforskriften, 2018). The mean nEQR was calculated based upon the results of the nEQR for these three indices (Appendix G)

3.6 Circulation current analysis

From June 26th, 2018 until August 9th, 2018 two current meter rigs were deployed in the area north (1 rig labeled P1) and east (1rig labeled P2) of the VEAS discharge area. The locations were chosen for their proximity to the area of interest and based upon previous currents studies done in the area (see Bjerkeng et al., 1978) and are shown in figure 3.1 and listed in table 2. Current meter P1 is an Aquadopp AQP 5608 operating in the 400 kHz range placed at 62m depth with a vertical resolution of 4 meters. The frequency of 400 kHz gives shorter vertical range than the Continental meter. The meter was set up to give a reading every 15 minutes with an averaging period set at 160 seconds. Current meter P2 is a Continental CNL 6117 operating in the 190 kHz range placed at a depth of 90m with vertical resolution of 10 meters. The 190 kHz

range allows for greater vertical range than the Aquadopp meter, but coarser resolution. The meter was set to give reading every 15 minutes with an averaging period set to 300 sec to conserve power for the test. The blanking distance (distance above the instrument for which no reading is possible) for both instruments was 2 meters. Figure 3.1 shows the mooring configuration of the two rigs.

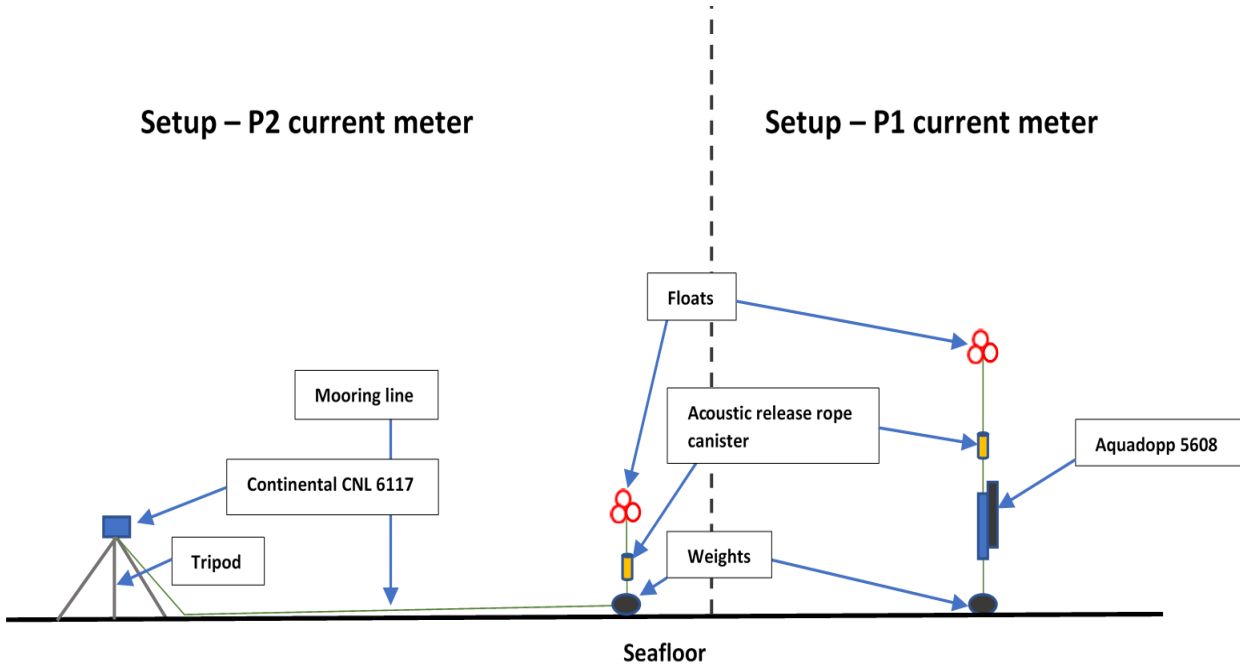

Figure 3.1 *Diagram of mooring configuration for current meter rigs.*

Both current meters utilize the acoustic doppler effect to measure current velocity and direction profiles through the water column (Nortek AS, 2017). These systems utilize 3 transducer beams to provide data for the 3 components of velocity; east, north, and up. The beams are angled 25° off the vertical access. The data collected by these current meters will be analyzed and plotted with MATLAB.

3.7 Reliability of analyses techniques

It is important, due to the comparison of data with different time stamps (relating to when the core was collected and processed) and preparations that occurred outside the authors control, to determine to what extent methodology, equipment and time influence results. This is especially true concerning TOC and metals analysis as these are used as part of determination of

environmental quality and final testing occurs outside of direct control. As such these analyses were subjected to additional scrutiny and testing (utilizing replicates, with blind samples and blanks, and in the case of the TOC a test conducted on a different machine) in order to determine the level of deviation among results. Figure 3.2 shows methodology used for the metals' analysis, though similar protocols were followed for TOC as well. Means were calculated for replicates measurements along with range of variation in the data sets through standard deviation of population calculations (Excel).

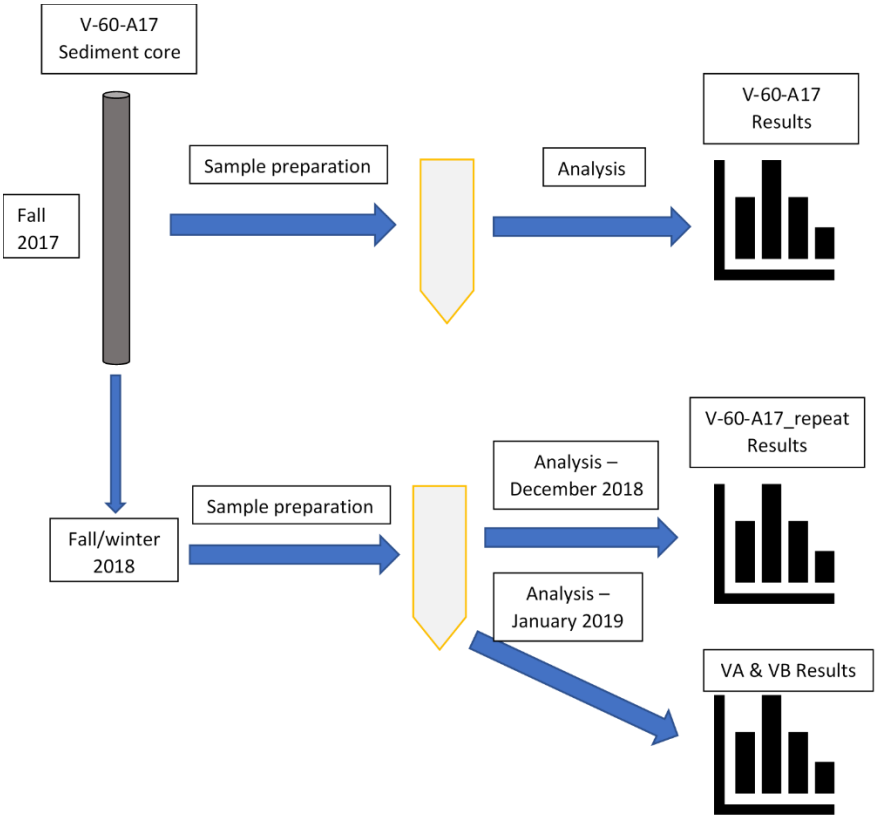

Figure 3.2 *Diagram explaining the process of additional protocols performed on metals analyses for the V-60-A17 core.*

4 Results

As a basis for putting subsequent test results in context, the salt corrected water content of the sediment cores was calculated and plotted (figure 4.1). The comparatively smoothed plot of the V-60-A18 core indicates little disturbance and matches well with the core notes (little signs of disturbance moving down core - Appendix A) and observations obtained during the time of sampling (figure 4.1, Appendix A). Based upon this result, this core (V-60-A18) was chosen for

radiometric dating (described below in section 4.1) as the replicate core (V-60-A18R) showed evidence of disturbance. Variations of water content (figure 4.1) in the additional cores and replicates match with core notes for these slices (Appendix A) and likely reflect disturbance and the presence of large clasts (rocks and shell fragments).

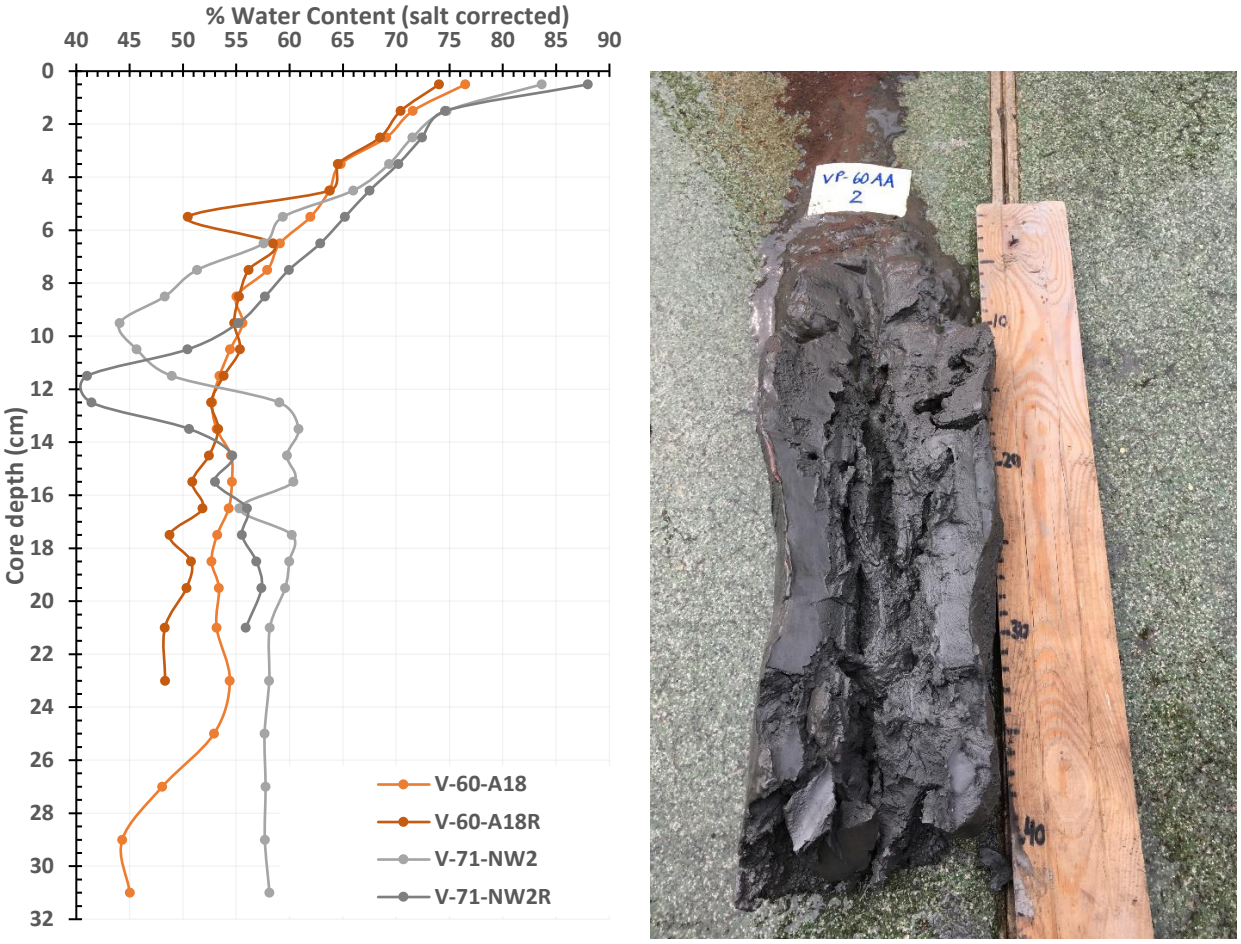

Figure 4.1 *Graph of salt corrected water content (left) for sediment cores collected on 03 May 2018 at 2 locations (table 2) along with image of split core from V-60-A18 location collected on same date. Note the relative uniformity throughout the core.*

The results for additional individual tests are described in detail below. Raw data for these tests can be found in Appendices (A-G).

4.1 Sediment radiometric dating

Concentrations of ^{226}Ra were relatively uniform throughout the V-60-A18 core with a mean value of 41 Bq kg^{-1} that is similar to those found in sediments in the Bekkelag basin below 17cm

collected at approximately the same time (full dating report can be found in the Appendix C) (Appleby and Piliposian, 2019). Total ^{210}Pb reaches values close to equilibrium with ^{226}Ra at around 10cm depth though there is a small level of disequilibrium down to 20cm depth (Appleby and Piliposian, 2019). Unsupported ^{210}Pb concentrations initially increase with depth, reaching a maximum in the 3-4cm section, followed by an exponential decline to 10cm suggesting a relatively uniform sedimentation rate for this part of the core (Appleby and Piliposian, 2019). The report by Appleby and Piliposian (2019) notes that concentrations after this depth (10-20cm) are close to the detection limit with a slightly higher value in the 20-22cm sample suggesting that the sediments at this depth may be relatively modern.

Core chronology based upon ^{210}Pb dating puts 1986 and 1953 in the 5-6cm and 8-9cm slices respectively using the CRS model with full chronology shown in figure 4.2 (Appleby and Piliposian, 2019). The absence of clear ^{137}Cs activity, both of the 1986 Chernobyl accident and 1960's nuclear weapons testing mean that the chronology is based solely on the ^{210}Pb results. Appleby and Piliposian (2019) postulate that a peak in the ^{137}Cs values in the 3-4cm sample are the result of sedimentological processes and not related to a particular event.

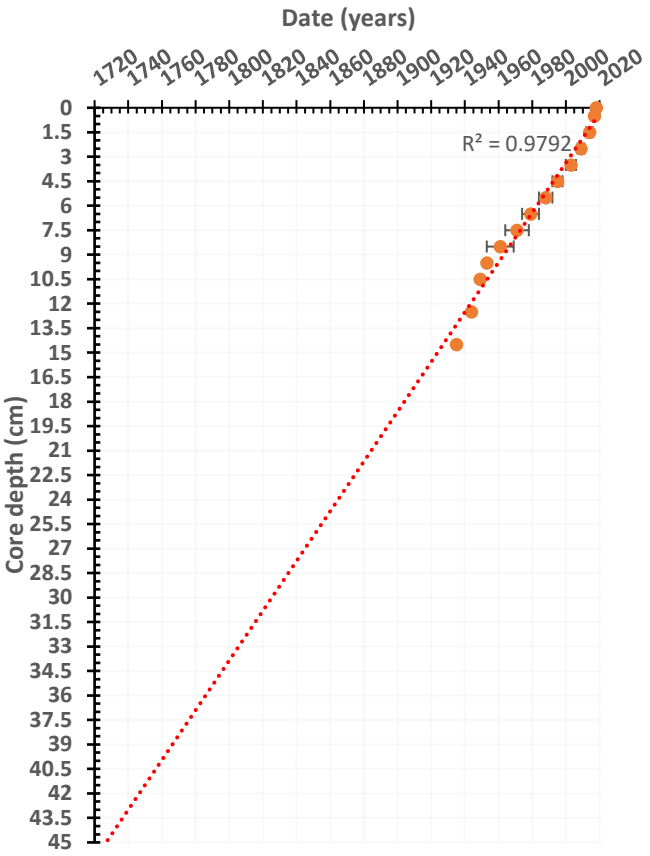

Figure 4.2 *Sediment chronology for V-60-A18 core based upon unsupported ^{210}Pb data from Appleby and Piliposian (2019). Dotted red line is extrapolation (linear - for data below 14.5cm) for down core dating with R^2 value shown for measure of regressive predictability. These values are used for comparison to other sediment cores for this area (V-60-A17 + Abdullah). Error bars are provided based upon reported data for the V-60-A18 core.*

Sedimentation rates for the V-60-A18 core (figure 4.3) appear relatively uniform from the 1960's to the early 2000's with mean values for this time period of 0.063 g cm^{-2} y^{-1} (0.12 cm y^{-1}), with a small increase in recent years (Appleby and Piliposian, 2019). Calculations suggest that there may have been a rapid accumulation in the 1940's, based upon low ^{210}Pb concentrations that is supported by data collected in the Bekkelag basin (Appendix C), though there are uncertainties for pre 1960 sediments (10cm and below) also shown in figure 4.2 (Appleby and Piliposian, 2019).

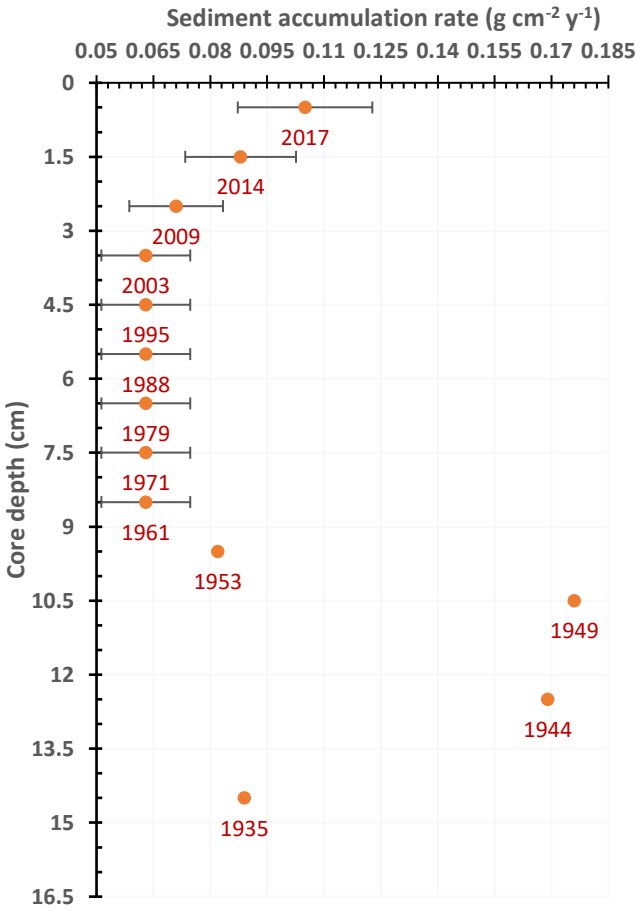

Figure 4.3 *Sediment accumulation rate with error bars for V-60-A18 core based upon data from Appleby and Piliposian (2019). Radiometric dates are shown in red.*

4.2 Total organic carbon (TOC) and nitrogen (TN)

TOC for the full cores and the surface samples was analyzed and reported as % organic carbon along with % nitrogen. Replicate analyses were performed on some samples and in these instances the mean value of all results was plotted. TOC is generally increasing moving up core from 1.1 and 1.7% at the bottom (core depth 31cm) to 4.8 and 6.2% at the top for the V-60-A18 and V-71-NW2 cores respectively (figure 4.4). Both sediment cores showed generally the same overall trend (increasing) though the V-71-NW2 core had continuously higher values. There is a slight decrease evident for the V-60-A18 core between the 1.5 to 0.5cm core depth, but this is not shown in the V-71-NW2 core. Surface samples (0.5cm depth) are varied, with the lowest surface value (3.9%) coming from the V-93-NE2 (located distally from the discharge area) site and the

largest occurring from the V-66-NW1 site (5.8%) which is reflected in the full core values as an increasing trend in TOC toward the north west from V-60-A18 site.

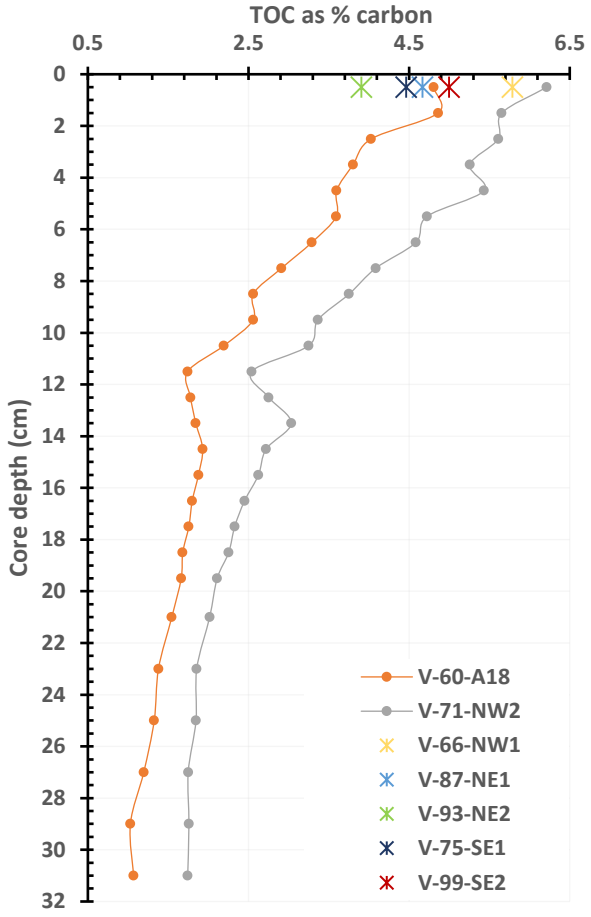

Figure 4.4 *TOC as percent carbon for sediment cores and surface samples from the study area. Note the overall increasing trend in TOC and that values tend to increase as one move toward the north west of the study area as evidenced by the values for the NW1 and NW2 samples. For positions of sites see figure 2.1.*

The ratio of organic carbon to nitrogen (an indicator of the source of carbon input; 0-7 marine, 7-20 soil) was calculated and plotted (figure 4.5) (Meyers, 1994; Nasir, 2016). The C:N ratios for both sediment cores increased moving up core with generally higher values for areas northwest of the V-60-A18 site as seen with TOC. Ratios suggest a change over from marine input of carbon as you move up core from a core depth of 12cm.

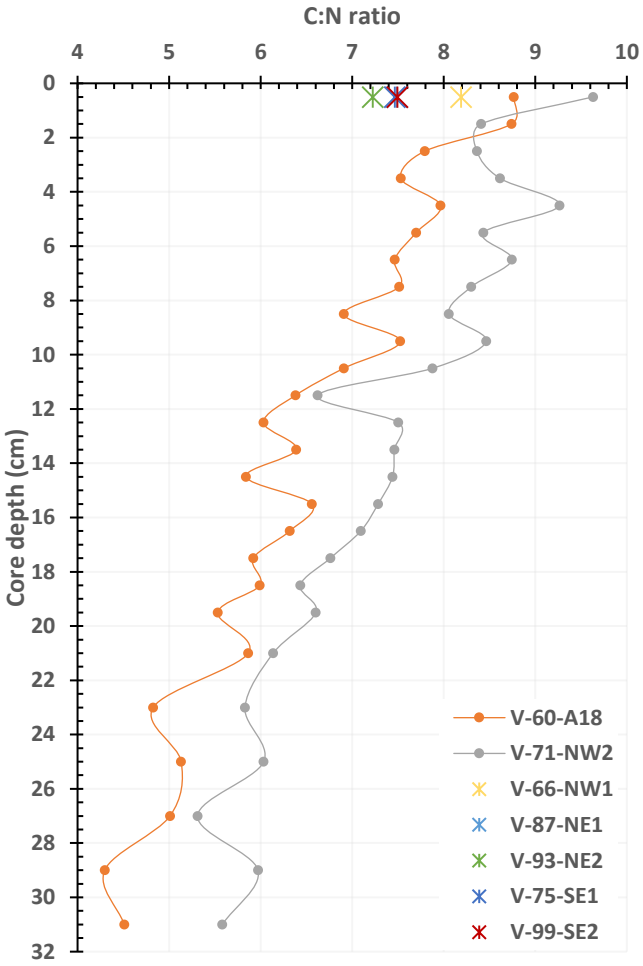

Figure 4.5 *Carbon nitrogen ratio (C:N) for full cores and surface samples from study area. Note the higher ratios (greater than 7) up core trending toward a terrestrial input of carbon. For positions of the sites see figure 2.1.*

4.3 Metals analysis

Core and surface sample sediments were analyzed for Copper (Cu), Cadmium (Cd), Zinc (Zn) and Lead (Pb) with the results plotted and shown in figure 4.6 (a.-d.). Mercury was also analyzed semi-qualitatively and as such the results are not presented, however, the overall trend follows those discussed in detail below.

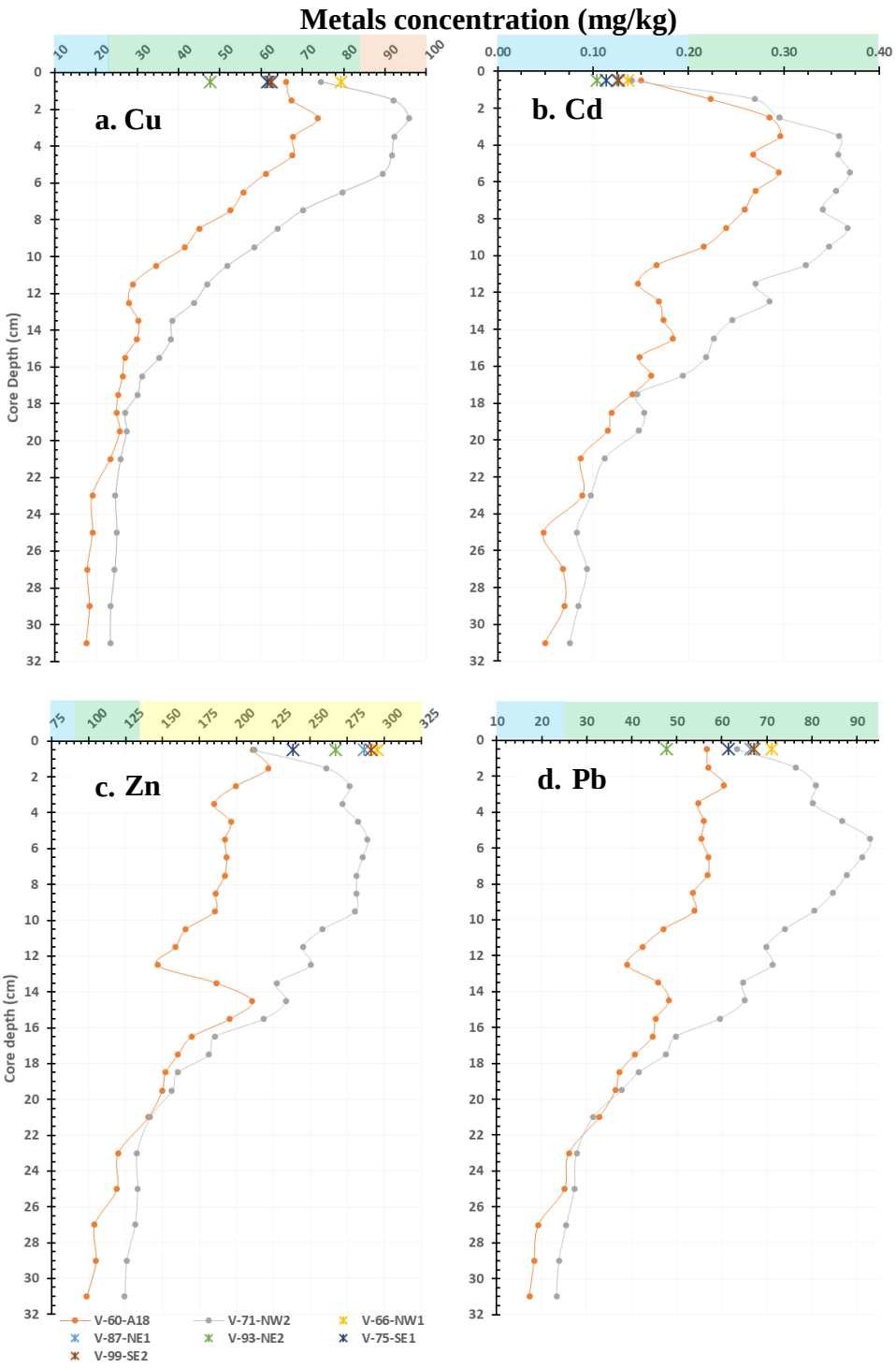

Figure 4.6 a.-d. *Metals concentrations for full core and surface samples from study area for Copper (**a.**), Cadmium (**b.**), Zinc (**c.**) and Lead (**d.**) in mg/kg. Colored banding on x-axis reflects current environmental quality boundaries for these metals as shown in table 1. For positions of the sites see figure 2.1.*

Both sediment cores follow the same general trend for all analyzed metals, that is increasing up core from the 20cm core depth. However, the rate at which this concentration increase occurs is

greater for the V-71-NW2 core and as such there is a distinct separation between the sediment cores from approximately 20cm up to approximately 2cm core depth were this difference begins to subside. There are several examples where the sediment cores behave differently, most pronounced would be approximate to the 12.5cm core depth where all metals' values (though not well pronounced in Cu) in the V-60-A18 core decreased while values for the V-71-NW2 core increased. Peaks for the various metals vary with core depth as is to be expected based upon their use and disposal histories and will be discussed in more detail below in relation to the work of Lepland et al. (2010). Again, there is some variability between the cores as to where these peaks occur with the peaks occurring farther up core in the V-60-A18 core than in the V-71-NW2 core.

There was great variability for the surface samples both in magnitude and assemblage. The closest correlation with the sediment cores occurs for Cd with all surface values relatively close to each other and to the values of the surfaces of the sediment cores. Surface values are higher than the full cores for Zn, while there is a more variable distribution for Cu and Pb.

4.4 Reliability of analyses techniques

As data for the 2018 core (V-60-A18) was processed and compared to the results of the 2017 core (V-60-A17) it became clear that there were some discrepancies, even though both cores were thought to come from the same location. This necessitated retesting the 2017 core, which revealed further discrepancies from the original 2017 data. As such, testing the reliability of analysis techniques (for metals and TOC analyses) was conducted including replicates, with blind samples and blanks, and in the case of the TOC a test conducted on a different machine.

For metal concentrations, variations in data exist for tests that were performed at the same time, with the same preparation, under blind conditions as shown in figure 4.7 (labelled VA and VB in methodology section, figure 3.2). In a follow up discussion with the lab technician who performed these tests, these variations could not be accounted for from standard analytical error, and the size of the error varied by metal (figure 4.7).

Looking at another comparison from the same metals' extraction (occurring in the fall of 2018) with the addition of time between testing (approximately 1 month) (figure 4.8) these deviations from the mean have grown. Again, the magnitude of the variations was varied between metals and differed between core depth with those shown in figure 4.7.

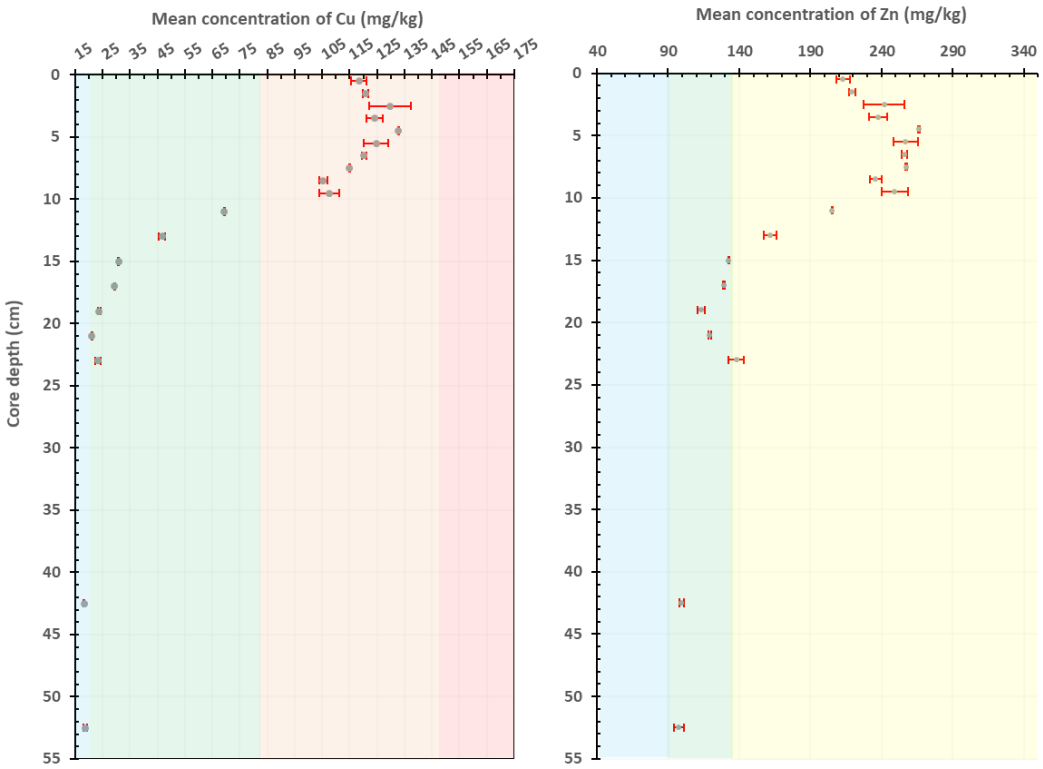

Figure 4.7 *Mean concentrations of Cu (left) and Zn (right) for the same extraction of two samples of the V-60-A17 core (VA and VB in figure 3.2). Note significant deviation from the mean exist here (as shown by error bars in red) and that these deviations are not uniform across the different metals. Colored background has been added corresponding to environmental quality standards discussed in table 1 for 2018 to show situations where uncertainty could lead to differing classification. Samples from 42.5 and 52.5cm core depth are from the Abdullah core.*

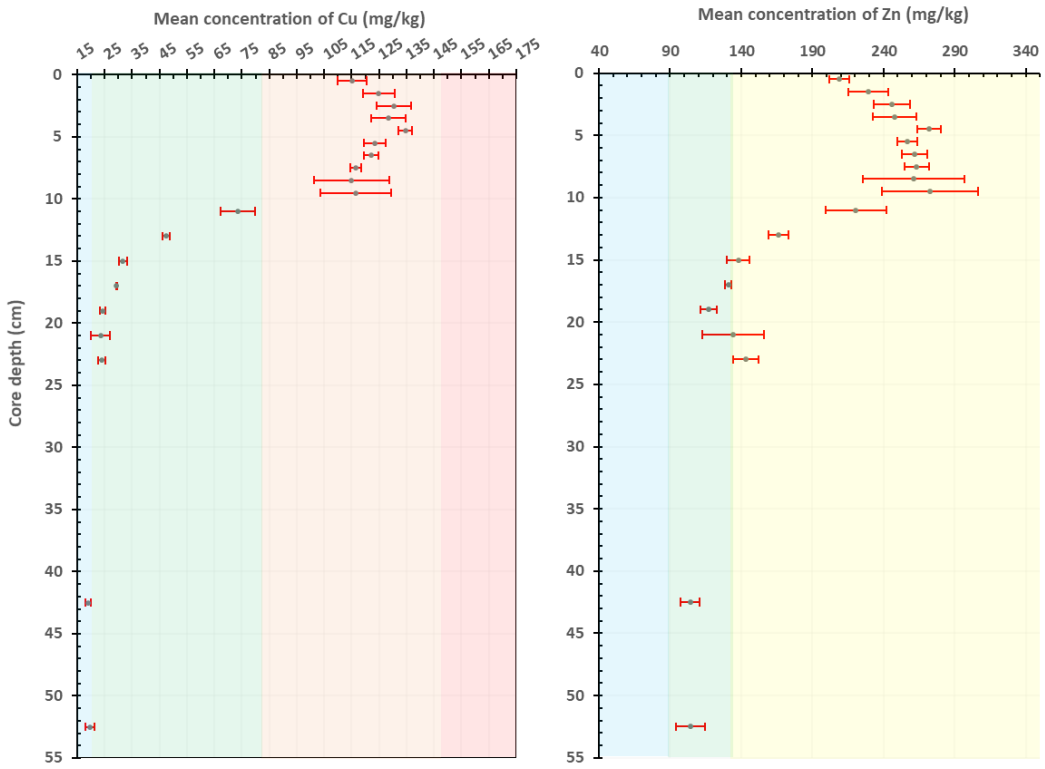

Figure 4.8 *Mean concentrations (3 analyses) of Cu (left) and Zn (right) from same extraction as shown in figure 4.7 with additional time between tests (approximately 1 month). The mean and deviations have been calculated from the results from the V-60-A17_repeat and the VA/VB blind test (figure 3.2). Note that deviations from the mean (red error bars) have grown (from those shown in figure 4.7) and this growth is not necessarily in uniformity with those seen in figure 4.7.*

As data was combined for all analyses of the 2017 sediment core (original 2017 preparation, the preparation prepared at end of 2018 (V-60-A17_repeat), along with the bling study performed at the beginning of 2019 (VA and VB)) (figure 4.9) these deviations grow dramatically. Variations of the values of concentrations for these metals at many more core depths is great enough to lead to uncertainty in placing environmental quality status.

The graphs shown here represent only the testing for Cu and Zn for continuity, but the patterns discussed apply to other metals tested (Cd and Pb).

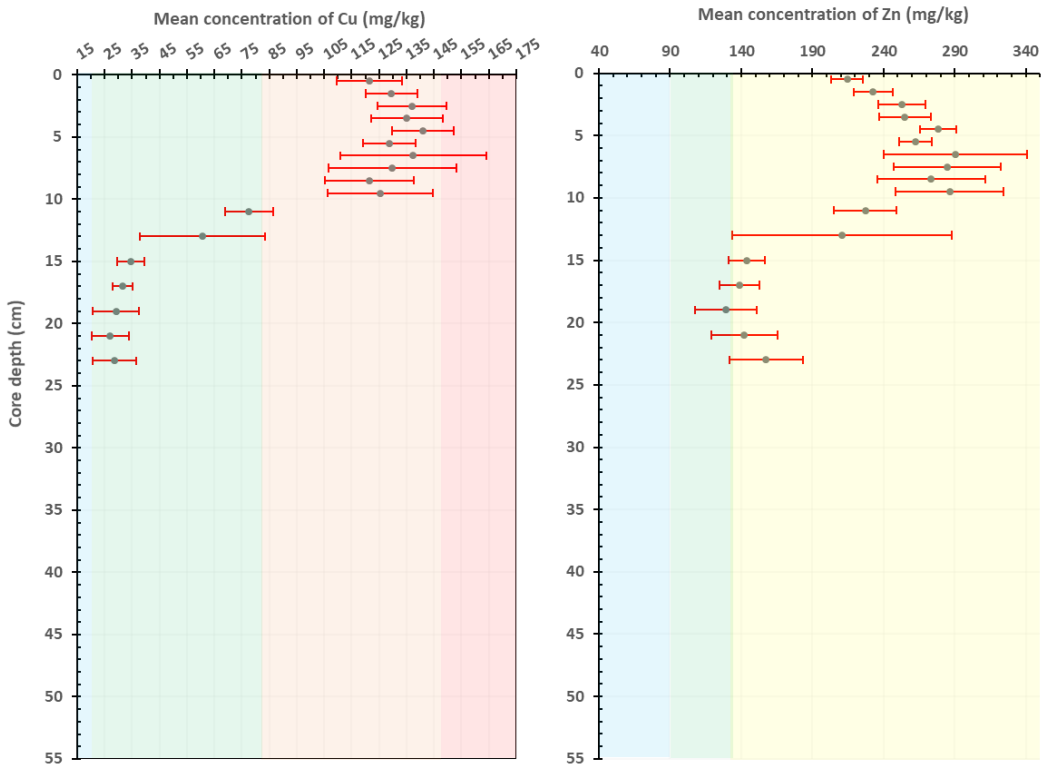

Figure 4.9 *Mean concentration for metals Cu (left) and Zn (right) for all preparations and tests (total of 4 analyses) of the V-60-A17 core as shown in figure 3.2 with error bars (red) showing deviations across all data. Note that the 42.5 and 52.5cm core depths (Abdullah core) are not shown here as they were not part of the 2017 testing of the V-60-A17 core.*

Analysis of the TOC methodology included analyzing deviation of the replicates given with the raw data for the retested V-60-A17 core provided by the University of Oslo (UiO)Biology Dept. Retesting of the 2017 core was also performed at an additional lab on a different apparatus (UiO Department of Geosciences) for comparison. Here comparison between the labs did not yield as much deviation as those experienced for the metals (figure 4.10). There does appear to be greater variation for the data obtained from the Biology department, but replicates were only provided for a few core depths and as such the analysis is not complete.

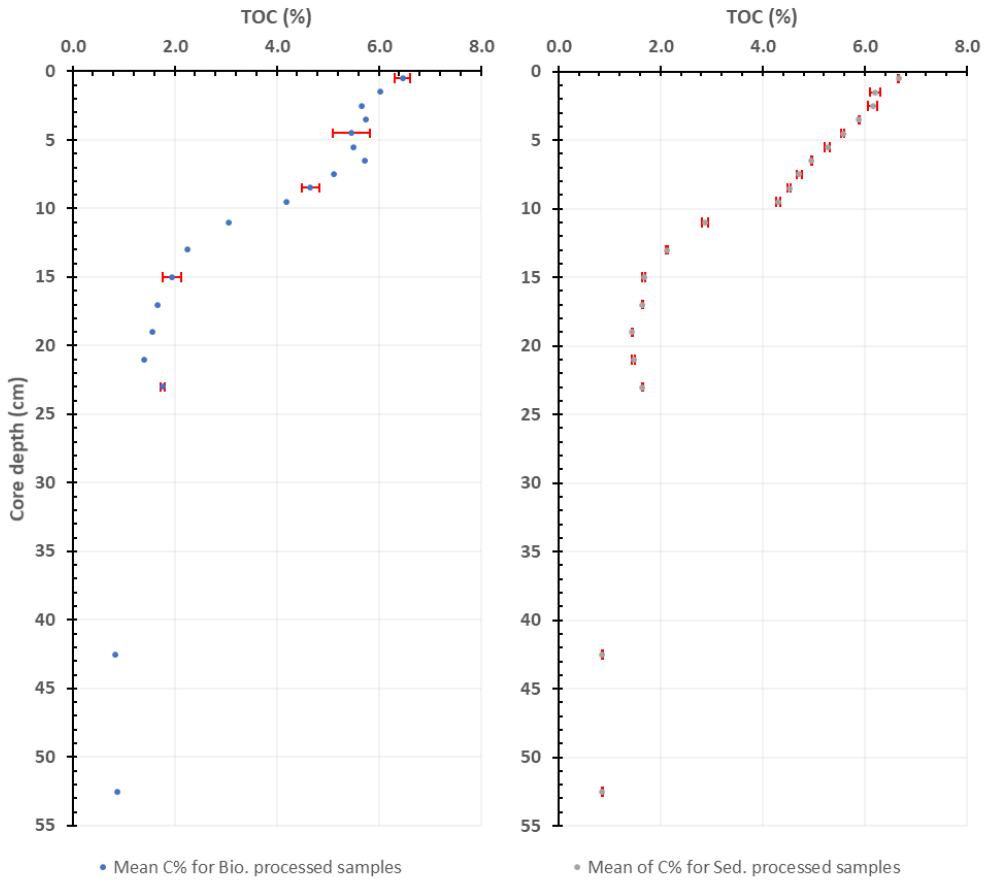

Figure 4.10 *Analysis of UiO Biology department processed samples (left) for TOC (%) and Geosciences department processed samples (right) with error bars (red) showing deviation from the mean for replicates (V-60-A17 core). Note that replicates were only available for 5 core depths for the Biology department processed sample.*

One parameter where significant variation did exist in the TN analyses was with the data for nitrogen (N) % (figure 4.11). Here the mean was calculated for data obtained from both the UiO Biology dept. and Geosciences dept. and plotted with standard deviation (error bars). In this instance, the greater variation came from the Geoscience data, as many values coming from the deeper core samples were abnormally low (including 0.0 readings), resulting in unrealistic C:N ratios (values ranged from a low of 9.08 to a high of 40.36) for this data set.

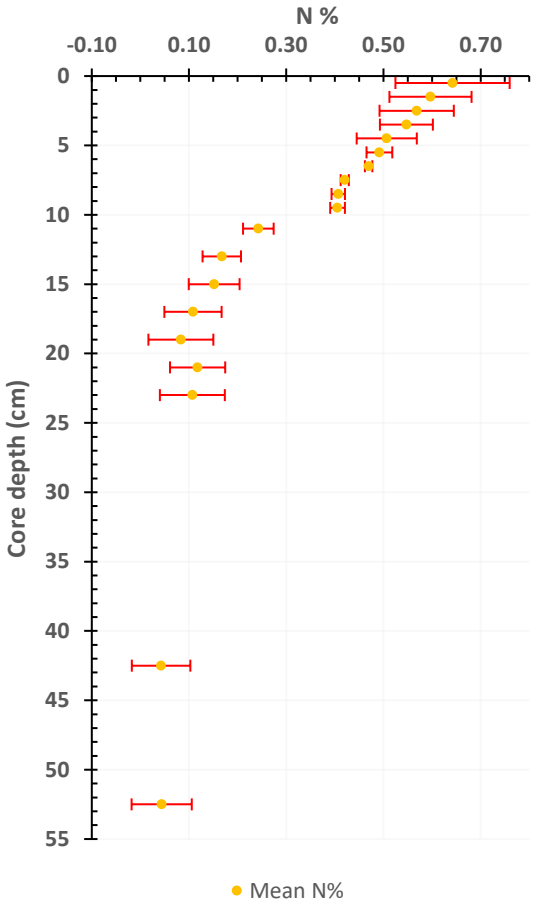

Figure 4.11 *Mean of N % for UiO Biology dept. and Geosciences dept. processed data along with standard deviations (error bars in red) showing higher uncertainty for V-60-A17 core.*

4.5 Micropaleontology

Diversity indices $H'_{(log2)}$ and ES_{100} for the V-60-A18 core showed a relatively homogeneous pattern throughout the core and remained consistently in good EcoQS with the exceptions of 4.5 and 9.5cm core depth where values for both indices dropped to moderate (figure 4.12).
The number of foram tests picked per gram of dried sediment varied up core, beginning on the low end (146/g dried sediment) at the bottom of the core, then increasing to a maximum of 694/g dried sediment at 3.5cm core depth before decreasing again toward the top of the core (figure 4.12). The number of species present, did not change as dramatically with core depth (figure 4.12) and this suggests domination by only a few species.

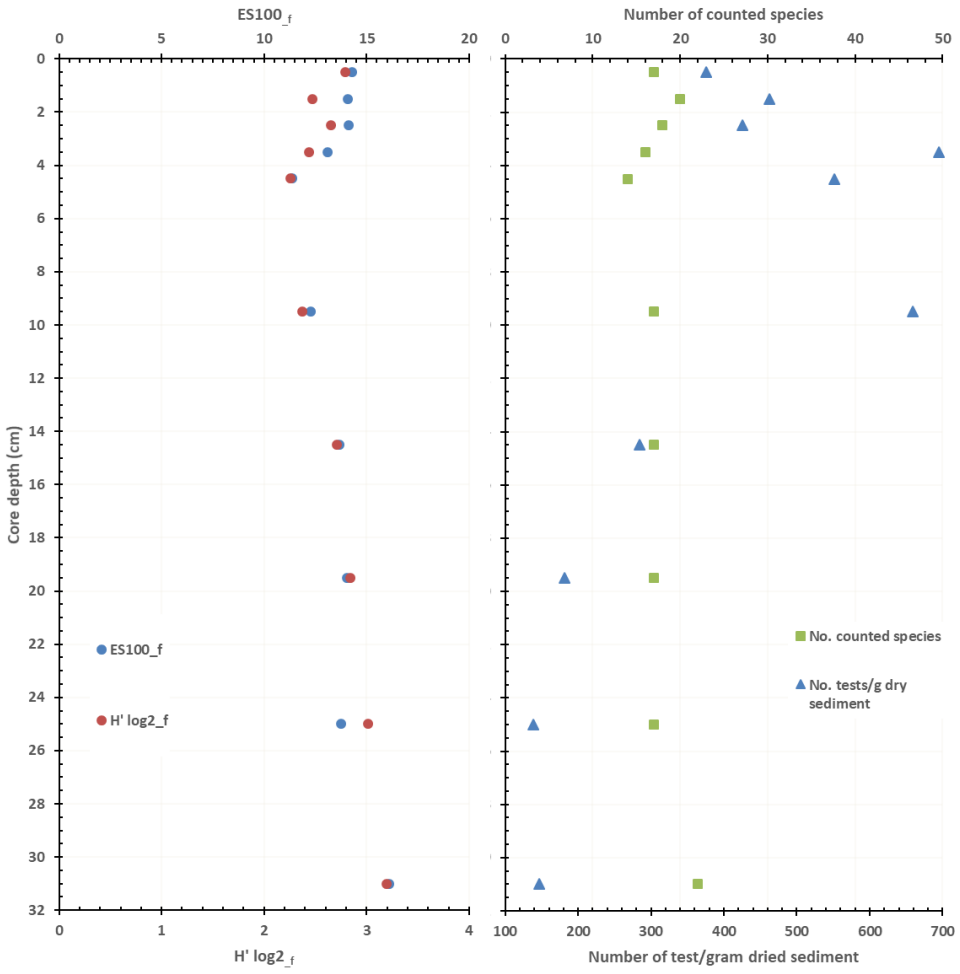

Figure 4.12 *Diversity indices ES_{100} and $H'_{(log2)}$ (left) for the V-60-A18 core showing relatively homogeneous pattern throughout the core. Number of counted species (right) shows little change throughout the core and when compared with the trend for number of tests per gram dried sediment that follows patterns seen in other variables and suggests domination of only a few species. Approximately 200 tests were picked per sample.*

The dominant species for most of the core was the calcareous foraminifera *Bulimina marginata* accounting for close to or just over 50% in nearly all analyzed samples except in 25 and 31cm core depth. At 25cm core depth the dominant species is *Nonionella iridea* (22.2%) and at 31cm core depth *Cassidulina laevigata* as the dominant species with 25.9% (see Appendix G). Cluster analysis of similarity shows a clear division of similarity between 9.5 and 14.5cm core depth (figure 4.13). There are also subdivisions occurring between the 14.5/19cm and 25/31cm samples and a division occurring in the upper most core depth (0.5cm) visible in figure 4.13.

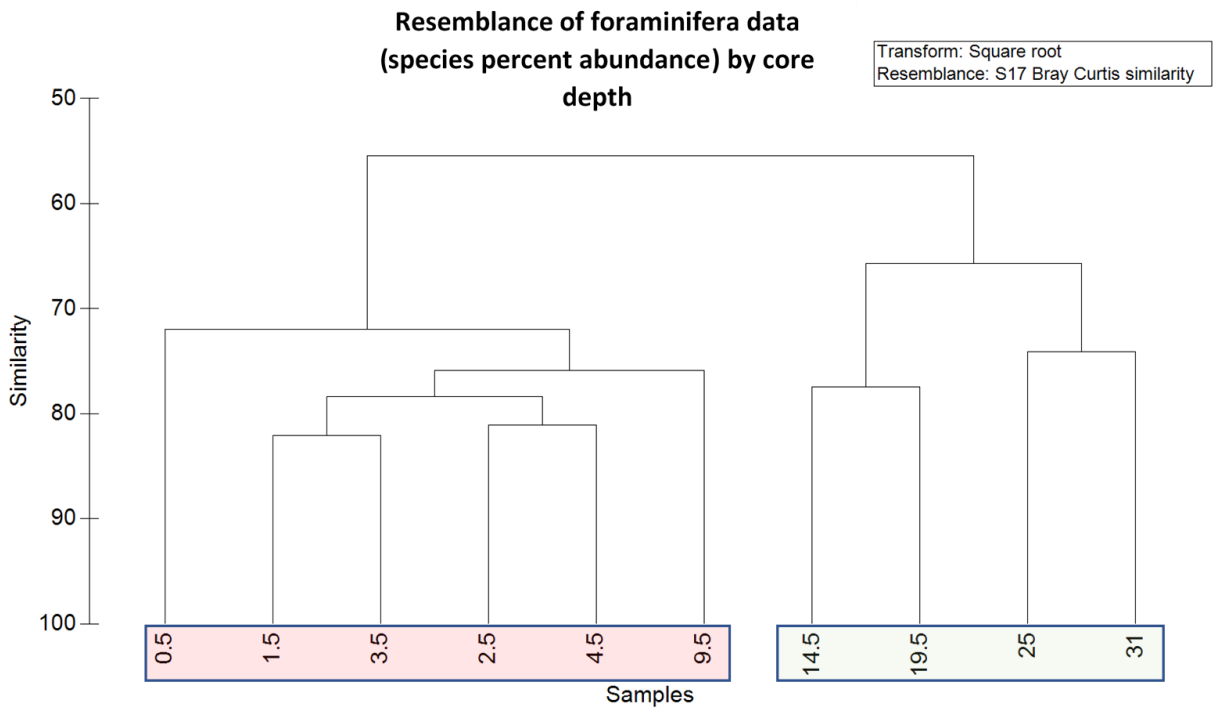

Figure 4.13 *Cluster diagram of similarity based upon relative species abundance (% in core V-60-A18). Colored boxes present major divisions in similarity.*

Foraminifera species where selected based upon ecological groupings (EG) related to the AZTI Marine Biotic Index (AMBI) for forams discussed in Alve et al. (2016) and plotted on an MDS diagram. Two EG 1 species (*Cassidulina laevigata* and *Hyalinea balthica*), one EG 3 species (*Bulimina marginata*) and one EG 5 species (*Stainforthia fusiformis*) were selected and plotted as shown in figure 4.14. The abundance of these species behaved as would be expected for their ecological groupings through the core with those in EG1 disappearing up core, *Bulimina marginata* reaching a maximum approximately mid core (as shown at 9.5cm core depth) and *Stainforthia fusiformis* increasing in abundance moving up core.

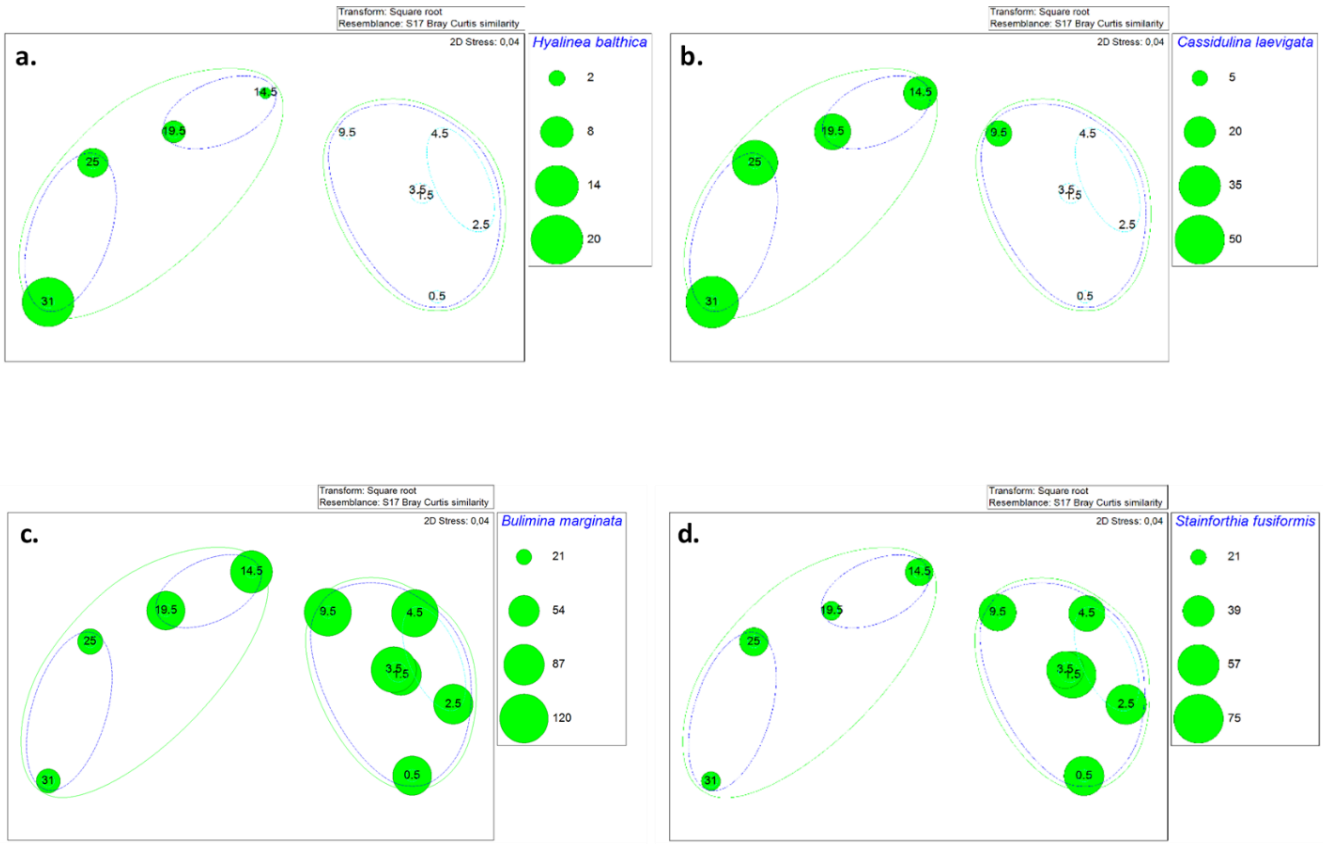

Figure 4.14 a.-d *Two-dimensional MDS-plots based on relative abundance showing the distribution of selected species in core V-60-A18.* ***a.*** *and* ***b.*** *show EG 1 species (Hyalinea balthica and Cassidulina laevigata respectively),* ***c.*** *shows EG 3 species Bulimina marginata and* ***d.*** *shows EG 5 species Stainforthia fusiformis. Numbers in the bubbles indicate the core depth of the sample.*

It was possible to view the relationships discussed above simply through the picked faunal slides (figure 4.16). At the 30-32cm core depth *Cassidulina laevigata* is still in abundance with less *Stainforthia fusiformis*. In comparison in the 0-1cm core depth *Stainforthia fusiformis* and *Bulimina marginata* dominate.

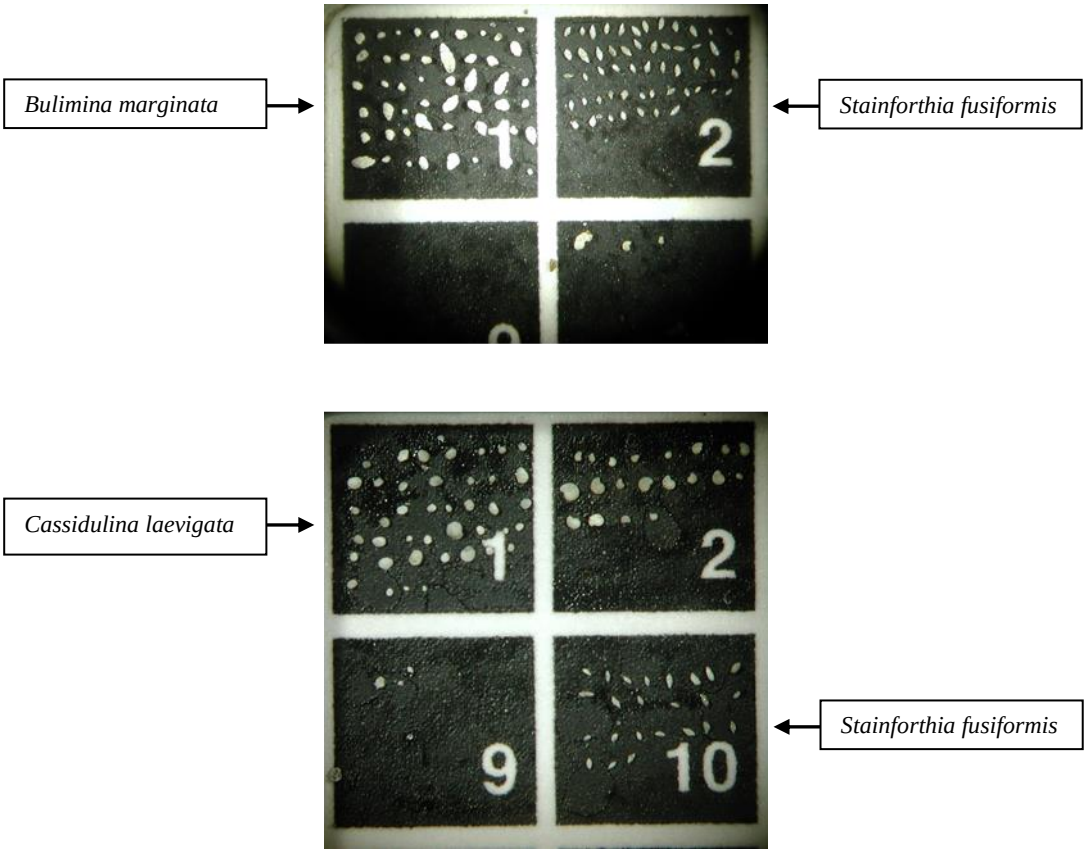

Figure 4.15 *Image of sections of picked faunal slide for 0-1cm core depth (top) and 30-32cm core depth (bottom). Note the change in relative abundance of Stainforthia fusiformis from the bottom of the sediment core (section 10 bottom image) to the top (section 2 top image). Cassidulina laevigata (section 1 bottom image) has vanished at the top of the core while numbers of Bulimina marginata (block 1 top image) are still strong. Images are of 15x magnified faunal slides and each block is approximately 5mm square.*

4.6 Circulation currents in the VEAS discharge area

Unfortunately, due to circumstances outside of the control of the author, finalized results are not available for circulation patterns in the VEAS discharge area. While unfortunate, a preliminary glimpse at the data did not reveal data inconsistent with what is know concerning the currents in this area and supported the work done in preparation for the building and operation of the VEAS plant shown in Bjerkeng et al., (1978).

Figure 4.16 shows a dye drop experiment from that report that parallels preliminary data from the P1 and P2 current meters. There is a current moving generally toward the southeast that varies in strength with depth (decrease in current as you move toward deeper depth,). Preliminary results show negligible current at deepest sample depth (approximately 85m).

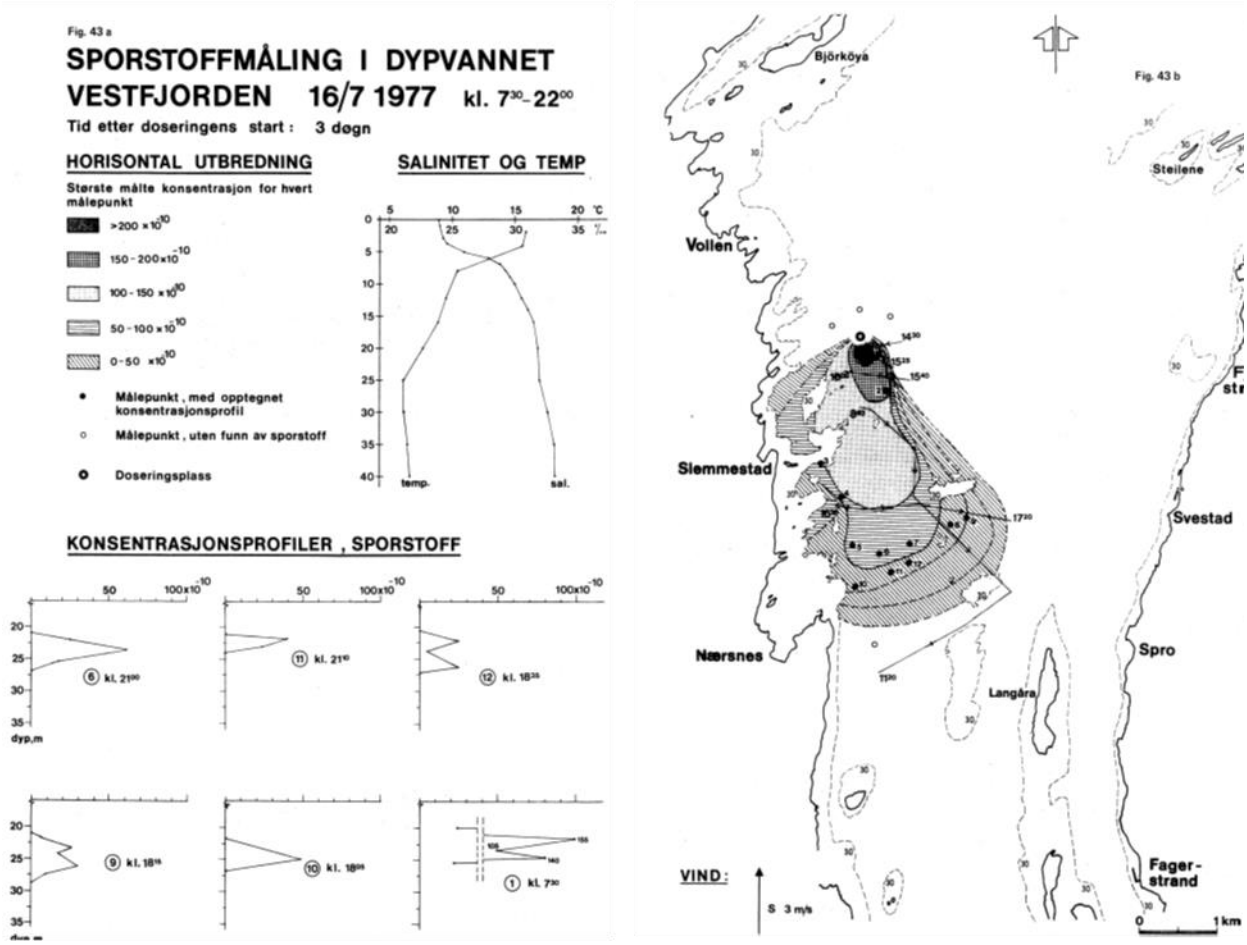

Figure 4.16 *Figure from a dye drop experiment conducted in 1977 in preparation for the building and operation of the VEAS wastewater treatment plant. Image of dye plume measurements after 3 days' time showing general current trending toward the south-southeast (Bjerkeng et al., 1978).*

5 Discussion

5.1 Validation of 2017 core results

In comparing the analyses from the 2017 core to the one that was collected at the same site in 2018 it became clear that outside of the general trends evident throughout the inner Oslofjord (better environmental quality deep in the core, worsening as you move up core before improving toward the surface) these two cores had little in common. Values for most analyses were far higher for the 2017 core than in the 2018 core. This occurred to such an extent that it facilitated the need to retest the 2017 core and analyze the methodologies used in order to gain some

understanding of the factors impacting the tests and how they might come to bear on assigning environmental quality status.

In figure 5.1 results of four supporting criteria (Cu, Cd, Zn, TOC) for determining the environmental quality status are plotted from three analyses runs (fall 2017 (V-60-A17), fall 2018 (V-60-A17_repeat), May 2018 (V-60-A18)) of samples from the same location. All values trend dramatically higher for the 2017 data, even when retested. This includes the mean values for all retests completed as part of the analysis of methodology (Section 3.7 and 4.4). These values would not impact the results sufficiently to bring the 2017 core back into range of the values of the 2018 core and as such are not part of the graphs in figure 5.1.

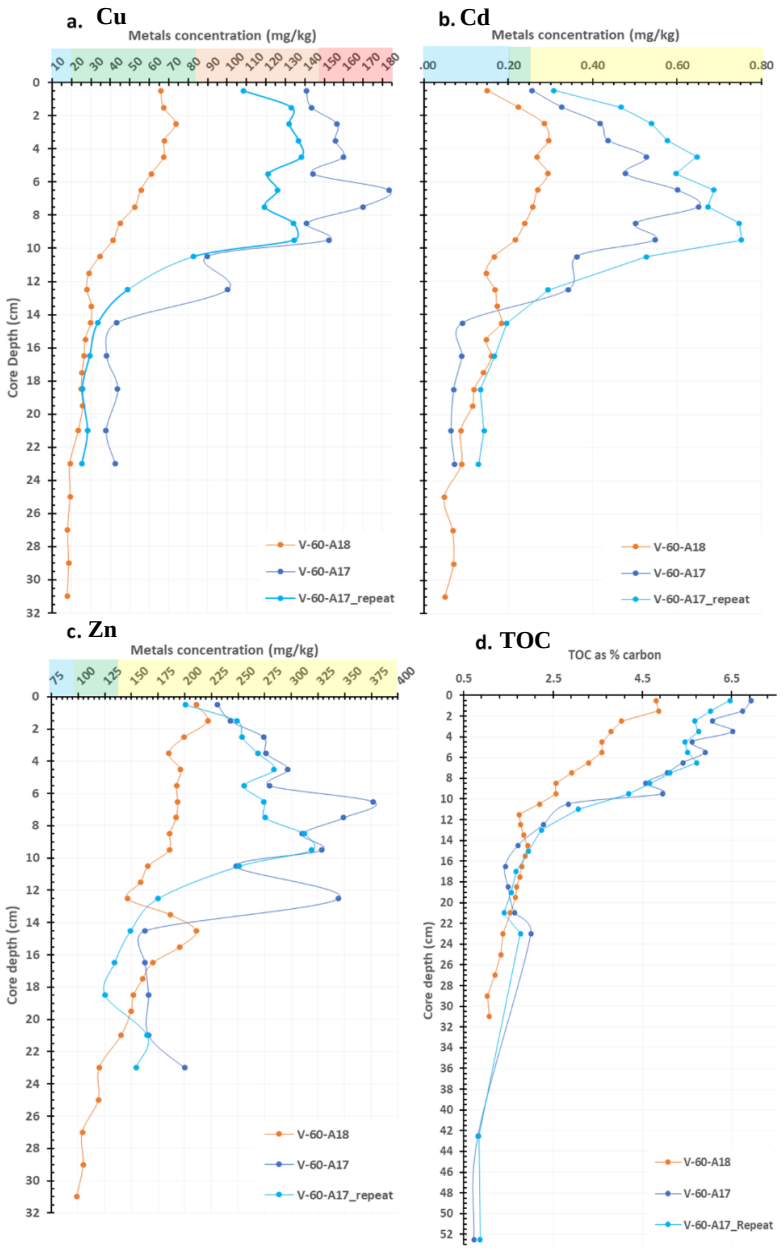

Figure 5.1 a.-d. *Comparison between 2017 core and 2018 core from the same location;* ***a.*** *Cu,* ***b.*** *Cd,* ***c.*** *Zn and* ***d.*** *TOC. TOC graph (**d.**) includes data from the Abdullah core sample collected (42.5 and 52.5cm core depth). Colored bars at top of graphs (Cu, Cd, Zn) indicate environmental quality boundaries as shown in table 1.*

Comparison of the micropaleontology data for these cores finds the differences are not as substantial as those mentioned above, and respective of the diversity indices (H'_{log2} and ES_{100}) there is little difference moving up core (figure 5.2). For the ES_{100} index, the 2017 core has overall better status than the 2018 with no areas identified as moderate, and two core depths showing very good status. For the H'_{log2}, the 2017 core is very similar to the 2018 core, but with

moderate EcoQS section seeming to trend further up core (2.5cm core depth is now in moderate status). Status boundaries for the surface core depths for both agree on good EcoQS at this level for both ES_{100} and H'_{log2}.

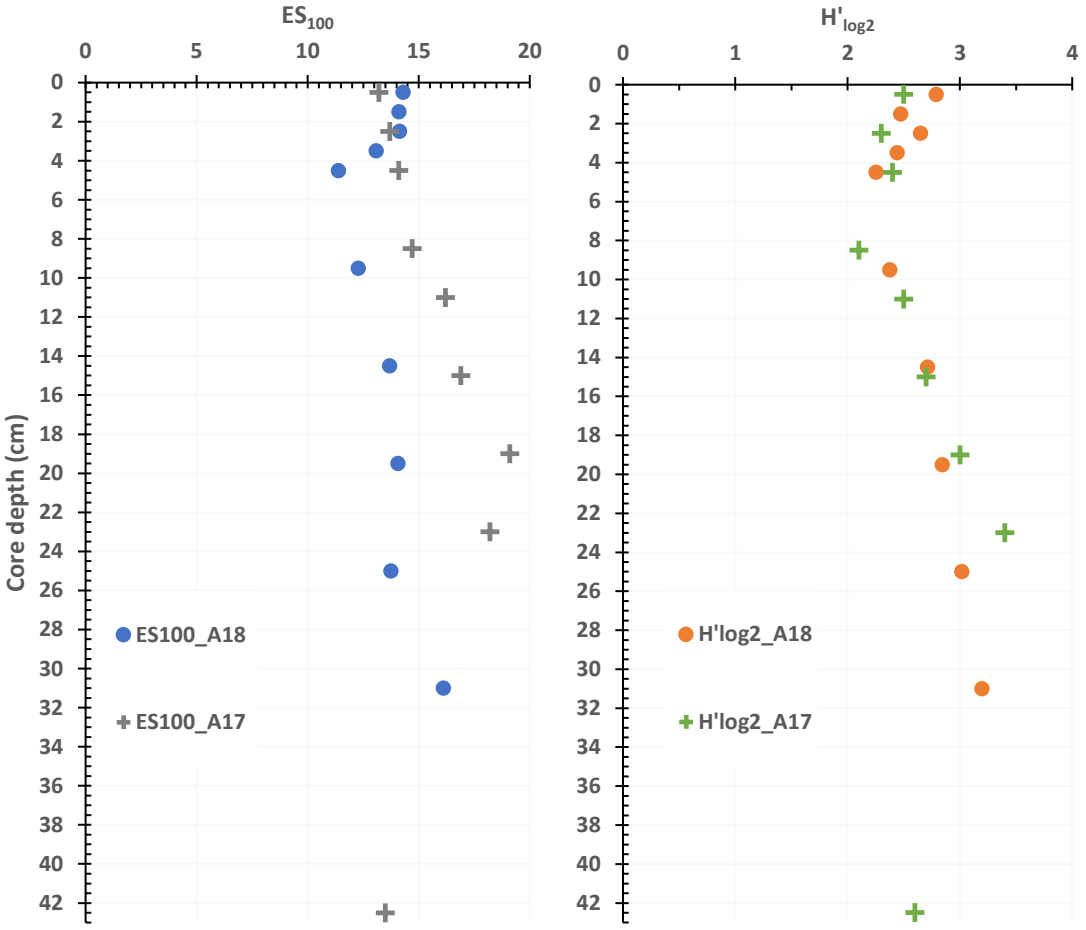

Figure 5.2 *Comparison of diversity indices ES_{100} (left) and H'log2 (right) for 2017 core (V-60-A17, A17 in legend) and 2018 core (V-60-A18, A18 in legend). Note the relative similarity between the cores unlike what is shown for supporting parameters in figure 5.1.*

Comparison of both cores with cluster analysis of similarity shows similar groupings (figure 5.3). This highlights not only the biological similarity of the cores, but also that the changes in environmental quality visible in the cores occur at a similar time frame (core depth) in each, particularly deep core (areas below 14.5cm core depth), mid core (from 2.5-14.5cm core depth) and surface (0.5cm core depth).

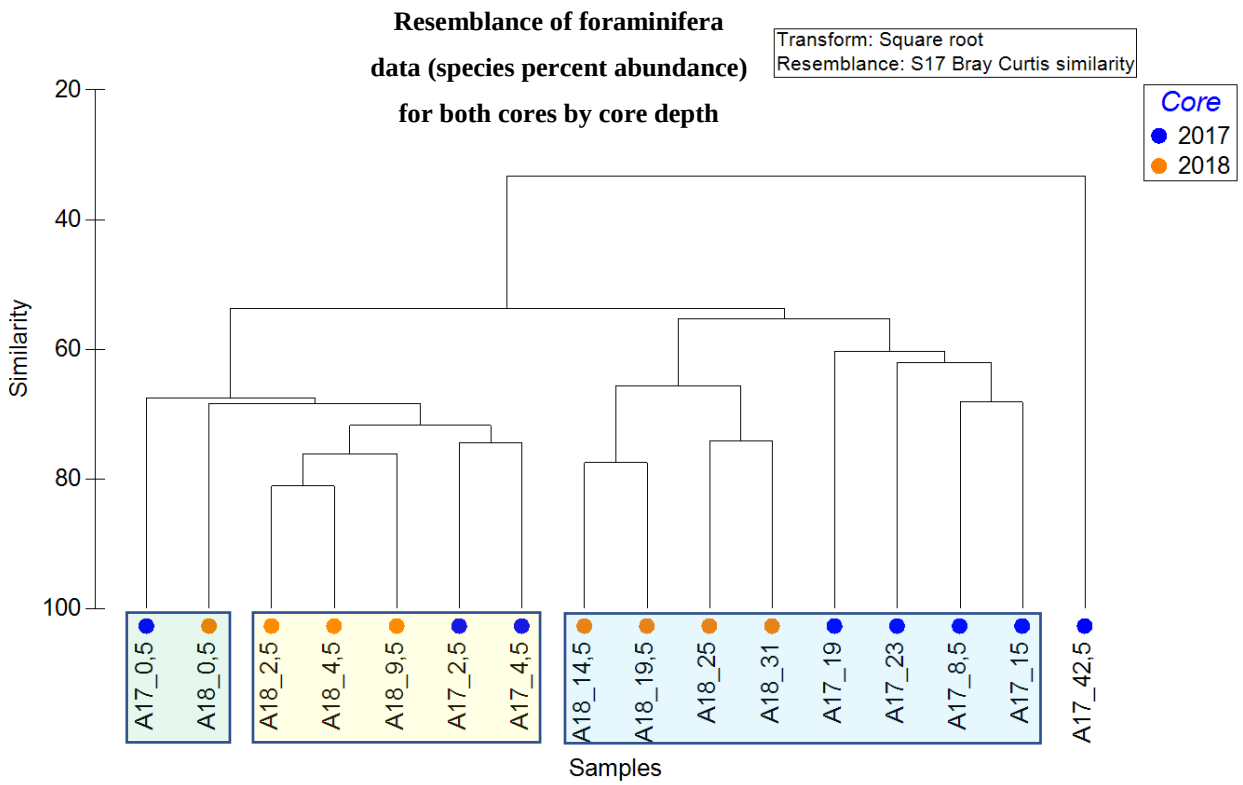

Figure 5.3 *Cluster diagram of similarity between 2017 (V-60-A17, A17)and 2018 (V-60-A18, A18) cores based upon core depth (value at end of sample name in cm). Colored boxes show major divisions in similarity. Note that sample A17_42.5 is from the Abdullah core and is included to highlight the differences at this core depth.*

When making these comparisons, it is important to note that there is some difference in the micropaleontology analysis of these cores both in resolution (shown to some degree in figure 5.2) as these cores were sliced at different intervals and in terms of the picking of forams different size fractions were analyzed (2017: 125-500µm; 2018: 63-500µm). Therefore, these analyses are not directly comparable, but nonetheless show the similarities in the overall trend. Based upon the differences discussed above, it is difficult to say with certainty that these cores came from the exact same location regardless of the coordinates shown on the GPS system in use on the research vessel. However, even accounting for all potential sources of error (GPS accuracy, deflection of the cable and instrument due to current at depth, drifting of the vessel) it is still probable that the 2018 core was collected not more than 15-20m from the original location. Given the differences that are seen above, it is clear that environmental conditions in the area and perhaps in the inner Oslofjord in general, are quite patchy. Consideration of this

patchiness is an important consideration for planning testing regimes for establishing overall EcoQS.

Additionally, analyses of the methodologies used for TOC and metals revealed that additional care and planning should be taken when preparing samples that will be used as supporting parameters for determination of environmental quality. Deviations in some core sections were enough to change (downgrading or improving) the environmental quality of the parameters tested for. Both random and systematic errors can be observed in the analysis discussed in Section 4.4. Time is also likely a factor when planning for and preparing samples, as testing revealed increased variation in data when accounting for all other variables except time. This may limit the viability of testing samples long after collection. Further studies should be completed to investigate the role of time as a variable for analysis, along with ways to limit the impact of errors in methodology.

5.2 Correlation with other work in the inner Oslofjord

Other studies have been conducted in the inner Oslofjord that relate to the work I have completed (Fagrådet, 2017; Hess et al., 2014; Lepland et al., 2010; and similar). However, most work is located either in the Bekkelag basin or far from the VEAS area. It is still important to look at how this study fits into the larger body of knowledge concerning the environmental quality status development of the inner Oslofjord.

Lepland et al. (2010) looked at the chronology of metals contamination (Al, Cd, Cu, Fe, Hg, and Mn) in sediments in the inner Oslofjord (Oslo harbor). Through radiometric dating of the cores collected they found chronological boundaries for peak metals contamination, specifically 1955-1960 for Cd and approximately 1970 for Cu reflecting high anthropogenic discharge periods (Lepland et al., 2010). In comparing the data collected for this thesis, it is clear that the new cores collected (V-60-A18 and V-71-NW2) do not match this convention (figure 5.4) with maximum values for these metals happening at a far later date (approximately 2009 for Cu and 1988 for Cd). This may be due to bioturbation especially for the V-71-NW2 core as core notes mention signs of this down to 14.5cm core depth (Appendix A).

There is, however, stronger correlation between the V-60-A17 core and chronographic maximum values for Cu (approximately 1979) and Cd (approximately 1967) discussed in Lepland et al. (2010). Additionally, the overall trend for the sediment accumulation rate is comparable

between the cores, though the magnitude of accumulation is less for the new cores and slightly out of phase with the Lepland et al. data (a large spike in sediment accumulation of 3 kg m^{-2} y^{-1} seen in 1954 seems to correlate to a spike of 1.76 kg m^{-2} y^{-1} in 1949) (figure 5.4).

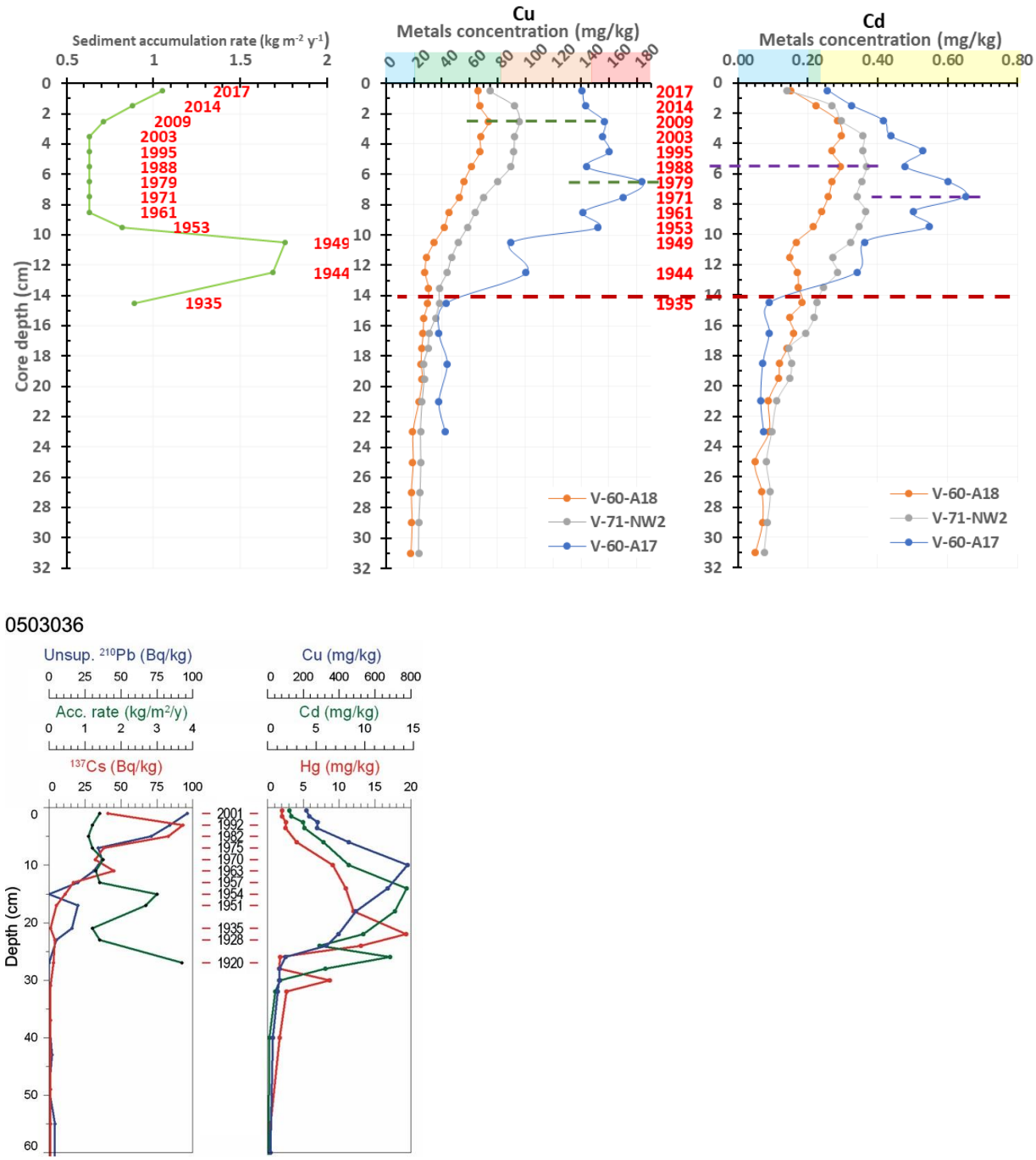

Figure 5.4 *Comparison of chronostratigraphic maximum values for metals (Cu: green dashed line and Cd: purple dashed line) between cores collected in the VEAS area in 2017 and 2018 (top) and site 0503036 from Lepland et al. (bottom) (2010). Sediment accumulation rates are also shown (far left, top: V-60-A18 and bottom: 0503036). Red dashed line (top) indicates approximate time of change from*

what might be called "reference" conditions. Colored bars at top of graphs (Cu and Cd; top) indicate environmental quality boundaries as shown in table 1.

Rational for these differences is likely the difference in location as the Lepland et al. data was collected in an area that was presumably closer to the actual source of contamination (Oslo harbor). As such, the magnitude of the values is greater for the Lepland et al. data and sediment transport would have delayed deposition in the area near VEAS resulting in the time lag shown in figure 5.4.

The consistently later peaks present in the 2018 cores (V-60-A18 and V-71-NW2) is more difficult to account for. It is possible that this is an artifact related to VEAS (though it might be expected in the V-60-A17 core as well, but the patchiness discussed in section 5.2 might explain this) or related to bioturbation or some other redistribution of the sediment.

Based upon the work of Croudace and Cundy, (1995) and Zhang et al. (2015) it is insufficient to look at the metals concentration data without also looking at the sedimentation accumulation rate as this can have significant effect on concentration. High sedimentation rates can dilute concentrations of metals and vice versa (Zhang et al., 2015). Sediment accumulation rate for the core is relatively stable with the exception of the period between 1961 to 1935, though the change in this period is not as great as in the Lepland et al. core (figure 5.4). Plots of the flux (calculated by sediment accumulation rate x metals concentration) for Cu and Cd (figure 5.5) reveal that the increased sediment accumulation rate seen for this period is likely responsible for slight dip in concentration for these metals observed during the same time period. Analysis of the flux up core (top 4cm core depth) for these metals shows that the sediment accumulation rate for Cu might also be responsible for lower concentrations at this level.

Dolven et al. (2013) looked at foraminifera as a way of determining past ecological status for sites in the inner Oslofjord. Of the sites discuss, Dk2 is the closest site to the VEAS study area though at 99m depth. ES_{100} and H'_{log2} from a core sampled at this site have high EcoQS (25.59 for ES_{100_f} and 3.94 for H'_{log2_f} indices at 6.5cm core depth, relative age 2009) compared to good EcoQS (14.14 for ES_{100_f} and 2.65 for H'_{log2_f} at 2.5cm core depth, relative age 2009) for the V-60-A18 core location. Dolven et al. also found greater numbers of species at this location/core depth (38 species at Dk2 compared to 18 at V-60-A18) and slightly greater numbers of tests (232 at Dk2 to 203 at V-60-A18). Again, this site (Dk2) is located away from the VEAS discharge and in deeper water which may account for some of the discrepancy.

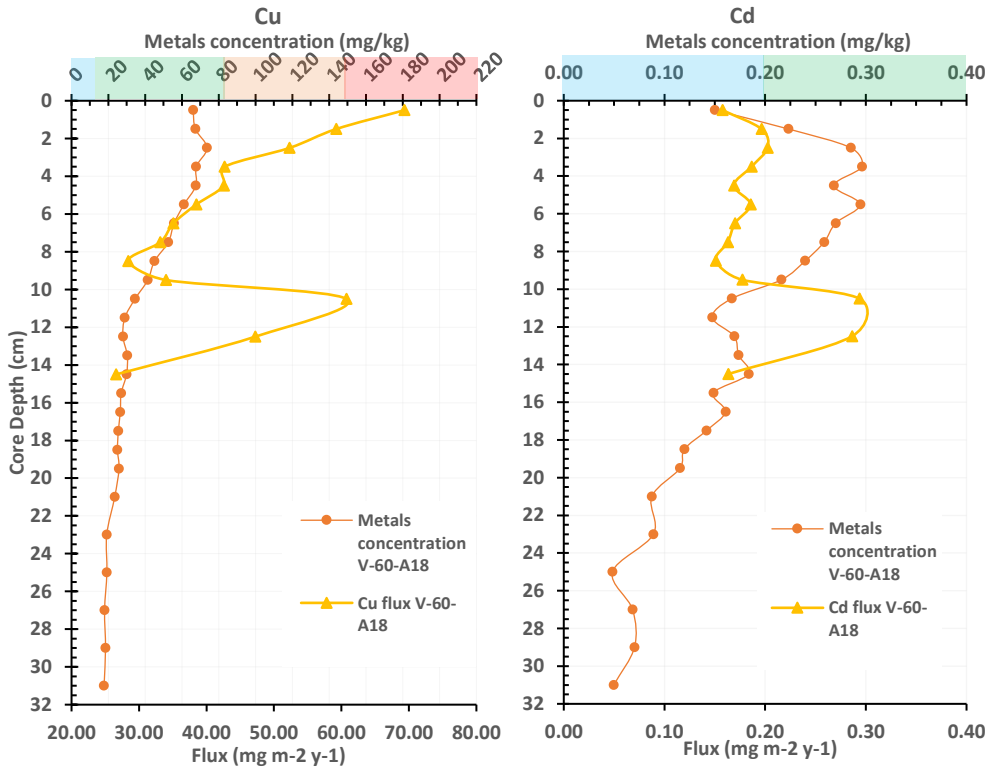

Figure 5.5 *Flux based upon sediment accumulation rate for Cu (left) and Cd (right) for the V-60-A18 core. High sediment accumulation rate seen between 10 -15cm core depth (figure 5.4) appears to be responsible for the slight decrease in concentration observed during the same period. Colored bars at top of graphs indicate environmental quality boundaries as shown in table 1.*

5.3 VEAS impact on the area

As shown in figure 5.6 it is clear that VEAS and other wastewater treatment facilities have had an impact on improving the overall quality of the inner Oslofjord. As phosphorus and nitrogen levels have decreased, so have incidents of eutrophicating algal blooms and in response, oxygen levels have increased (figure 5.6). VEAS is having an impact locally as well, with concentrations for metals declining after the plant became operational (1982, approximately the 5.5cm core depth), correlating well with VEAS's own values for these metals (figure 2.9, figure 4.6 a.-d.).

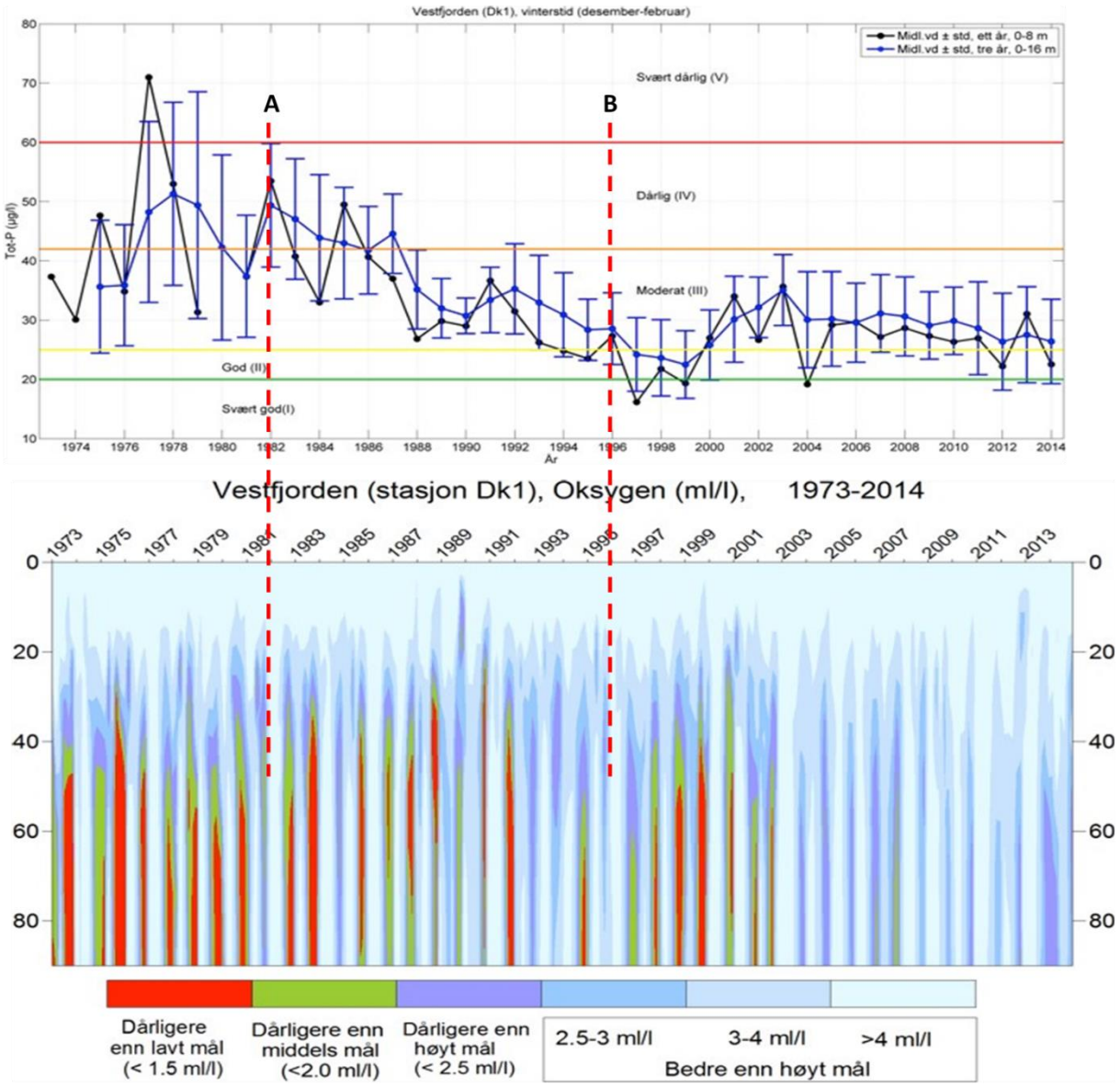

Figure 5.6 *Total phosphorous (Tot-P) in µg/L (top) and oxygen in mL/L (bottom) for station Dk1 in Vestfjorden (years 1973-2014) inner Oslofjord from Berge et al (2015). Dashed red line* ***A****, shows the beginning of operation of the VEAS plant. Total phosphorous begins to decrease considerably (top) and oxygen levels improve (bottom) with more oxygen at depth. Dashed red line* ***B****, shows date when VEAS began limiting nitrogen discharge leading to greatly improved oxygen levels in Vestfjorden (bottom).*

One parameter where it is more difficult to draw a positive correlation is with the input of organic carbon. TOC for the study area is shown to be increasing (figure 4.4) which is not consistent with the discharge values presented by VEAS (figure 2.8). Figure 5.7 shows these graphs side by side synced by date. The opposite trends between them seem to suggest another source of organic carbon for this part of Vestfjorden or another process at work. This other

process might be diagenetic in nature either through action on the organic matter itself (protection/competition) or acting through processes impacting remineralization and burial (Arndt et al., 2013; Burdige, 2007). Additional support for these hypotheses lies in the higher values shown for supporting factors (TOC – figure 4.4, metals figure 4.6 a.-d.) from the V-71-NW2 location that is approximately 300m NNE of the discharge network. Given what is known about the currents in this area, it is unlikely that VEAS is responsible for these values, though it could be responsible for the delayed peaks shown at the V-60-A18 data.

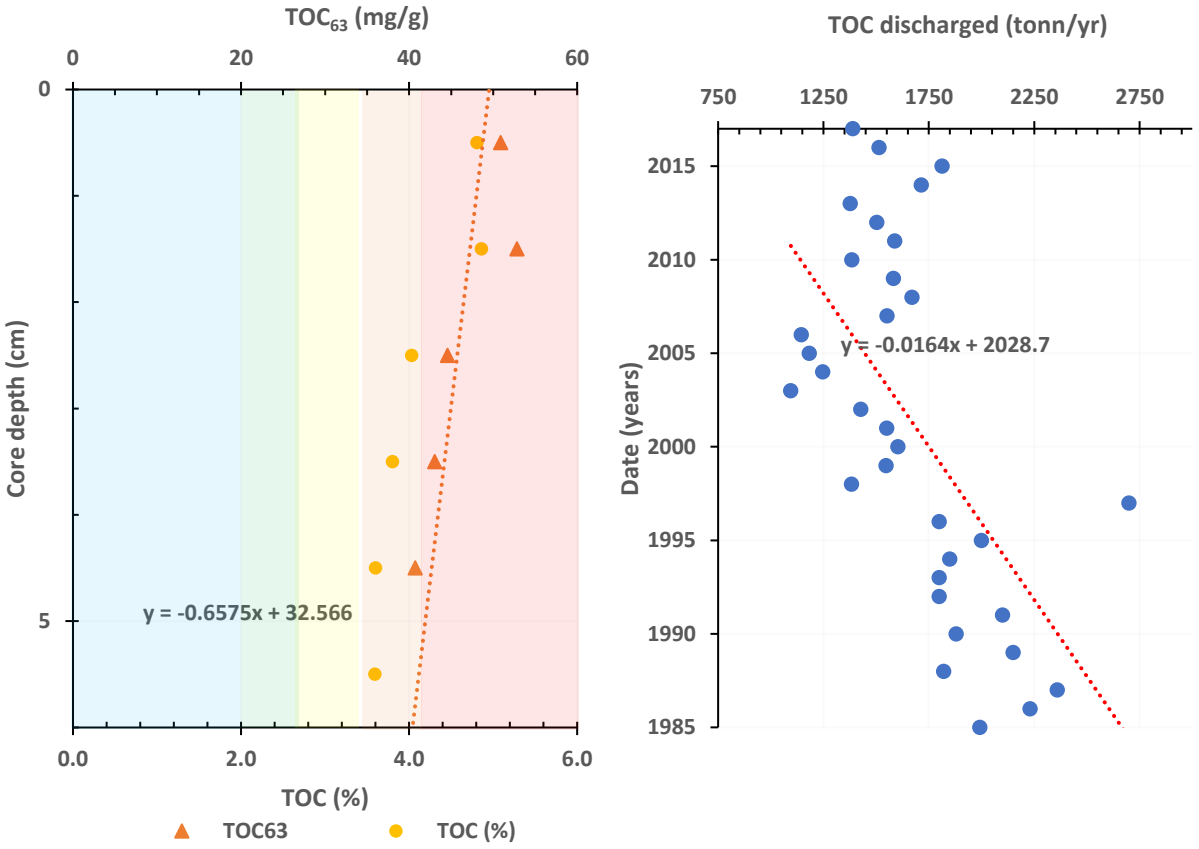

Figure 5.7 *TOC as TOC_{63} and TOC % for V-60-A18 core (left) and TOC discharged by VEAS in ton/year (right). Core depth has been synced with dates from historic data from VEAS (core depth of 6cm is approximately 1985 based upon radiometric dating). Colored banding (left) is for environmental quality boundaries for TOC_{63} from Klassifisering av miljøtilstand i vann: Økologisk og kjemisk klassifiseringssystem for kystvann, grunnvann, innsjøer og elver (2018) with TOC_{63} values calculated based on data for 63-500µm fraction from foram data.*

It is important to note that the reduced values of these supporting factors work to downgrade the overall EcoQS for the area from the good status present from the foraminifera analysis of diversity indices ES_{100} and H'_{log2} in section 4.5 to moderate/not good based upon values present for Zn.

5.4 Efficacy of foraminifera as biological indicators

Several studies such as Alve (2000), Alve et al. (2009) and Bouchet et al. (2012) have looked at the efficacy of using benthic foraminifera as biological quality indicators from marine environments with the data from this study supporting this approach. As shown in table 3, when paired with the radiometric dating of the core, the ES_{100} and H'_{log2} diversity indices seem to tell the story of the Oslofjord present in other studies and in other supporting data shown in this thesis (figures 5.2, 5.4) that is; a change from good to moderate EcoQS occurring around 1920-1935 that improves starting in the mid 1990's.

Table 3 *Diversity indices ES_{100_f} and H'_{log2_f} along with the Norwegian Quality Index (NQI_f) and the mean normalized Ecological Quality Ratio (nEQR) for the V-60-A18 core by core depth correlated with radiometric dating. Note that purple shaded dates are extrapolated based upon regression trend line shown in figure 4.2 and that _f indicates colored shading based upon foram boundaries for these indices.*

Core depth (cm)	Date	ES_{100_f}	H'_{log2_f}	NQI_f	Mean $nEQR_f$
0.5	2017	14.29	2.79	0.46	0.65
1.5	2014	14.10	2.47	0.44	0.62
2.5	2009	14.14	2.65	0.45	0.63
3.5	2003	13.09	2.44	0.44	0.60
4.5	1995	11.38	2.25	0.42	0.51
9.5	1953	12.28	2.38	0.45	0.57
14.5	1935	13.69	2.71	0.50	0.67
19.5	1880	14.06	2.84	0.52	0.69
25	1860	13.75	3.02	0.51	0.69
31	1820	16.11	3.20	0.58	0.77

NQI (table 3) seems to paint a more nuanced picture of EcoQS in this area with 31cm core depth equating to "high" status and a return to "moderate" status occurring in 2014 (1.5cm core depth) based upon boundaries put forth in Alve et al. (2019). The change in 2014 would be in keeping with the algal bloom reported by Fagrådet for vann og avløpsteknisk samarbeid i indre Oslofjord (2014) and suggests that this index may be more sensitive to ecological changes than other indices. The high status present at 31cm core depth may likely be showing true "reference" conditions at this depth.

As seen in table 3, nEQR reflects similar EcoQS to the ES_{100} and H'_{log2} indices and loses the features of the NQI. As ES_{100} is overrepresented in the mean nEQR (appearing both in the

nEQR for ES_{100} along with the NQI calculations) this is not surprising and might be a consideration when utilizing this index.

Additionally, core data supports the work done by Alve et al. (2016) related to Foram-AMBI. As shown in figure 4.15, patterns of faunal succession are visible in the core and are likely related to TOC values present in the core at these depths. When selected species abundances (based upon ecological groups) are plotted against TOC there is a strong degree of confidence (R^2) with the trend lines (polynomial regression). These trends correspond well with those shown in Alve et al. (2016, figure 2) for response to environmental stress (TOC) for members of specific ecological groups.

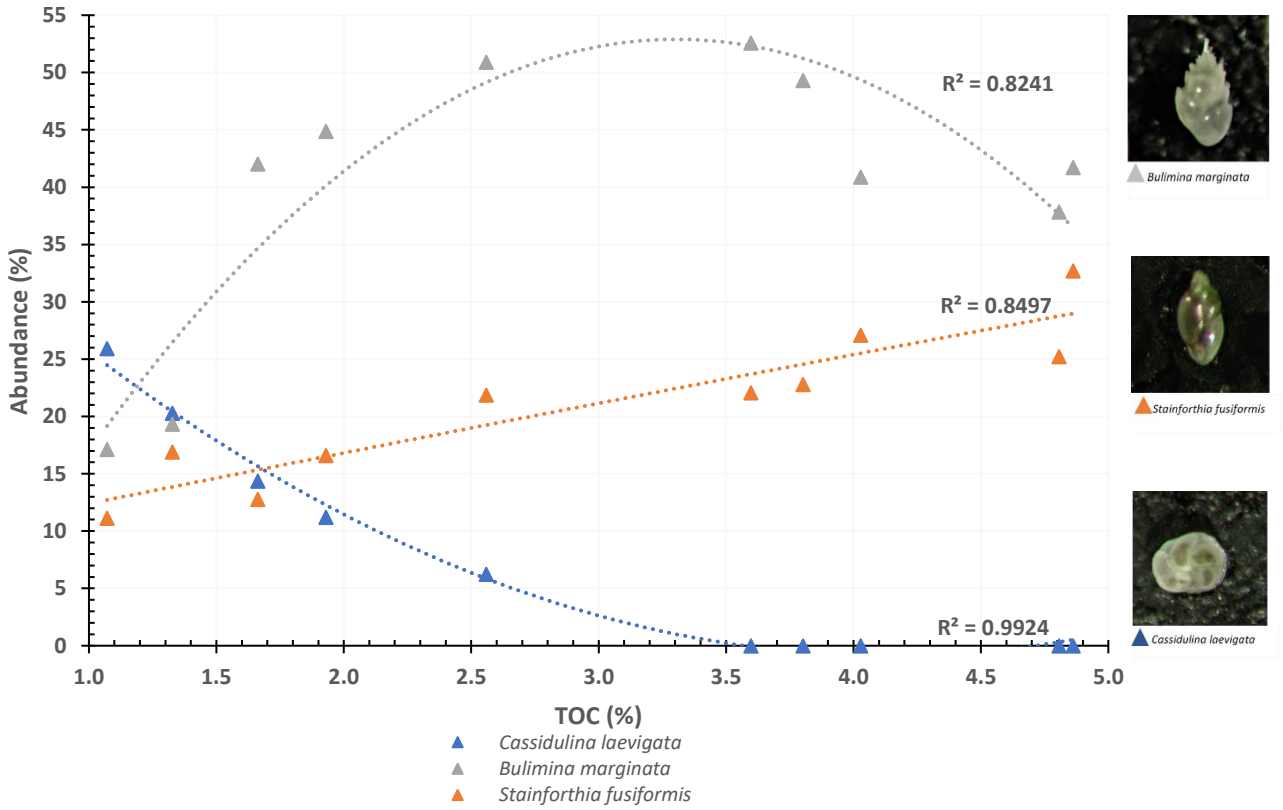

Figure 5.8 *Relationship between abundance (%) and TOC (C %) for EG 1 species (Cassidulina laevigata), EG 3 species (Bulimina marginata) and EG 5 species (Stainforthia fusiformis). Trendlines (polynomial regression) match patterns discussed in Alve et al. (2016). Inset images of species taken at 110x magnification from picked faunal slides of V-60-A18 core.*

6 Conclusions

- It is not possible based upon the data gathered from the V-60-A18 core to confirm the values present in the core collected at the same location in 2017 (V-60-A17). This is due to the patchy nature of this area (as observed from the comparison of the data) and the higher overall values confirmed with repeated testing of the V-60-A17 core. Additionally, boundaries for the biological and chemical parameters for determining EcoQS have changed since 2017, though this would not have changed the outcome. The EcoQS is classified as not good for both years, though Cu is the driving supporting chemical parameter for the 2017 core and Zn is driving supporting parameter for the 2018 core. Biologically there is little difference evident between the cores based upon micropaleontological analysis.
- The overall trend observed in the geochemical analysis is consistent with those observed at other sites throughout the inner Oslofjord. Temporal analysis shows a proximal start (1920-1935) to the degradation of the inner Oslofjord consistent with other dated cores in the inner Oslofjord. Peaks of supporting chemical parameters for the V-60-A17 core seem to be consistent with those discussed in Lepland et al. (2010). Delayed peaks in the V-60-A18/V-71-NW2 cores may be the result of bioturbation (see Appendix A for core notes).
- It is not possible to conclude that VEAS is having an impact of the area proximal to the discharge pipes based upon the studies that have been conducted. This is due to the apparently patchy nature of the study area. Additionally, TOC seems to be increasing in the study area though it is decreasing through VEAS discharge. Chemical parameters also appear to be higher at the core collected father from the discharge outlet suggesting that some other mechanism may be responsible. It does seem clear to conclude that wastewater treatment plants like VEAS are having an overall positive impact on the ecological health of the inner Oslofjord.
- Foraminifera appear to be an effective tool in determining past and present EcoQS along with temporal changes in the environment when combined with core dating. Diversity indices (ES_{100}, H'_{log2}) for both cores (V-60-A17, V-60-A18) describe a picture of changing EcoQS consistent with other data and historical evidence throughout the inner

Oslofjord. The work of Alve et al. (2019) in setting boundaries for forams in the NQI appears to provide an even more nuanced look at this data with a tool capable of detecting environmental anomalies absent in ES_{100} and H'_{log2} indices. Limitations of this tool seem to involve the resolution that the core is sliced at, access to good dated profiles of the core, and ensuring that there are enough individual forams present at each interval to analyze with PRIMER.

- Analysis of the methodology for the geochemical parameters (TOC and heavy metals) seemed to reveal large errors present in these analyses inconsistent with what would be expected. This suggests random and systemic errors are present and must be accounted for when planning and carrying out testing regimes. It appears that time may be a factor in some instances and tests should be carried out as soon as possible from sampling to ensure good results. This may also imply a limitation to the time limit for retesting samples. Outside laboratories should be included in the testing regime (especially when results are to be used by governmental bodies for management purposes) to provide the best possible outcome.
- Due to the absence of finalized data it is impossible to determine the impact fjord circulation is playing on the discharge from VEAS. If historical discharge patterns continue to drive circulation in this area, then further research should be conducted to the area SE of the discharge area for potential changes.

References

Alve, E., 2000. Environmental Stratigraphy: A case study in reconstructing bottom water oxygen conditions in Frierfjord, Norway, over the past five centuries, in: Environmental Micropaleontology: The Application of Microfossils to Environmental Geology. Kluwer Academic/Plenum Publishers, New York, pp. 323–350.

Alve, E., Hess, S., Bouchet, V.M.P., Dolven, J.K., Rygg, B., 2019. Intercalibration of benthic foraminiferal and macrofaunal biotic indices: An example from the Norwegian Skagerrak coast (NE North Sea). Ecol. Indic. 96, 107–115. https://doi.org/10.1016/j.ecolind.2018.08.037

Alve, E., Korsun, S., Schönfeld, J., Dijkstra, N., Golikova, E., Hess, S., Husum, K., Panieri, G., 2016. Foram-AMBI: A sensitivity index based on benthic foraminiferal faunas from North-East Atlantic and Arctic fjords, continental shelves and slopes. Mar. Micropaleontol. 122, 1–12. https://doi.org/10.1016/j.marmicro.2015.11.001

Alve, E., Lepland, A., Magnusson, J., Backer-Owe, K., 2009. Monitoring strategies for re-establishment of ecological reference conditions: Possibilities and limitations. Mar. Pollut. Bull. 59, 297–310. https://doi.org/10.1016/j.marpolbul.2009.08.011

Appleby, P.G., 2001. Chronostratigraphic techniques in recent sediments, in: Tracking Environmental Change Using Lake Sediments. Kluwer Academic Publishers, Dordrecht, The Netherlands.

Appleby, P.G., Piliposian, G.T., 2019. Radiometric dating of two marine sediment cores from inner Oslofjord, Norway. Environmental Radioactivity Research Centre, University of Liverpool.

Arndt, S., Jørgensen, B.B., LaRowe, D.E., Middelburg, J.J., Pancost, R.D., Regnier, P., 2013. Quantifying the degradation of organic matter in marine sediments: A review and synthesis. Earth-Sci. Rev. 123, 53–86. https://doi.org/10.1016/j.earscirev.2013.02.008

Arnesen, V., 2001. The pollution and protection of the inner Oslofjord: redefining the goals of wastewater treatment policy in the 20th century. AMBIO J. Hum. Environ. 30, 282–286.

Baalsrud, K., Magnusson, J., 2002. Indre Oslofjord: Natur og Miljø. Bokbinderet Johnsen AS, Skien.

Bakke, T., Källqvist, T., Ruus, A., Breedveld, G.D., Hylland, K., 2010. Development of sediment quality criteria in Norway. J. Soils Sediments 10, 172–178. https://doi.org/10.1007/s11368-009-0173-y

Berge, J.A., Amundsen, R., Gitmark, J.K., Gundersen, H., Johnsen, T.M., Ledang, A.B., Lømsland, E.R., Magnusson, J., Staalstrøm, A., Strand, D., Hylland, K., Holth, T.F., 2015. Overvåking av Indre Oslofjord i 2014 (No. L.NR. 6833-2015). Norsk Institutt for Vannforskning.

Bjerkeng, B., Göransson, C.G., Magnusson, J., Baalsrud, K., 1978. Undersøkelse av alternative utslippssteder for avløpsvann fra sentralrenseanlegg vest - DEL II Figurer (Figures No. 0-132/76). Norsk Institutt for Vannforskning.

Borja, A., Franco, J., Pérez, V., 2000. A Marine Biotic Index to Establish the Ecological Quality of Soft-Bottom Benthos Within European Estuarine and Coastal Environments. Mar. Pollut. Bull. 40, 1100–1114. https://doi.org/10.1016/S0025-326X(00)00061-8

Bouchet, V.M.P., Alve, E., Rygg, B., Telford, R.J., 2012. Benthic foraminifera provide a promising tool for ecological quality assessment of marine waters. Ecol. Indic. 23, 66–75. https://doi.org/10.1016/j.ecolind.2012.03.011

Bray, J.R., Curtiss, J.T., 1957. An Ordination of the Upland Forest Communities of Southern Wisconsin. Ecol. Monogr. 27, 325–349. https://doi.org/10.2307/1942268
Burdige, D.J., 2007. Preservation of Organic Matter in Marine Sediments: Controls, Mechanisms, and an Imbalance in Sediment Organic Carbon Budgets? Chem. Rev. 107, 467–485. https://doi.org/10.1021/cr050347q
Clark, K.R., Gorley, R.N., 2006. Primer v6: User manual/tutorial.
Coccioni, R., 2000. Benthic foraminifera as bioindicators of heavy metal pollution: A case study from the Goro lagoon (Italy), in: Environmental Micropaleontology: The Application of Microfossils to Environmental Geology. Kluwer Academic/Plenum Publishers, New York, pp. 71–103.
Croudace, I.W., Cundy, A.B., 1995. Heavy metal and hydrocarbon pollution in recent sediments from Southampton Water, Southern England: A geochemical and isotopic study. Environ. Sci. Technol. 29, 1288–1296.
Direktoratsgruppen for gjennomføringen av vannforskriften, 2018. Klassifisering av miljøtilstand i vann: Økologisk og kjemisk klassifiseringssystem for kystvann, grunnvann, innsjøer og elver (No. 02:2018).
Dolven, J.K., Alve, E., Rygg, B., Magnusson, J., 2013. Defining past ecological status and in situ reference conditions using benthic foraminifera: A case study from the Oslofjord, Norway. Ecol. Indic. 29, 219–233. https://doi.org/10.1016/j.ecolind.2012.12.031
European Commission, Directorate-General for the Environment, 2003. Transitional and coastal waters: typology, reference conditions and classification systems. No 5. No 5. OPOCE, Luxembourg.
European Union, 2000. Directive 2000/60/EC of the European Parliament and of the Council of 23 October 2000 establishing a framework for Community action in the field of water policy.
Fagrådet for vann og avløpsteknisk samarbeid i indre Oslofjord, 2019. Rapporter [WWW Document]. Rapporter. URL http://www.indre-oslofjord.no/rapporter/ (accessed 4.5.19).
Fagrådet for vann og avløpsteknisk samarbeid i indre Oslofjord, 2017. Årsberetning 2017 (Annual report). Fagrådet for vann og avløpsteknisk samarbeid i indre Oslofjord.
Fagrådet for vann og avløpsteknisk samarbeid i indre Oslofjord, 2014. Årsberetning 2014. Fagrådet for vann og avløpsteknisk samarbeid i indre Oslofjord.
Gade, H.G., 1971. Hydrographic investigations in the Oslofjord : a study of water circulation and exchange processes : 1. Universitetet, Bergen.
Grall, J., Glémarec, M., 1997. Using biotic indices to estimate macrobenthic community perturbations in the Bay of Brest. Estuar. Coast. Shelf Sci. 44, 43–53. https://doi.org/10.1016/S0272-7714(97)80006-6
Hess, S., Alve, E., Reuss, N.S., 2014. Benthic foraminiferal recovery in the Oslofjord (Norway): Responses to capping and re-oxygenation. Estuar. Coast. Shelf Sci. 147, 87–102. https://doi.org/10.1016/j.ecss.2014.05.012
Hurlbert, S.H., 1971. The Nonconcept of Species Diversity: A Critique and Alternative Parameters. Ecology 52, 577–586. https://doi.org/10.2307/1934145
Institute of Marine Research, 2014. Fjords - water exchange and currents [WWW Document]. Inst. Mar. Res. URL https://www.imr.no/temasider/kyst_og_fjord/fjorder_vannutskiftning_og_strom/en (accessed 5.5.18).

Kröncke, I., Reiss, H., 2010. Influence of macrofauna long-term natural variability on benthic indices used in ecological quality assessment. Mar. Pollut. Bull. 60, 58–68. https://doi.org/10.1016/j.marpolbul.2009.09.001

Lepland, Aivo, Andersen, T.J., Lepland, Aave, Arp, H.P.H., Alve, E., Breedveld, G.D., Rindby, A., 2010. Sedimentation and chronology of heavy metal pollution in Oslo harbor, Norway. Mar. Pollut. Bull. 60, 1512–1522. https://doi.org/10.1016/j.marpolbul.2010.04.017

Libæk, I., Stenersen, Ø., Aase, J., 1999. History of Norway. Grøndahl Dreyer.

Meyers, P.A., 1994. Preservation of elemental and isotopic source identification of sedimentary organic matter. Chem. Geol. 114, 289–302. https://doi.org/10.1016/0009-2541(94)90059-0

Miljødirektoratet, 2015a. Klassifisering av miljøtilstand i vann: Økologisk og kjemisk klassifi seringssystem for kystvann, grunnvann, innsjøer og elver (No. Veileder 02:2013 – revidert 2015).

Miljødirektoratet, 2015b. Grenseverdier for klassifisering av vann, sediment og biota (No. M 608).

Nannestad, Å., 2019a. VEAS. [Email].

Nannestad, Å., 2019b. Thesis: Copper abnormalities. [Email].

Nannestad, Å.D., 2018. SV: VEAS Trip and Master's thesis. [Email].

Nasir, A., 2016. The Use of C/N Ratio in Assessing the Influence of Land-Based Material in Coastal Water of South Sulawesi and Spermonde Archipelago, Indonesia. Front. Mar. Sci. https://doi.org/10.3389/fmars.2016.00266

Norconsult, 2018. Toktrapport 15.05.2018: Miljøovervåkning av Indre Oslofjord.

Norges Geologiske Undersøkelse, 2018. Oslofjord 1m resolution bathymetry data.

Norges Geologiske Undersøkelse, 2015. Marine sediment map VEAS basin.

Nortek AS, 2017. The comprehensive manual 2017.

Ørsted, H., 1970. Filipstadkaia around 1970. http://www.oslohavn.no/en/news/2012/The+Ports+Cultural+Heritage.b7C_wljK3m.ips

OSPAR Commission (Ed.), 2000. Quality status report 2000. London.

Oug, E., Christiansen, M.E., Dobbe, K., Rønning, A.-H., Bakken, T., Kongsrud, J.A., 2015. Mapping of marine benthic invertebrates in the Oslofjord and the Skagerrak: sampling data of museum collections from 1950-1955 and from recent investigations. Fauna Nor. 35, 35. https://doi.org/10.5324/fn.v35i0.1944

Sætre, R. (Ed.), 2007. The Norwegian coastal current - Oceanography and climate. Tapir Academic Press, Trondheim.

Shannon, C.E., Weaver, W., 1963. The Mathematical Theory of Communication. University of Illinois Press, Urbana.

Staalstrøm, A., Røed, L.P., 2016. Vertical mixing and internal wave energy fluxes in a sill fjord. J. Mar. Syst. 159, 15–32. https://doi.org/10.1016/j.jmarsys.2016.02.005

Syvitski, J.P.M., Burrell, D.C., Skei, J.M., 1987. Fjords : processes and products. Springer, New York.

Vestfjorden Avløpsselskap, 2013. Årsrapport 2013 (Yearly report). VEAS.

Vestfjorden Avløpsselskap, n.d. Vann: En renere Oslofjord [WWW Document]. VEAS En Renere Oslo. URL http://www.veas.nu/home/produkter/vann (accessed 11.8.17).

Wilse, A.B., 1935. The grain silo is being built 1935. http://www.oslohavn.no/en/news/2012/The+Ports+Cultural+Heritage.b7C_wljK3m.ips.

WoRMS Editorial Board, 2019. World Register of Marine Species [WWW Document]. World Regist. Mar. Species. URL http://www.marinespecies.org at VLIZ. Accessed 05-30-2019. doi:10.14284/170

Zhang, Y., Lu, X., Shao, X., Liu, H., Xing, M., Zhao, F., Li, X., Yuan, M., 2015. Influence of Sedimentation Rate on the Metal Contamination in Sediments of Bohai Bay, China. Bull. Environ. Contam. Toxicol. 95, 507–512. https://doi.org/10.1007/s00128-015-1599-0

Appendices

Appendix A: Sediment core data

Table 4 *Notes of sediment core composition for cores and replicates taken at time of slicing 03 May 2018. Shaded cells indicate no data for that interval.*

Core interval (cm)	Core depth (cm)	Core V-60-A18	Core V-60-A18R	Core V-71-NW2	Core V-71-NW2R
0-1	**0.5**	Soft/high water content; Feels sandy	Soft/high water content; Feels sandy	Black and brown top; Fluffy; Shell fragments	Many worm tubes on top; Black; Extremely soupy
1-2	**1.5**	Soft/high water content; Feels sandy	Soft/high water content; Feels sandy	Black and brown top; Fluffy; Shell fragments	
2-3	**2.5**	Sandy			
3-4	**3.5**	Sandy		Soft; High water content	
4-5	**4.5**	Sandy	Some signs of bioturbation; Possible worms	Small shell fragments	
5-6	**5.5**	Sandy		Some burrows	Shell fragments
6-7	**6.5**	Sandy; Starting to see less water		Big burrows	
7-8	**7.5**	Sandy; Starting to see less water		Shell fragments	Large worm
8-9	**8.5**	Shell fragments	Small worm		
9-10	**9.5**	Low water; firming up		Shell fragments and stones	Bioturbation
10-11	**10.5**	Stone fragments		Stones	Bioturbation
11-12	**11.5**	Fragments of vegetation?		Stones	Stones
12-13	**12.5**	Worm	Worm	Stiffening up	Stones
13-14	**13.5**				Less stones
14-15	**14.5**		Less water; firming	Stiff; Some bioturbation	Worms
15-16	**15.5**	Quite homogeneous			Worms
16-17	**16.5**	Quite homogeneous			
17-18	**17.5**	Firming	Shell fragment		
18-19	**18.5**	Firming	Shell fragment		
19-20	**19.5**	Firming		Empty tube	
20-22	**21**	Firming			End of core
22-24	**23**	Firming	End of core		
24-26	**25**	Firming			
26-28	**27**	Firming			
28-30	**29**	Quite firm			
30-32	**31**	End of core		End of core – 1.5cm sample	

Table 5 *Sample weights and water content for V-60-A18 sediment core collected 03 May 2018 in 60m water depth. Note that italicized data has been processed. All massing done with Sartorius Basic T digital balance S/N 509481.*

Box No.	Core name	Core interval (cm)	Core depth (cm)	Empty box weight (g)	Box + wet sample weight (g)	Wet sample weight (g)	Box + dry sample weight (g)	*Dry sample weight (g)*	*% Water*	*Salt corrected dry sample weight (g)*	*% Water (salt corrected)*	Weight of material sent for radiometric dating (g)	*Material left after sampling (g)*
1	**V-60-A18**	**0-1**	**0.5**	9.129	72.715	*63.59*	25.633	*16.50*	*74.0*	*14.95*	*76.49*	6.024	*8.926*
2	**V-60-A18**	**1-2**	**1.5**	9.075	75.525	*66.45*	29.488	*20.41*	*69.3*	*18.89*	*71.57*	6.069	*12.825*
3	**V-60-A18**	**2-3**	**2.5**	9.088	76.312	*67.22*	31.360	*22.27*	*66.9*	*20.79*	*69.08*	6.078	*14.711*
4	**V-60-A18**	**3-4**	**3.5**	9.088	68.941	*59.85*	31.394	*22.31*	*62.7*	*21.07*	*64.80*	6.089	*14.978*
5	**V-60-A18**	**4-5**	**4.5**	9.076	80.275	*71.20*	36.347	*27.27*	*61.7*	*25.82*	*63.73*	6.096	*19.725*
6	**V-60-A18**	**5-6**	**5.5**	9.081	71.760	*62.68*	34.160	*25.08*	*60.0*	*23.84*	*61.97*	6.064	*17.774*
7	**V-60-A18**	**6-7**	**6.5**	9.090	88.155	*79.07*	42.924	*33.83*	*57.2*	*32.34*	*59.10*	6.105	*26.236*
8	**V-60-A18**	**7-8**	**7.5**	9.119	79.318	*70.20*	39.967	*30.85*	*56.1*	*29.55*	*57.91*	6.182	*23.367*
9	**V-60-A18**	**8-9**	**8.5**	9.123	89.772	*80.65*	46.806	*37.68*	*53.3*	*36.27*	*55.03*	6.028	*30.237*
10	**V-60-A18**	**9-10**	**9.5**	9.089	87.938	*78.85*	45.501	*36.41*	*53.8*	*35.01*	*55.60*	6.357	*28.655*
11	**V-60-A18**	**10-11**	**10.5**	9.141	90.371	*81.23*	47.566	*38.43*	*52.7*	*37.01*	*54.44*	6.042	*30.970*
12	**V-60-A18**	**11-12**	**11.5**	9.138	90.058	*80.92*	48.204	*39.07*	*51.7*	*37.68*	*53.43*	6.094	*31.591*
13	**V-60-A18**	**12-13**	**12.5**	9.139	87.473	*78.33*	47.470	*38.33*	*51.1*	*37.01*	*52.75*	6.175	*30.836*
14	**V-60-A18**	**13-14**	**13.5**	9.134	88.323	*79.19*	47.571	*38.44*	*51.5*	*37.09*	*53.16*	6.755	*30.337*
15	**V-60-A18**	**14-15**	**14.5**	9.142	89.924	*80.78*	47.295	*38.15*	*52.8*	*36.75*	*54.51*	6.610	*30.136*
16	**V-60-A18**	**15-16**	**15.5**	9.093	83.774	*74.68*	44.306	*35.21*	*52.8*	*33.91*	*54.59*	6.623	*27.288*
17	**V-60-A18**	**16-17**	**16.5**	9.100	81.226	*72.13*	43.313	*34.21*	*52.6*	*32.96*	*54.30*	6.951	*26.011*
18	**V-60-A18**	**17-18**	**17.5**	9.279	88.859	*79.58*	47.870	*38.59*	*51.5*	*37.24*	*53.21*	6.835	*30.403*
19	**V-60-A18**	**18-19**	**18.5**	9.126	80.535	*71.41*	44.116	*34.99*	*51.0*	*33.79*	*52.68*	6.931	*26.857*
20	**V-60-A18**	**19-20**	**19.5**	9.145	86.547	*77.40*	46.553	*37.41*	*51.7*	*36.09*	*53.38*	6.720	*29.368*
21	**V-60-A18**	**20-22**	**21**	9.145	151.972	*142.83*	78.470	*69.33*	*51.5*	*66.90*	*53.16*	7.761	*59.138*
22	**V-60-A18**	**22-24**	**23**	9.146	147.651	*138.51*	74.704	*65.56*	*52.7*	*63.15*	*54.41*	7.789	*55.362*
23	**V-60-A18**	**24-26**	**25**	9.138	152.780	*143.64*	79.195	*70.06*	*51.2*	*67.63*	*52.92*	7.056	*60.573*
24	**V-60-A18**	**26-28**	**27**	9.142	174.275	*165.13*	97.451	*88.31*	*46.5*	*85.77*	*48.06*	7.661	*78.113*

Box No.	Core name	Core interval (cm)	Core depth (cm)	Empty box weight (g)	Box + wet sample weight (g)	Wet sample weight (g)	Box + dry sample weight (g)	*Dry sample weight (g)*	*% Water*	*Salt corrected dry sample weight (g)*	*% Water (salt corrected)*	Weight of material sent for radiometric dating (g)	*Material left after sampling (g)*
25	**V-60-A18**	**28-30**	**29**	9.134	166.369	*157.24*	98.930	*89.80*	*42.9*	*87.57*	*44.31*	7.568	*80.003*
26	**V-60-A18**	**30-32**	**31**	9.225	169.656	*160.43*	99.729	*90.50*	*43.6*	*88.20*	*45.03*	7.982	*80.214*

Table 6 *Sample weights and water content for V-60-A18R sediment core collected 03 May 2018 in 60m water depth. This is a replicate sediment core of the V-60-A18 core. Note that italicized data has been processed. All massing done with Sartorius Basic T digital balance S/N 509481.*

Box No.	Core name	Core interval (cm)	Core depth (cm)	Empty box weight (g)	Box + wet sample weight (g)	*Wet sample weight (g)*	Box + dry sample weight (g)	*Dry sample weight (g)*	*% Water*	*Salt corrected dry sample weight (g)*	*% Water (salt corrected)*
1	**V-60-A18R**	**0-1**	**0.5**	9.146	76.075	*66.93*	28.115	*18.97*	*71.7*	*17.39*	74.02
2	**V-60-A18R**	**1-2**	**1.5**	9.151	63.678	*54.53*	26.506	*17.36*	*68.2*	*16.13*	70.42
3	**V-60-A18R**	**2-3**	**2.5**	9.077	77.192	*68.12*	32.032	*22.96*	*66.3*	*21.46*	68.49
4	**V-60-A18R**	**3-4**	**3.5**	9.085	82.520	*73.44*	36.635	*27.55*	*62.5*	*26.04*	64.55
5	**V-60-A18R**	**4-5**	**4.5**	8.448	78.055	*69.61*	35.077	*26.63*	*61.7*	*25.21*	63.78
6	**V-60-A18R**	**5-6**	**5.5**	9.077	84.325	*75.25*	47.564	*38.49*	*48.9*	*37.27*	50.47
7	**V-60-A18R**	**6-7**	**6.5**	9.088	80.477	*71.39*	40.079	*30.99*	*56.6*	*29.66*	58.46
8	**V-60-A18R**	**7-8**	**7.5**	9.096	77.589	*68.49*	40.355	*31.26*	*54.4*	*30.03*	56.16
9	**V-60-A18R**	**8-9**	**8.5**	9.135	83.458	*74.32*	43.692	*34.56*	*53.5*	*33.24*	55.27
10	**V-60-A18R**	**9-10**	**9.5**	9.169	86.498	*77.33*	45.473	*36.30*	*53.1*	*34.95*	54.80
11	**V-60-A18R**	**10-11**	**10.5**	9.121	81.296	*72.18*	42.630	*33.51*	*53.6*	*32.23*	55.34
12	**V-60-A18R**	**11-12**	**11.5**	9.135	83.587	*74.45*	44.793	*35.66*	*52.1*	*34.38*	53.83
13	**V-60-A18R**	**12-13**	**12.5**	9.137	83.420	*74.28*	45.562	*36.43*	*51.0*	*35.18*	52.65
14	**V-60-A18R**	**13-14**	**13.5**	9.142	73.852	*64.71*	40.456	*31.31*	*51.6*	*30.21*	53.31
15	**V-60-A18R**	**14-15**	**14.5**	9.138	92.907	*83.77*	50.372	*41.23*	*50.8*	*39.83*	52.45
16	**V-60-A18R**	**15-16**	**15.5**	9.219	82.791	*73.57*	46.561	*37.34*	*49.2*	*36.15*	50.87

Box No.	Core name	Core interval (cm)	Core depth (cm)	Empty box weight (g)	Box + wet sample weight (g)	*Wet sample weight (g)*	Box + dry sample weight (g)	*Dry sample weight (g)*	*% Water*	*Salt corrected dry sample weight (g)*	*% Water (salt corrected)*
17	**V-60-A18R**	**16-17**	**16.5**	9.210	88.034	*78.82*	48.468	*39.26*	*50.2*	*37.95*	51.85
18	**V-60-A18R**	**17-18**	**17.5**	9.211	108.342	*99.13*	61.551	*52.34*	*47.2*	*50.80*	48.76
19	**V-60-A18R**	**18-19**	**18.5**	9.094	119.223	*110.13*	65.095	*56.00*	*49.1*	*54.21*	50.77
20	**V-60-A18R**	**19-20**	**19.5**	9.144	95.323	*86.18*	53.329	*44.19*	*48.7*	*42.80*	50.34
21	**V-60-A18R**	**20-22**	**21**	9.141	156.797	*147.66*	87.750	*78.61*	*46.8*	*76.33*	48.31
22	**V-60-A18R**	**22-24**	**23**	9.125	162.123	*153.00*	90.529	*81.40*	*46.8*	*79.04*	48.34

Table 7 *Sample weights and water content for V-71-NW2 sediment core collected 03 May 2018 in 71m water depth. Note that italicized data has been processed. All massing done with Sartorius Basic T digital balance S/N 509481.*

Box No.	Core name	Core interval (cm)	Core depth (cm)	Empty box weight (g)	Box + wet sample weight (g)	*Wet sample weight (g)*	Box + dry sample weight (g)	*Dry sample weight (g)*	*% Water*	*Salt corrected dry sample weight (g)*	*% Water (salt corrected)*
1	**V-71-NW2**	**0-1**	**0.5**	9.137	64.902	*55.77*	19.743	*10.61*	*81.0*	*9.12*	*83.65*
2	**V-71-NW2**	**1-2**	**1.5**	9.136	70.963	*61.83*	26.237	*17.10*	*72.3*	*15.63*	*74.73*
3	**V-71-NW2**	**2-3**	**2.5**	9.135	68.951	*59.82*	27.532	*18.40*	*69.2*	*17.03*	*71.53*
4	**V-71-NW2**	**3-4**	**3.5**	9.139	70.904	*61.77*	29.442	*20.30*	*67.1*	*18.93*	*69.34*
5	**V-71-NW2**	**4-5**	**4.5**	9.137	76.312	*67.18*	33.402	*24.27*	*63.9*	*22.85*	*65.99*
6	**V-71-NW2**	**5-6**	**5.5**	9.136	84.748	*75.61*	41.290	*32.15*	*57.5*	*30.72*	*59.37*
7	**V-71-NW2**	**6-7**	**6.5**	9.143	68.380	*59.24*	35.366	*26.22*	*55.7*	*25.13*	*57.57*
8	**V-71-NW2**	**7-8**	**7.5**	9.142	82.975	*73.83*	46.287	*37.15*	*49.7*	*35.93*	*51.33*
9	**V-71-NW2**	**8-9**	**8.5**	9.131	92.783	*83.65*	53.665	*44.53*	*46.8*	*43.24*	*48.31*
10	**V-71-NW2**	**9-10**	**9.5**	9.204	104.185	*94.98*	63.669	*54.47*	*42.7*	*53.13*	*44.06*
11	**V-71-NW2**	**10-11**	**10.5**	9.210	89.442	*80.23*	53.974	*44.76*	*44.2*	*43.59*	*45.67*
12	**V-71-NW2**	**11-12**	**11.5**	9.211	85.022	*75.81*	49.087	*39.88*	*47.4*	*38.69*	*48.96*
13	**V-71-NW2**	**12-13**	**12.5**	9.215	85.039	*75.82*	41.708	*32.49*	*57.1*	*31.06*	*59.03*

Box No.	Core name	Core interval (cm)	Core depth (cm)	Empty box weight (g)	Box + wet sample weight (g)	*Wet sample weight (g)*	Box + dry sample weight (g)	*Dry sample weight (g)*	*% Water*	*Salt corrected dry sample weight (g)*	*% Water (salt corrected)*
14	**V-71-NW2**	**13-14**	**13.5**	9.210	80.867	*71.66*	38.662	*29.45*	*58.9*	*28.06*	*60.84*
15	**V-71-NW2**	**14-15**	**14.5**	9.210	86.470	*77.26*	41.778	*32.57*	*57.8*	*31.09*	*59.76*
16	**V-71-NW2**	**15-16**	**15.5**	9.114	93.304	*84.19*	44.116	*35.00*	*58.4*	*33.38*	*60.35*
17	**V-71-NW2**	**16-17**	**16.5**	9.129	89.987	*80.86*	46.706	*37.58*	*53.5*	*36.15*	*55.29*
18	**V-71-NW2**	**17-18**	**17.5**	9.122	73.698	*64.58*	36.049	*26.93*	*58.3*	*25.68*	*60.23*
19	**V-71-NW2**	**18-19**	**18.5**	9.109	79.940	*70.83*	38.814	*29.71*	*58.1*	*28.35*	*59.98*
20	**V-71-NW2**	**19-20**	**19.5**	9.113	74.094	*64.98*	36.608	*27.50*	*57.7*	*26.26*	*59.59*
21	**V-71-NW2**	**20-22**	**21**	9.121	145.096	*135.98*	68.549	*59.43*	*56.3*	*56.90*	*58.15*
22	**V-71-NW2**	**22-24**	**23**	9.137	144.573	*135.44*	68.409	*59.27*	*56.2*	*56.76*	*58.09*
23	**V-71-NW2**	**24-26**	**25**	9.139	143.402	*134.26*	68.460	*59.32*	*55.8*	*56.85*	*57.66*
24	**V-71-NW2**	**26-28**	**27**	9.140	146.003	*136.86*	69.488	*60.35*	*55.9*	*57.82*	*57.75*
25	**V-71-NW2**	**28-30**	**29**	9.089	163.221	*154.13*	77.151	*68.06*	*55.8*	*65.22*	*57.68*
26	**V-71-NW2**	**30-32**	**31**	9.086	114.264	*105.18*	55.090	*46.00*	*56.3*	*44.05*	*58.12*

Table 8 *Sample weights and water content for V-71-NW2R sediment core collected 03 May 2018 in 71m water depth. This is a replicate sediment core of the V-71-NW2 core. Note that italicized data has been processed. All massing done with Sartorius Basic T digit balance S/N 509481.*

Box No.	Core name	Core interval (cm)	Core depth (cm)	Empty box weight (g)	Box + wet sample weight (g)	*Wet sample weight (g)*	Box + dry sample weight (g)	*Dry sample weight (g)*	*% Water*	*Salt corrected dry sample weight (g)*	*% Water (salt corrected)*
1	**V-71-NW2R**	**0-1**	**0.5**	9.085	82.312	*73.23*	19.952	*10.87*	*85.2*	*8.81*	*87.97*
2	**V-71-NW2R**	**1-2**	**1.5**	9.109	70.560	*61.45*	26.186	*17.08*	*72.2*	*15.61*	*74.59*
3	**V-71-NW2R**	**2-3**	**2.5**	9.075	70.725	*61.65*	27.500	*18.43*	*70.1*	*17.00*	*72.43*
4	**V-71-NW2R**	**3-4**	**3.5**	9.087	78.983	*69.90*	31.487	*22.40*	*68.0*	*20.83*	*70.19*
5	**V-71-NW2R**	**4-5**	**4.5**	9.082	71.470	*62.39*	30.695	*21.61*	*65.4*	*20.27*	*67.51*

Box No.	Core name	Core interval (cm)	Core depth (cm)	Empty box weight (g)	Box + wet sample weight (g)	*Wet sample weight (g)*	Box + dry sample weight (g)	*Dry sample weight (g)*	*% Water*	*Salt corrected dry sample weight (g)*	*% Water (salt corrected)*
6	**V-71-NW2R**	**5-6**	**5.5**	9.084	78.430	*69.35*	34.666	*25.58*	*63.1*	*24.14*	*65.19*
7	**V-71-NW2R**	**6-7**	**6.5**	9.094	77.848	*68.75*	35.995	*26.90*	*60.9*	*25.52*	*62.88*
8	**V-71-NW2R**	**7-8**	**7.5**	8.836	96.585	*87.75*	45.670	*36.83*	*58.0*	*35.15*	*59.94*
9	**V-71-NW2R**	**8-9**	**8.5**	8.681	86.975	*78.29*	43.239	*34.56*	*55.9*	*33.11*	*57.70*
10	**V-71-NW2R**	**9-10**	**9.5**	8.401	96.146	*87.75*	49.254	*40.85*	*53.4*	*39.31*	*55.20*
11	**V-71-NW2R**	**10-11**	**10.5**	9.104	68.468	*59.36*	39.489	*30.39*	*48.8*	*29.43*	*50.43*
12	**V-71-NW2R**	**11-12**	**11.5**	9.111	121.731	*112.62*	77.016	*67.91*	*39.7*	*66.43*	*41.01*
13	**V-71-NW2R**	**12-13**	**12.5**	9.134	93.161	*84.03*	59.470	*50.34*	*40.1*	*49.22*	*41.42*
14	**V-71-NW2R**	**13-14**	**13.5**	9.135	87.596	*78.46*	49.168	*40.03*	*49.0*	*38.76*	*50.59*
15	**V-71-NW2R**	**14-15**	**14.5**	9.126	90.880	*81.75*	47.642	*38.52*	*52.9*	*37.09*	*54.63*
16	**V-71-NW2R**	**15-16**	**15.5**	9.136	92.581	*83.45*	49.760	*40.62*	*51.3*	*39.21*	*53.01*
17	**V-71-NW2R**	**16-17**	**16.5**	9.130	77.090	*67.96*	40.236	*31.11*	*54.2*	*29.89*	*56.02*
18	**V-71-NW2R**	**17-18**	**17.5**	9.131	95.277	*86.15*	48.956	*39.83*	*53.8*	*38.30*	*55.54*
19	**V-71-NW2R**	**18-19**	**18.5**	9.141	87.499	*78.36*	44.343	*35.20*	*55.1*	*33.78*	*56.89*
20	**V-71-NW2R**	**19-20**	**19.5**	9.092	81.450	*72.36*	41.265	*32.17*	*55.5*	*30.85*	*57.37*
21	**V-71-NW2R**	**20-22**	**21**	9.083	149.139	*140.06*	73.352	*64.27*	*54.1*	*61.77*	*55.90*

Table 9 *Sample weights and water content for surface sediment cores collected 03 May 2018 in various water depths (depth of collection corresponds to numerical value in the center of the core name. Note that italicized data has been processed. All massing done with Sartorius Basic T digital balance S/N 509481.*

Box No.	Core name	Core interval (cm)	Core depth (cm)	Empty box weight (g)	Box + wet sample weight (g)	*Wet sample weight (g)*	Box + dry sample weight (g)	*Dry sample weight (g)*	*% Water*	*Salt corrected dry sample weight (g)*	*% Water (salt corrected)*	Notes
1/2	**V-75-SE1**	**0-1**	**0.5**	9.139	130.919	*121.78*	35.342	*26.20*	*78.5*	*23.05*	81.07	Core tops from Gemini corer combined 1/2

Box No.	Core name	Core interval (cm)	Core depth (cm)	Empty box weight (g)	Box + wet sample weight (g)	*Wet sample weight (g)*	Box + dry sample weight (g)	*Dry sample weight (g)*	*% Water*	*Salt corrected dry sample weight (g)*	*% Water (salt corrected)*	Notes
2/2	**V-75-SE1**	**0-1**	**0.5**	9.136	165.463	*156.33*	42.164	*33.03*	*78.9*	*28.96*	81.48	Core tops from Gemini corer combined 2/2
1/2	**V-99-SE2**	**0-1**	**0.5**	9.139	152.361	*143.22*	40.320	*31.18*	*78.2*	*27.48*	80.81	Core tops from Gemini corer combined 1/2
2/2	**V-99-SE2**	**0-1**	**0.5**	9.145	145.387	*136.24*	40.030	*30.89*	*77.3*	*27.41*	79.88	Core tops from Gemini corer combined 2/2
1/2	**V-87-NE1**	**0-1**	**0.5**	9.141	145.327	*136.19*	35.49	*26.35*	*80.7*	*22.72*	83.32	Core tops from Gemini corer combined 1/2
2/2	**V-87-NE1**	**0-1**	**0.5**	9.144	147.968	*138.82*	36.55	*27.40*	*80.3*	*23.72*	82.91	Core tops from Gemini corer combined 2/2
1/2	**V-93-NE2**	**0-1**	**0.5**	9.143	152.339	*143.20*	32.612	*23.47*	*83.6*	*19.52*	86.37	Core tops from Gemini corer combined 1/2
2/2	**V-93-NE2**	**0-1**	**0.5**	9.139	153.665	*144.53*	35.491	*26.35*	*81.8*	*22.45*	84.46	Core tops from Gemini corer combined 2/2
1/2	**V-66-NW1**	**0-1**	**0.5**	9.146	126.841	*117.70*	32.900	*23.75*	*79.8*	*20.65*	82.45	Core tops from Gemini corer combined 1/2
2/2	**V-66-NW1**	**0-1**	**0.5**	9.142	176.255	*167.11*	43.560	*34.42*	*79.4*	*30.04*	82.02	Core tops from Gemini corer combined 2/2

Appendix B: CTD raw data

Table 10 *CTD raw data for location V-93-NE2 collected on 03 May 2018.*

Depth of measurement (m)	Temperature (°C)	Salinity (PSU)	Density (sigma-t, Kg/m³)	Fluorescence (Seapoint)	Fluorescence WET Labs WETstar (mg/m³)	Turbidity, Seapoint (FTU)	Sound Velocity (Chen-Millero, m/s)	Oxygen, SBE 43 (% saturation)	Oxygen, SBE 43 (mg/L)
0.5	8.7148	21.0552	16.2597	1.027E+00	0.6452	0.799	1468.04	99.56678	10.115540
1.0	8.7143	21.0563	16.2606	1.062E+00	0.6438	0.755	1468.05	99.52533	10.111370
1.5	8.7122	21.0611	16.2646	1.072E+00	0.6435	0.740	1468.06	99.49985	10.108950
2.0	8.7097	21.0670	16.2695	1.102E+00	0.6450	0.722	1468.06	99.43534	10.102600
2.5	8.7090	21.0688	16.2710	1.127E+00	0.6450	0.722	1468.07	99.37125	10.096130
3.0	8.7102	21.0667	16.2692	1.152E+00	0.6511	0.741	1468.08	99.47862	10.106890
3.5	8.7081	21.0720	16.2736	1.199E+00	0.6501	0.712	1468.09	99.64483	10.123930
4.0	8.6948	21.0979	16.2955	1.200E+00	0.6495	0.720	1468.07	99.66878	10.127760
4.5	8.6752	21.1284	16.3217	1.184E+00	0.6545	0.715	1468.04	99.64635	10.128050
5.0	8.6132	21.2263	16.4059	1.128E+00	0.6512	0.684	1467.93	99.49582	10.120730
5.5	8.5233	21.3523	16.5154	1.081E+00	0.6338	0.678	1467.75	99.68901	10.153120
6.0	8.1764	22.0381	17.0938	1.002E+00	0.5977	0.643	1467.25	99.94572	10.215480
6.5	7.9831	22.4197	17.4155	9.789E-01	0.5878	0.652	1466.97	99.70988	10.211690
7.0	7.8757	22.6760	17.6289	9.040E-01	0.5848	0.627	1466.87	99.37617	10.185900
7.5	7.7532	22.8829	17.8054	8.709E-01	0.5743	0.622	1466.66	98.98899	10.161420
8.0	7.5214	23.3118	18.1686	8.097E-01	0.5558	0.591	1466.28	99.66805	10.257740
8.5	7.3917	23.6172	18.4231	7.450E-01	0.5440	0.580	1466.15	101.64958	10.472470
9.0	7.2647	23.8604	18.6285	6.755E-01	0.5319	0.578	1465.96	102.72409	10.597750
9.5	7.1460	24.2129	18.9187	5.877E-01	0.5219	0.590	1465.93	103.10370	10.641910
10.0	6.9896	24.5683	19.2155	5.264E-01	0.4945	0.566	1465.76	103.19929	10.666010
10.5	6.6591	25.2137	19.7596	4.622E-01	0.4722	0.586	1465.25	103.54106	10.739240
11.0	6.4709	25.5415	20.0383	4.221E-01	0.4527	0.738	1464.91	103.84762	10.795640
11.5	6.3193	25.7983	20.2569	3.965E-01	0.4393	0.603	1464.63	104.00911	10.832930
12.0	6.1739	26.0464	20.4679	3.816E-01	0.4152	0.569	1464.36	104.23949	10.876600
12.5	6.0946	26.0663	20.4921	3.906E-01	0.3968	0.562	1464.07	104.52965	10.926000
13.0	5.9546	26.2905	20.6836	3.457E-01	0.3683	0.538	1463.80	105.04586	11.000260
13.5	5.5898	27.0587	21.3277	3.091E-01	0.3431	0.530	1463.28	105.68052	11.106780
14.0	5.4613	27.7779	21.9088	2.986E-01	0.3457	0.521	1463.67	106.64122	11.188550
14.5	5.4735	28.1465	22.1987	3.012E-01	0.3451	0.508	1464.20	107.27241	11.223920
15.0	5.6137	28.2681	22.2799	2.981E-01	0.3466	0.502	1464.93	107.30770	11.180990
15.5	5.7873	28.4956	22.4408	3.966E-01	0.3524	0.485	1465.93	108.26980	11.217640
16.0	6.0498	28.8371	22.6810	2.792E-01	0.3497	0.473	1467.43	110.06999	11.307740
16.5	6.5925	29.8561	23.4199	2.646E-01	0.3447	0.477	1470.89	111.08676	11.192430
17.0	6.9482	30.2885	23.7162	2.564E-01	0.3426	0.471	1472.84	110.44664	11.004410
17.5	7.1059	30.4179	23.7977	2.483E-01	0.3308	0.452	1473.63	108.38222	10.750420
18.0	7.3473	30.8280	24.0884	2.790E-01	0.3302	0.467	1475.09	104.80461	10.310510

Depth of measurement (m)	Temperature (°C)	Salinity (PSU)	Density (sigma-t, Kg/m³)	Fluorescence (Seapoint)	Fluorescence WET Labs WETstar (mg/m³)	Turbidity, Seapoint (FTU)	Sound Velocity (Chen-Millero, m/s)	Oxygen, SBE 43 (% saturation)	Oxygen, SBE 43 (mg/L)
18.5	7.5362	31.1255	24.2968	2.540E-01	0.3463	0.463	1476.20	96.43543	9.427290
19.0	7.6838	31.4866	24.5601	2.657E-01	0.3763	0.496	1477.22	81.55043	7.927530
19.5	7.9349	31.7062	24.6973	2.496E-01	0.3451	0.483	1478.47	70.21174	6.776250
20.0	7.9743	31.7664	24.7389	2.459E-01	0.3542	0.505	1478.70	62.67988	6.040980
20.5	7.7433	31.7680	24.7728	2.323E-01	0.3703	0.552	1477.83	56.59489	5.483250
21.0	7.7051	31.7847	24.7913	2.428E-01	0.3720	0.563	1477.71	52.96523	5.135630
21.5	7.8642	31.8848	24.8474	2.280E-01	0.3595	0.546	1478.45	50.14465	4.841550
22.0	7.8692	31.9481	24.8964	2.368E-01	0.3521	0.538	1478.56	48.44473	4.674840
22.5	7.8343	31.9839	24.9295	2.361E-01	0.3544	0.542	1478.48	51.38245	4.961010
23.0	8.0109	32.0536	24.9590	2.271E-01	0.3324	0.508	1479.24	54.63488	5.251570
23.5	7.9484	32.0579	24.9714	2.154E-01	0.3278	0.512	1479.02	54.85984	5.280540
24.0	7.9132	32.0746	24.9895	2.297E-01	0.3268	0.495	1478.91	53.58883	5.161820
24.5	7.9464	32.0899	24.9967	2.184E-01	0.3215	0.505	1479.07	53.40065	5.139290
25.0	7.8598	32.1054	25.0213	2.086E-01	0.3258	0.508	1478.77	52.46949	5.059090
25.5	7.8814	32.1389	25.0445	2.047E-01	0.3289	0.507	1478.90	51.91829	5.002400
26.0	7.7091	32.1602	25.0856	2.176E-01	0.3312	0.540	1478.27	52.37651	5.065630
26.5	7.6418	32.1541	25.0903	1.984E-01	0.3542	0.526	1478.02	52.51933	5.087430
27.0	7.5931	32.1584	25.1004	2.074E-01	0.3342	0.540	1477.84	53.10272	5.149500
27.5	7.6543	32.2014	25.1256	2.295E-01	0.3226	0.564	1478.14	53.94266	5.222190
28.0	7.7139	32.2304	25.1400	2.050E-01	0.3171	0.534	1478.41	55.60031	5.374410
28.5	7.7256	32.2983	25.1917	1.998E-01	0.3091	0.541	1478.55	57.71973	5.575170
29.0	7.8749	32.3241	25.1908	3.384E-01	0.2977	0.512	1479.16	59.40567	5.717730
29.5	7.8335	32.3422	25.2109	2.571E-01	0.3034	0.511	1479.03	60.14059	5.793230
30.0	7.7788	32.3432	25.2195	1.908E-01	0.3050	0.512	1478.83	60.32262	5.817940
30.5	7.7020	32.3937	25.2699	1.963E-01	0.2917	0.514	1478.61	59.00018	5.698710
31.0	7.9502	32.4690	25.2937	1.942E-01	0.2580	0.466	1479.66	55.70078	5.346970
31.5	7.9007	32.4816	25.3108	1.752E-01	0.2535	0.569	1479.50	54.08915	5.197650
32.0	7.8396	32.5255	25.3540	2.024E-01	0.2447	0.478	1479.33	55.04848	5.295650
32.5	7.8220	32.5558	25.3802	1.887E-01	0.2344	0.455	1479.30	56.55901	5.442050
33.0	7.8214	32.5817	25.4007	2.252E-01	0.2298	0.444	1479.34	54.91008	5.282570
33.5	7.8277	32.6174	25.4278	2.151E-01	0.2203	0.429	1479.42	53.58870	5.153520
34.0	7.8399	32.6590	25.4588	1.798E-01	0.2146	0.421	1479.53	54.43700	5.232220
34.5	7.8351	32.6704	25.4684	1.969E-01	0.2094	0.422	1479.53	55.78447	5.361910
35.0	7.8264	32.6828	25.4794	1.873E-01	0.2090	0.441	1479.52	56.89379	5.469180
35.5	7.7869	32.6956	25.4950	1.768E-01	0.2049	0.444	1479.39	57.48408	5.530420
36.0	7.7198	32.7202	25.5239	1.858E-01	0.2022	0.434	1479.18	57.65741	5.554650
36.5	7.6873	32.7457	25.5486	2.347E-01	0.1942	0.441	1479.09	57.76694	5.568390
37.0	7.6628	32.7646	25.5669	1.821E-01	0.1940	0.438	1479.03	57.72375	5.566630
37.5	7.6412	32.7773	25.5799	1.826E-01	0.1895	0.434	1478.97	58.05733	5.601090
38.0	7.6015	32.8044	25.6068	1.778E-01	0.1794	0.424	1478.86	58.92509	5.688930

Depth of measurement (m)	Temperature (°C)	Salinity (PSU)	Density (sigma-t, Kg/m³)	Fluorescence (Seapoint)	Fluorescence WET Labs WETstar (mg/m³)	Turbidity, Seapoint (FTU)	Sound Velocity (Chen-Millero, m/s)	Oxygen, SBE 43 (% saturation)	Oxygen, SBE 43 (mg/L)
38.5	7.5701	32.8225	25.6254	2.112E-01	0.1760	0.416	1478.77	59.76455	5.773420
39.0	7.5544	32.8273	25.6315	2.046E-01	0.1699	0.412	1478.72	60.21422	5.818760
39.5	7.5190	32.8459	25.6510	2.575E-01	0.1657	0.414	1478.62	60.63131	5.863080
40.0	7.4898	32.8647	25.6698	1.973E-01	0.1663	0.416	1478.54	61.80386	5.979710
40.5	7.4954	32.8588	25.6644	1.790E-01	0.1664	0.422	1478.56	62.81768	6.077240
41.0	7.4803	32.8713	25.6763	1.962E-01	0.1642	0.429	1478.53	63.41449	6.136600
41.5	7.4503	32.8917	25.6966	1.839E-01	0.1634	0.428	1478.45	64.25781	6.221650
42.0	7.4181	32.9149	25.7193	1.778E-01	0.1577	0.433	1478.36	65.12943	6.309700
42.5	7.4054	32.9212	25.7261	1.886E-01	0.1553	0.436	1478.33	65.12838	6.311160
43.0	7.3862	32.9363	25.7406	1.828E-01	0.1551	0.433	1478.28	64.94078	6.295120
43.5	7.3720	32.9481	25.7518	1.813E-01	0.1533	0.450	1478.25	64.94884	6.297460
44.0	7.3512	32.9646	25.7677	1.821E-01	0.1495	0.458	1478.20	65.28841	6.332710
44.5	7.3272	32.9838	25.7861	1.715E-01	0.1509	0.455	1478.14	65.81373	6.386370
45.0	7.2977	33.0066	25.8082	1.885E-01	0.1528	0.457	1478.06	66.23273	6.430400
45.5	7.2858	33.0148	25.8162	1.740E-01	0.1502	0.464	1478.03	66.67373	6.474620
46.0	7.2695	33.0242	25.8259	1.710E-01	0.1470	0.467	1477.99	66.98196	6.506590
46.5	7.2479	33.0383	25.8399	1.709E-01	0.1465	0.480	1477.93	67.15880	6.526390
47.0	7.2315	33.0506	25.8519	1.824E-01	0.1438	0.468	1477.89	67.21376	6.533650
47.5	7.2327	33.0477	25.8494	1.748E-01	0.1447	0.471	1477.90	67.02373	6.515120
48.0	7.2102	33.0617	25.8635	1.726E-01	0.1428	0.474	1477.84	66.90970	6.506790
48.5	7.1950	33.0725	25.8741	1.715E-01	0.1421	0.485	1477.80	67.07461	6.524640
49.0	7.1672	33.0921	25.8933	1.721E-01	0.1391	0.480	1477.73	67.34154	6.553930
49.5	7.1582	33.0989	25.8999	1.709E-01	0.1384	0.478	1477.71	67.46532	6.567040
50.0	7.1552	33.1015	25.9024	1.793E-01	0.1361	0.496	1477.71	67.58561	6.579080
50.5	7.1226	33.1228	25.9236	1.710E-01	0.1344	0.484	1477.62	67.74523	6.598630
51.0	7.0876	33.1427	25.9440	1.726E-01	0.1304	0.480	1477.51	68.04654	6.632450
51.5	7.0750	33.1491	25.9508	1.709E-01	0.1296	0.487	1477.48	68.59600	6.687660
52.0	7.0610	33.1592	25.9606	1.785E-01	0.1323	0.504	1477.45	68.84325	6.713460
52.5	7.0552	33.1637	25.9649	1.709E-01	0.1327	0.525	1477.44	69.08600	6.737840
53.0	7.0392	33.1742	25.9754	1.709E-01	0.1331	0.529	1477.40	69.67065	6.796890
53.5	7.0302	33.1804	25.9815	1.709E-01	0.1340	0.536	1477.38	70.16168	6.845920
54.0	7.0268	33.1826	25.9836	1.726E-01	0.1343	0.526	1477.38	70.30234	6.860090
54.5	7.0326	33.1783	25.9795	1.709E-01	0.1337	0.531	1477.40	70.05158	6.834900
55.0	7.0219	33.1852	25.9864	1.788E-01	0.1338	0.540	1477.38	69.77469	6.809250
55.5	7.0071	33.1957	25.9966	1.704E-01	0.1316	0.538	1477.34	69.64362	6.798300
56.0	6.9995	33.2006	26.0015	1.704E-01	0.1304	0.532	1477.33	69.38947	6.774450
56.5	6.9906	33.2069	26.0077	1.709E-01	0.1296	0.537	1477.31	69.31375	6.768170
57.0	6.9942	33.2038	26.0048	1.709E-01	0.1275	0.537	1477.33	69.24541	6.761070
57.5	6.9847	33.2102	26.0111	1.709E-01	0.1316	0.553	1477.31	69.26419	6.764100
58.0	6.9778	33.2152	26.0159	1.726E-01	0.1320	0.556	1477.29	69.34291	6.772640

Depth of measurement (m)	Temperature (°C)	Salinity (PSU)	Density (sigma-t, Kg/m³)	Fluorescence (Seapoint)	Fluorescence WET Labs WETstar (mg/m³)	Turbidity, Seapoint (FTU)	Sound Velocity (Chen-Millero, m/s)	Oxygen, SBE 43 (% saturation)	Oxygen, SBE 43 (mg/L)
58.5	6.9680	33.2218	26.0225	1.710E-01	0.1316	0.551	1477.27	69.29338	6.769020
59.0	6.9641	33.2245	26.0251	1.726E-01	0.1296	0.552	1477.27	69.30281	6.770440
59.5	6.9562	33.2306	26.0310	1.715E-01	0.1302	0.554	1477.25	69.35750	6.776740
60.0	6.9408	33.2413	26.0415	1.715E-01	0.1299	0.554	1477.22	69.49016	6.791630
60.5	6.9328	33.2469	26.0470	1.732E-01	0.1322	0.586	1477.20	69.49154	6.792760
61.0	6.9221	33.2542	26.0542	1.728E-01	0.1319	0.609	1477.18	69.28701	6.774110
61.5	6.9198	33.2560	26.0559	1.726E-01	0.1334	0.604	1477.18	69.26080	6.771830
62.0	6.9210	33.2554	26.0552	1.720E-01	0.1339	0.615	1477.19	69.36639	6.781990
62.5	6.9201	33.2560	26.0559	1.715E-01	0.1346	0.634	1477.20	69.54376	6.799440
63.0	6.9207	33.2552	26.0552	1.732E-01	0.1334	0.620	1477.20	69.14485	6.760390
63.5	6.9119	33.2613	26.0611	1.750E-01	0.1352	0.640	1477.19	68.67283	6.715340
64.0	6.9044	33.2666	26.0663	1.721E-01	0.1330	0.623	1477.17	68.56307	6.705530
64.5	6.9003	33.2695	26.0692	1.715E-01	0.1348	0.620	1477.17	68.53892	6.703660
65.0	6.8964	33.2722	26.0718	1.736E-01	0.1325	0.640	1477.16	68.33341	6.684040
65.5	6.8959	33.2728	26.0723	1.766E-01	0.1344	0.676	1477.17	68.15058	6.666220
66.0	6.8933	33.2749	26.0743	1.771E-01	0.1352	0.672	1477.17	68.04518	6.656210
66.5	6.8851	33.2807	26.0800	1.733E-01	0.1335	0.654	1477.15	67.84388	6.637530
67.0	6.8775	33.2865	26.0856	1.721E-01	0.1330	0.622	1477.14	67.71873	6.626180
67.5	6.8741	33.2894	26.0884	1.710E-01	0.1316	0.626	1477.14	67.55079	6.610140
68.0	6.8735	33.2897	26.0886	1.720E-01	0.1320	0.616	1477.15	67.53297	6.608470
68.5	6.8690	33.2931	26.0919	1.772E-01	0.1321	0.656	1477.14	67.65244	6.620700
69.0	6.8658	33.2952	26.0940	1.717E-01	0.1325	0.634	1477.14	67.68651	6.624420
69.5	6.8648	33.2961	26.0948	1.709E-01	0.1304	0.602	1477.15	67.67490	6.623410
70.0	6.8640	33.2968	26.0955	1.704E-01	0.1308	0.611	1477.15	67.71181	6.627120
70.5	6.8597	33.3002	26.0988	1.787E-01	0.1294	0.585	1477.15	67.84880	6.641040
71.0	6.8578	33.3018	26.1003	1.778E-01	0.1288	0.590	1477.15	67.99353	6.655420
71.5	6.8541	33.3046	26.1030	1.709E-01	0.1287	0.588	1477.15	68.08152	6.664480
72.0	6.8507	33.3071	26.1054	1.726E-01	0.1280	0.598	1477.15	68.14200	6.670810
72.5	6.8493	33.3081	26.1064	1.715E-01	0.1291	0.590	1477.15	68.09924	6.666800
73.0	6.8484	33.3086	26.1069	1.703E-01	0.1299	0.579	1477.15	68.09823	6.666810
73.5	6.8458	33.3105	26.1087	1.709E-01	0.1293	0.606	1477.16	68.23655	6.680680
74.0	6.8446	33.3115	26.1097	1.709E-01	0.1295	0.601	1477.16	68.48579	6.705220
74.5	6.8425	33.3124	26.1107	1.721E-01	0.1295	0.606	1477.16	68.67780	6.724300
75.0	6.8409	33.3138	26.1120	1.733E-01	0.1290	0.589	1477.16	68.65341	6.722090
75.5	6.8403	33.3144	26.1125	1.715E-01	0.1257	0.579	1477.17	68.53505	6.710580
76.0	6.8393	33.3150	26.1131	1.721E-01	0.1246	0.597	1477.18	68.60296	6.717350
76.5	6.8379	33.3162	26.1143	1.709E-01	0.1272	0.630	1477.18	68.78795	6.735630
77.0	6.8371	33.3174	26.1153	1.721E-01	0.1277	0.582	1477.19	68.82711	6.739540
77.5	6.8367	33.3180	26.1158	1.715E-01	0.1256	0.580	1477.19	68.93573	6.750200
78.0	6.8350	33.3193	26.1171	1.716E-01	0.1254	0.594	1477.20	69.15034	6.771430

Depth of measurement (m)	Temperature (°C)	Salinity (PSU)	Density (sigma-t, Kg/m³)	Fluorescence (Seapoint)	Fluorescence WET Labs WETstar (mg/m³)	Turbidity, Seapoint (FTU)	Sound Velocity (Chen-Millero, m/s)	Oxygen, SBE 43 (% saturation)	Oxygen, SBE 43 (mg/L)
78.5	6.8338	33.3204	26.1182	1.716E-01	0.1271	0.604	1477.20	69.26186	6.782490
79.0	6.8331	33.3209	26.1186	1.785E-01	0.1246	0.586	1477.21	69.25237	6.781640
79.5	6.8328	33.3209	26.1187	1.709E-01	0.1271	0.592	1477.22	69.31382	6.787710
80.0	6.8313	33.3221	26.1199	1.721E-01	0.1260	0.595	1477.22	69.23309	6.779980
80.5	6.8293	33.3232	26.1210	1.750E-01	0.1248	0.593	1477.22	69.21752	6.778720
81.0	6.8282	33.3237	26.1215	1.711E-01	0.1253	0.604	1477.23	69.15250	6.772510
81.5	6.8276	33.3244	26.1221	1.709E-01	0.1260	0.589	1477.23	69.08234	6.765690
82.0	6.8275	33.3246	26.1223	1.726E-01	0.1273	0.614	1477.24	69.11873	6.769260
82.5	6.8269	33.3250	26.1227	1.720E-01	0.1260	0.589	1477.25	69.12152	6.769610
83.0	6.8266	33.3252	26.1229	1.817E-01	0.1256	0.591	1477.26	69.17159	6.774560
83.5	6.8266	33.3253	26.1230	1.721E-01	0.1274	0.598	1477.26	69.32762	6.789830
84.0	6.8261	33.3256	26.1233	1.720E-01	0.1252	0.593	1477.27	69.37085	6.794130
84.5	6.8262	33.3257	26.1233	1.714E-01	0.1235	0.615	1477.28	69.43588	6.800480
85.0	6.8259	33.3261	26.1237	1.733E-01	0.1244	0.592	1477.29	69.49735	6.806520
85.5	6.8259	33.3264	26.1239	1.709E-01	0.1259	0.590	1477.29	69.34404	6.791500
86.0	6.8262	33.3266	26.1240	1.709E-01	0.1264	0.588	1477.30	69.27163	6.784350
86.5	6.8267	33.3267	26.1241	1.720E-01	0.1275	0.586	1477.31	69.23568	6.780750
87.0	6.8267	33.3270	26.1243	1.720E-01	0.1269	0.603	1477.32	69.34741	6.791680
87.5	6.8261	33.3274	26.1247	1.720E-01	0.1261	0.592	1477.33	69.57409	6.813960
88.0	6.8264	33.3279	26.1250	1.709E-01	0.1295	0.589	1477.34	69.39330	6.796180
88.5	6.8271	33.3279	26.1249	1.783E-01	0.1310	0.616	1477.35	69.06108	6.763540
89.0	6.8277	33.3279	26.1248	1.737E-01	0.1324	0.575	1477.36	68.92509	6.750140
89.5	6.8278	33.3279	26.1249	1.736E-01	0.1307	0.590	1477.37	68.85787	6.743530
90.0	6.8277	33.3280	26.1250	1.745E-01	0.1314	0.583	1477.38	68.61141	6.719400
90.5	6.8278	33.3281	26.1250	1.747E-01	0.1318	0.571	1477.39	68.23829	6.682840
91.0	6.8278	33.3281	26.1250	1.773E-01	0.1328	0.575	1477.39	67.92385	6.652050
91.5	6.8279	33.3283	26.1251	1.734E-01	0.1327	0.595	1477.40	67.74650	6.634660
92.0	6.8281	33.3284	26.1252	1.726E-01	0.1308	0.574	1477.41	67.64404	6.624590
92.5	6.8282	33.3283	26.1251	1.737E-01	0.1338	0.582	1477.42	67.71883	6.631890
93.0	6.8284	33.3282	26.1250	1.727E-01	0.1331	0.632	1477.43	67.59373	6.619620
93.5	6.8283	33.3280	26.1249	1.789E-01	0.1317	0.605	1477.44	67.34549	6.595330

Table 11 *CTD raw data for location V-71-NW2 collected on 03 May 2018.*

Depth of measurement (m)	Temperature (°C)	Salinity (PSU)	Density (sigma-t, Kg/m³)	Fluorescence (Seapoint)	Fluorescence, WET Labs WETstar (mg/m³)	Turbidity, Seapoint (FTU)	Sound Velocity (Chen-Millero, m/s)	Oxygen, SBE 43 (% saturation)	Oxygen, SBE 43 (mg/L)
0.5	8.6900	21.0268	16.2406	9.944E-01	0.6483	0.761	1467.91	100.09486	10.17687
1.0	8.6904	21.0277	16.2412	1.027E+00	0.6461	0.748	1467.92	99.49412	10.11563
1.5	8.6705	21.0696	16.2764	1.126E+00	0.6498	0.735	1467.91	99.77032	10.14559
2.0	8.6709	21.1109	16.3086	1.117E+00	0.6490	0.716	1467.97	99.78963	10.14474

Depth of measurement (m)	Temperature (°C)	Salinity (PSU)	Density (sigma-t, Kg/m³)	Fluorescence (Seapoint)	Fluorescence, WET Labs WETstar (mg/m³)	Turbidity, Seapoint (FTU)	Sound Velocity (Chen-Millero, m/s)	Oxygen, SBE 43 (% saturation)	Oxygen, SBE 43 (mg/L)
2.5	8.6683	21.1272	16.3217	1.131E+00	0.6497	0.730	1467.98	99.73013	10.13825
3.0	8.6480	21.1576	16.3480	1.239E+00	0.6485	0.723	1467.95	99.67802	10.13567
3.5	8.6631	21.1234	16.3193	1.306E+00	0.6476	0.702	1467.98	99.83595	10.15046
4.0	8.5754	21.2671	16.4424	1.217E+00	0.6495	0.688	1467.82	100.16872	10.19535
4.5	8.5164	21.3824	16.5398	1.172E+00	0.6458	0.678	1467.74	100.29244	10.21419
5.0	8.4455	21.5685	16.6939	1.160E+00	0.6411	0.716	1467.70	100.28860	10.21815
5.5	8.4570	21.5493	16.6774	1.195E+00	0.6371	0.697	1467.73	100.10235	10.19773
6.0	8.5072	21.4252	16.5743	1.174E+00	0.6262	0.694	1467.78	99.81205	10.16459
6.5	8.1027	22.1462	17.1870	9.011E-01	0.5686	0.616	1467.10	100.62648	10.29574
7.0	7.6088	23.0716	17.9702	8.099E-01	0.5646	0.644	1466.31	101.57034	10.44859
7.5	7.6015	23.1470	18.0301	7.563E-01	0.5610	0.587	1466.39	101.82235	10.47117
8.0	7.5702	23.1991	18.0746	7.044E-01	0.5490	0.578	1466.33	101.38020	10.42976
8.5	7.6573	23.0352	17.9361	6.689E-01	0.5323	0.559	1466.48	99.75922	10.25320
9.0	7.6547	23.0533	17.9505	6.215E-01	0.5324	0.564	1466.50	101.48331	10.42978
9.5	7.1341	24.2450	18.9452	5.591E-01	0.5205	0.571	1465.93	103.84876	10.71951
10.0	6.7076	25.0231	19.6045	4.629E-01	0.4685	0.564	1465.20	104.92090	10.88352
10.5	6.6434	25.1110	19.6807	4.365E-01	0.4450	0.560	1465.06	105.33779	10.93702
11.0	6.6300	25.1401	19.7051	4.413E-01	0.4512	0.563	1465.05	104.55974	10.85760
11.5	6.6926	25.0295	19.6111	4.095E-01	0.4384	0.565	1465.17	102.49975	10.63573
12.0	6.5765	25.2307	19.7821	4.027E-01	0.4173	0.564	1464.96	103.25440	10.72962
12.5	5.9443	26.2677	20.6668	3.842E-01	0.3942	0.538	1463.72	105.92382	11.09650
13.0	5.7353	26.6790	21.0129	3.437E-01	0.3674	0.540	1463.39	107.43144	11.28005
13.5	5.5576	27.0482	21.3226	3.221E-01	0.3490	0.536	1463.14	107.93580	11.35334
14.0	5.5284	27.2321	21.4708	3.042E-01	0.3475	0.542	1463.26	106.44904	11.19111
14.5	5.7292	26.7614	21.0786	3.005E-01	0.3461	0.535	1463.49	104.82700	11.00210
15.0	5.6136	28.1711	22.2035	2.962E-01	0.3531	0.510	1464.81	107.23008	11.17982
15.5	6.0129	29.4301	23.1528	2.741E-01	0.3555	0.492	1468.02	110.12821	11.27910
16.0	6.1947	29.5352	23.2149	2.551E-01	0.3599	0.515	1468.89	111.97892	11.41176
16.5	6.2657	29.6305	23.2816	2.604E-01	0.3551	0.506	1469.31	112.15421	11.40360
17.0	6.4453	29.8626	23.4432	2.636E-01	0.3514	0.480	1470.32	111.58232	11.28023
17.5	6.4673	29.9320	23.4947	2.549E-01	0.3481	0.468	1470.50	108.31720	10.94187
18.0	7.2034	30.8294	24.1085	2.383E-01	0.3539	0.506	1474.53	98.95225	9.76726
18.5	7.4309	31.1083	24.2975	2.314E-01	0.3678	0.494	1475.77	91.34951	8.95283
19.0	7.4334	31.2018	24.3706	2.473E-01	0.3761	0.560	1475.91	86.08462	8.43093
19.5	7.5452	31.4405	24.5430	2.350E-01	0.3783	0.585	1476.64	84.00630	8.19367
20.0	7.3420	31.0626	24.2734	2.189E-01	0.3762	0.639	1475.39	78.69047	7.72894
20.5	7.5757	31.5458	24.6213	2.151E-01	0.3722	0.542	1476.91	65.87894	6.41810
21.0	7.6899	31.7634	24.7767	2.554E-01	0.3698	0.550	1477.62	58.66646	5.69115
21.5	7.6695	31.7973	24.8061	2.132E-01	0.3804	0.576	1477.60	56.50739	5.48307
22.0	7.6206	31.8449	24.8503	2.049E-01	0.3779	0.564	1477.48	57.47751	5.58167
22.5	7.6235	31.8447	24.8497	2.032E-01	0.3746	0.570	1477.50	59.88050	5.81467

Depth of measurement (m)	Temperature (°C)	Salinity (PSU)	Density (sigma-t, Kg/m³)	Fluorescence (Seapoint)	Fluorescence, WET Labs WETstar (mg/m³)	Turbidity, Seapoint (FTU)	Sound Velocity (Chen-Millero, m/s)	Oxygen, SBE 43 (% saturation)	Oxygen, SBE 43 (mg/L)
23.0	7.6295	31.8304	24.8377	2.330E-01	0.3681	0.550	1477.51	59.28020	5.75614
23.5	7.6573	31.9432	24.9224	2.035E-01	0.3675	0.541	1477.76	57.57192	5.58259
24.0	7.6625	31.9356	24.9157	2.000E-01	0.3497	0.507	1477.78	57.64745	5.58952
24.5	7.7304	31.9899	24.9489	2.076E-01	0.3424	0.511	1478.12	58.33874	5.64581
25.0	7.7287	32.0262	24.9775	1.986E-01	0.3414	0.520	1478.16	58.67090	5.67683
25.5	7.6980	32.0686	25.0152	2.000E-01	0.3365	0.526	1478.11	58.83425	5.69504
26.0	7.6742	32.0910	25.0361	1.970E-01	0.3339	0.531	1478.06	58.92678	5.70625
26.5	7.6208	32.1015	25.0519	1.949E-01	0.3333	0.541	1477.87	58.19559	5.64192
27.0	7.5956	32.1255	25.0742	1.954E-01	0.3300	0.543	1477.81	56.87110	5.51581
27.5	7.6080	32.1151	25.0643	2.092E-01	0.3295	0.548	1477.86	56.53529	5.48206
28.0	7.5870	32.1494	25.0942	2.063E-01	0.3281	0.537	1477.83	57.04651	5.53305
28.5	7.5736	32.1668	25.1096	2.137E-01	0.3302	0.530	1477.80	57.95131	5.62187
29.0	7.5662	32.1831	25.1235	2.146E-01	0.3246	0.531	1477.80	58.86866	5.71123
29.5	7.5734	32.1761	25.1170	2.073E-01	0.3223	0.533	1477.83	59.28169	5.75062
30.0	7.5782	32.2103	25.1432	1.830E-01	0.3116	0.508	1477.90	59.46594	5.76657
30.5	7.6169	32.2471	25.1667	2.040E-01	0.3176	0.565	1478.10	59.74046	5.78669
31.0	7.6034	32.2666	25.1840	1.874E-01	0.2962	0.504	1478.08	60.06818	5.81947
31.5	7.5445	32.2995	25.2180	2.153E-01	0.2800	0.527	1477.91	60.23134	5.84187
32.0	7.5882	32.2875	25.2025	1.932E-01	0.2753	0.511	1478.07	60.03564	5.81754
32.5	7.5983	32.4124	25.2992	1.827E-01	0.2533	0.550	1478.27	59.52617	5.76215
33.0	7.6192	32.4782	25.3480	1.832E-01	0.2449	0.556	1478.44	59.39361	5.74409
33.5	7.6377	32.5186	25.3771	1.838E-01	0.2312	0.502	1478.57	59.81627	5.78101
34.0	7.6328	32.5013	25.3643	1.895E-01	0.2233	0.469	1478.54	60.09499	5.80925
34.5	7.6276	32.4911	25.3569	2.049E-01	0.2231	0.517	1478.51	59.91087	5.79253
35.0	7.6430	32.5374	25.3912	1.853E-01	0.2235	0.526	1478.64	59.11485	5.71183
35.5	7.6563	32.5812	25.4237	1.849E-01	0.2152	0.485	1478.75	58.25700	5.62563
36.0	7.6636	32.6243	25.4565	1.768E-01	0.1985	0.449	1478.84	57.82844	5.58175
36.5	7.6669	32.6166	25.4500	1.776E-01	0.1964	0.450	1478.85	57.88054	5.58663
37.0	7.6704	32.6629	25.4859	1.913E-01	0.1935	0.512	1478.93	58.02883	5.59881
37.5	7.6564	32.7370	25.5461	1.895E-01	0.1896	0.541	1478.98	57.92818	5.58817
38.0	7.6459	32.7845	25.5849	1.998E-01	0.1882	0.557	1479.00	57.89633	5.58469
38.5	7.6154	32.8340	25.6281	1.873E-01	0.1837	0.625	1478.96	58.05737	5.60230
39.0	7.6162	32.8218	25.6184	1.867E-01	0.1842	0.581	1478.95	58.07195	5.60406
39.5	7.6378	32.7866	25.5877	1.902E-01	0.1811	0.531	1479.00	58.01219	5.59683
40.0	7.5802	32.8591	25.6528	1.885E-01	0.1762	0.551	1478.88	58.12136	5.61204
40.5	7.5361	32.8804	25.6757	1.827E-01	0.1742	0.488	1478.74	58.40844	5.64465
41.0	7.4786	32.9189	25.7141	1.786E-01	0.1733	0.494	1478.58	58.71220	5.68000
41.5	7.4494	32.9439	25.7378	1.737E-01	0.1714	0.498	1478.51	58.73490	5.68506
42.0	7.4062	32.9683	25.7630	1.818E-01	0.1680	0.499	1478.38	58.77220	5.69337
42.5	7.3774	32.9715	25.7695	1.810E-01	0.1649	0.489	1478.28	59.33978	5.75202
43.0	7.3869	32.9676	25.7651	1.813E-01	0.1615	0.480	1478.32	60.46612	5.86005

Depth of measurement (m)	Temperature (°C)	Salinity (PSU)	Density (sigma-t, Kg/m³)	Fluorescence (Seapoint)	Fluorescence, WET Labs WETstar (mg/m³)	Turbidity, Seapoint (FTU)	Sound Velocity (Chen-Millero, m/s)	Oxygen, SBE 43 (% saturation)	Oxygen, SBE 43 (mg/L)
43.5	7.4197	32.9493	25.7462	1.983E-01	0.1600	0.487	1478.43	61.64309	5.97038
44.0	7.4527	32.9312	25.7273	2.136E-01	0.1612	0.495	1478.55	62.81466	6.08000
44.5	7.2721	33.0300	25.8301	1.720E-01	0.1560	0.504	1477.98	63.95696	6.21211
45.0	7.2340	33.0538	25.8541	1.733E-01	0.1525	0.477	1477.87	64.15519	6.23585
45.5	7.2192	33.0633	25.8636	3.754E-01	0.1534	0.474	1477.83	63.95792	6.21839
46.0	7.2117	33.0675	25.8678	2.491E-01	0.1523	0.479	1477.82	63.48666	6.17346
46.5	7.1984	33.0757	25.8761	2.186E-01	0.1499	0.489	1477.79	63.01340	6.12898
47.0	7.2011	33.0732	25.8738	3.261E-01	0.1483	0.486	1477.80	64.64463	6.28737
47.5	7.1537	33.1031	25.9038	1.959E-01	0.1473	0.489	1477.66	66.53583	6.47706
48.0	7.1476	33.1066	25.9074	1.708E-01	0.1454	0.496	1477.65	67.34724	6.55681
48.5	7.1313	33.1162	25.9172	1.709E-01	0.1461	0.498	1477.61	67.77007	6.60003
49.0	7.1146	33.1270	25.9279	1.757E-01	0.1446	0.500	1477.57	67.71056	6.59629
49.5	7.1085	33.1304	25.9315	1.776E-01	0.1446	0.509	1477.55	67.53068	6.57954
50.0	7.0917	33.1411	25.9422	1.859E-01	0.1438	0.515	1477.51	67.78903	6.60678
50.5	7.0840	33.1453	25.9465	1.706E-01	0.1431	0.515	1477.50	68.08977	6.63709
51.0	7.0584	33.1618	25.9630	1.754E-01	0.1403	0.510	1477.42	68.22994	6.65395
51.5	7.0500	33.1677	25.9688	1.715E-01	0.1399	0.516	1477.41	68.11787	6.64403
52.0	7.0442	33.1718	25.9728	1.785E-01	0.1399	0.534	1477.40	67.79405	6.61316
52.5	7.0322	33.1787	25.9799	1.747E-01	0.1377	0.551	1477.37	67.81840	6.61705
53.0	7.0168	33.1894	25.9903	1.822E-01	0.1404	0.545	1477.33	68.41812	6.67746
53.5	7.0094	33.1945	25.9954	1.847E-01	0.1410	0.581	1477.32	68.78071	6.71376
54.0	7.0054	33.1964	25.9974	1.844E-01	0.1410	0.588	1477.31	68.72010	6.70838
54.5	6.9998	33.1996	26.0007	1.716E-01	0.1398	0.575	1477.30	68.62092	6.69943
55.0	6.9943	33.2029	26.0040	1.728E-01	0.1376	0.555	1477.29	68.53343	6.69159
55.5	6.9894	33.2061	26.0073	1.739E-01	0.1362	0.543	1477.29	68.17301	6.65700
56.0	6.9854	33.2088	26.0099	1.713E-01	0.1369	0.571	1477.28	67.76269	6.61742
56.5	6.9798	33.2126	26.0136	1.709E-01	0.1389	0.537	1477.27	68.09388	6.65046
57.0	6.9768	33.2144	26.0155	1.709E-01	0.1357	0.537	1477.27	68.76002	6.71589
57.5	6.9754	33.2154	26.0164	1.742E-01	0.1351	0.539	1477.28	69.26852	6.76574
58.0	6.9718	33.2179	26.0189	1.724E-01	0.1356	0.538	1477.27	69.50979	6.78976
58.5	6.9664	33.2217	26.0226	1.724E-01	0.1331	0.549	1477.27	69.61137	6.80035
59.0	6.9580	33.2274	26.0282	1.722E-01	0.1335	0.548	1477.25	69.57361	6.79772
59.5	6.9532	33.2311	26.0318	1.723E-01	0.1367	0.582	1477.24	69.45515	6.78673
60.0	6.9465	33.2359	26.0364	1.710E-01	0.1385	0.577	1477.23	69.42430	6.78454
60.5	6.9345	33.2441	26.0445	1.815E-01	0.1398	0.618	1477.20	69.47056	6.79057
61.0	6.9304	33.2470	26.0474	1.860E-01	0.1413	0.632	1477.20	69.48456	6.79245
61.5	6.9205	33.2536	26.0539	1.903E-01	0.1408	0.659	1477.18	69.39002	6.78447
62.0	6.9137	33.2581	26.0583	1.885E-01	0.1441	0.675	1477.17	69.08599	6.75559
62.5	6.9044	33.2639	26.0642	1.837E-01	0.1445	0.691	1477.14	68.14788	6.66503
63.0	6.8966	33.2694	26.0696	1.890E-01	0.1453	0.710	1477.13	66.98454	6.55220
63.5	6.8949	33.2708	26.0709	1.864E-01	0.1463	0.735	1477.13	66.18137	6.47382

Depth of measurement (m)	Temperature (°C)	Salinity (PSU)	Density (sigma-t, Kg/m³)	Fluorescence (Seapoint)	Fluorescence, WET Labs WETstar (mg/m³)	Turbidity, Seapoint (FTU)	Sound Velocity (Chen-Millero, m/s)	Oxygen, SBE 43 (% saturation)	Oxygen, SBE 43 (mg/L)
64.0	6.8886	33.2754	26.0754	1.878E-01	0.1473	0.733	1477.12	65.74098	6.43148
64.5	6.8856	33.2787	26.0783	1.949E-01	0.1471	0.750	1477.12	65.64207	6.42212
65.0	6.8847	33.2796	26.0792	1.933E-01	0.1482	0.772	1477.13	65.65606	6.42358
65.5	6.8836	33.2806	26.0801	1.942E-01	0.1492	0.815	1477.13	65.53156	6.41151
66.0	6.8832	33.2811	26.0806	1.947E-01	0.1493	0.839	1477.14	65.27967	6.38691
66.5	6.8818	33.2829	26.0822	1.960E-01	0.1520	0.859	1477.14	65.02309	6.36193
67.0	6.8799	33.2854	26.0844	2.088E-01	0.1572	0.901	1477.15	64.58436	6.31918
67.5	6.8774	33.2879	26.0867	2.208E-01	0.1550	0.926	1477.15	64.09365	6.27143
68.0	6.8770	33.2884	26.0871	2.066E-01	0.1528	0.905	1477.16	63.60187	6.22335
68.5	6.8836	33.2820	26.0812	1.997E-01	0.1527	0.914	1477.18	63.39450	6.20238
69.0	6.8805	33.2851	26.0841	1.978E-01	0.1521	0.912	1477.18	63.59908	6.22270
69.5	6.8810	33.2849	26.0838	1.958E-01	0.1529	0.905	1477.19	63.66154	6.22876
70.0	6.8762	33.2909	26.0892	2.142E-01	0.1592	0.959	1477.19	63.61203	6.22435
70.5	6.8804	33.2854	26.0843	2.057E-01	0.1515	10.166	1477.21	62.46453	6.11170

Table 12 *CTD raw data for location V-99-SE2 collected on 03 May 2018.*

Depth of measurement (m)	Temperature (°C)	Salinity (PSU)	Density (sigma-t, Kg/m³)	Fluorescence (Seapoint)	Fluorescence, WET Labs WETstar (mg/m³)	Turbidity, Seapoint (FTU)	Sound Velocity (Chen-Millero, m/s)	Oxygen, SBE 43 (% saturation)	Oxygen, SBE 43 (mg/L)
0.5	8.6727	21.1367	16.3286	9.905E-01	0.6541	0.699	1467.98	100.05397	10.16951
1.0	8.6789	21.1136	16.3098	1.020E+00	0.6554	0.703	1467.98	100.34001	10.19865
1.5	8.6802	21.1065	16.3040	1.052E+00	0.6541	0.714	1467.99	100.11972	10.17643
2.0	8.6778	21.1108	16.3077	1.084E+00	0.6561	0.718	1467.99	100.24118	10.18906
2.5	8.6762	21.1134	16.3099	1.098E+00	0.6560	0.705	1468.00	99.94892	10.15955
3.0	8.6736	21.1173	16.3133	1.100E+00	0.6553	0.766	1468.00	99.91420	10.15636
3.5	8.6646	21.1397	16.3319	1.077E+00	0.6548	0.678	1468.00	100.01343	10.16708
4.0	8.6399	21.1921	16.3759	1.058E+00	0.6560	0.687	1467.98	99.68944	10.13646
4.5	8.6194	21.2236	16.4030	1.056E+00	0.6518	0.679	1467.95	99.70376	10.14063
5.0	8.6073	21.2409	16.4180	1.063E+00	0.6420	0.673	1467.93	99.97594	10.17000
5.5	8.5407	21.3434	16.5063	1.062E+00	0.6235	0.670	1467.80	100.18633	10.20024
6.0	8.4389	21.5292	16.6640	1.059E+00	0.6182	0.649	1467.65	100.02451	10.19539
6.5	8.4162	21.5691	16.6980	1.039E+00	0.6067	0.650	1467.61	100.01291	10.19690
7.0	8.3907	21.6233	16.7434	9.946E-01	0.5886	0.620	1467.59	100.03391	10.20146
7.5	8.3181	21.7722	16.8687	8.555E-01	0.5829	0.621	1467.50	100.12864	10.21836
8.0	8.1287	22.1304	17.1717	7.670E-01	0.5652	0.592	1467.21	100.58469	10.28597
8.5	7.8997	22.5896	17.5584	6.915E-01	0.5506	0.580	1466.89	100.96107	10.34841
9.0	7.8717	22.6542	17.6123	5.692E-01	0.5211	0.567	1466.86	101.27753	10.38322
9.5	7.5498	23.3668	18.2084	5.696E-01	0.5026	0.560	1466.49	101.23189	10.40805
10.0	7.2953	23.8567	18.6221	4.930E-01	0.4957	0.561	1466.09	101.39421	10.45331
10.5	7.1831	24.0959	18.8226	4.715E-01	0.4789	0.564	1465.95	101.93916	10.52064

Depth of measurement (m)	Temperature (°C)	Salinity (PSU)	Density (sigma-t, Kg/m³)	Fluorescence (Seapoint)	Fluorescence, WET Labs WETstar (mg/m³)	Turbidity, Seapoint (FTU)	Sound Velocity (Chen-Millero, m/s)	Oxygen, SBE 43 (% saturation)	Oxygen, SBE 43 (mg/L)
11.0	7.0441	24.3978	19.0755	4.340E-01	0.4580	0.583	1465.78	102.12997	10.55381
11.5	6.9216	24.6281	19.2701	3.829E-01	0.4199	0.556	1465.59	102.96655	10.65484
12.0	7.0047	24.4728	19.1388	3.800E-01	0.4032	0.559	1465.74	103.80076	10.73111
12.5	6.7922	24.8762	19.4796	3.730E-01	0.3963	0.536	1465.40	104.02631	10.77973
13.0	6.1493	26.0276	20.4557	3.388E-01	0.3649	0.512	1464.25	104.66529	10.92893
13.5	5.6417	26.9905	21.2684	3.233E-01	0.3474	0.527	1463.41	105.75771	11.10617
14.0	5.5281	27.3887	21.5945	3.140E-01	0.3461	0.546	1463.45	105.09330	11.03712
14.5	5.4893	27.6409	21.7977	2.968E-01	0.3456	0.522	1463.62	103.23321	10.83363
15.0	5.4237	28.2796	22.3090	3.000E-01	0.3478	0.502	1464.17	104.32431	10.91862
15.5	5.7097	29.1008	22.9267	2.961E-01	0.3552	0.495	1466.38	108.55958	11.22266
16.0	6.2860	29.7929	23.4072	2.873E-01	0.3563	0.481	1469.58	111.12051	11.28066
16.5	6.6124	30.0906	23.6023	2.690E-01	0.3541	0.477	1471.26	111.61962	11.22334
17.0	6.9571	30.5327	23.9069	2.677E-01	0.3484	0.466	1473.18	112.41094	11.18012
17.5	7.4001	31.1340	24.3218	2.851E-01	0.3533	0.473	1475.67	110.25724	10.81205
18.0	7.6383	31.4081	24.5047	2.509E-01	0.3495	0.481	1476.94	100.01848	9.73719
18.5	7.6744	31.4969	24.5695	2.477E-01	0.3447	0.489	1477.19	85.99583	8.36031
19.0	7.7296	31.6549	24.6859	2.632E-01	0.3534	0.524	1477.61	74.09889	7.18696
19.5	7.6219	31.6885	24.7272	2.587E-01	0.3652	0.536	1477.25	63.12331	6.13589
20.0	7.5746	31.7341	24.7696	2.456E-01	0.3640	0.529	1477.13	54.45589	5.29768
20.5	7.5767	31.8159	24.8336	2.112E-01	0.3666	0.565	1477.25	50.73033	4.93233
21.0	7.5770	31.8764	24.8811	2.225E-01	0.3610	0.545	1477.33	50.78002	4.93518
21.5	7.5757	31.8965	24.8970	2.274E-01	0.3590	0.540	1477.36	53.30273	5.17983
22.0	7.5698	31.9323	24.9260	2.031E-01	0.3536	0.546	1477.39	56.55311	5.49514
22.5	7.5682	31.9620	24.9495	2.208E-01	0.3409	0.586	1477.43	59.27116	5.75832
23.0	7.5749	31.9856	24.9671	2.004E-01	0.3401	0.556	1477.49	60.75670	5.90087
23.5	7.5461	32.0189	24.9973	2.001E-01	0.3443	0.549	1477.43	61.23996	5.95040
24.0	7.5535	32.0343	25.0084	2.118E-01	0.3356	0.550	1477.49	61.24714	5.94949
24.5	7.5999	32.0675	25.0280	1.990E-01	0.3309	0.555	1477.72	60.86545	5.90489
25.0	7.6333	32.0852	25.0373	2.106E-01	0.3288	0.545	1477.87	60.63469	5.87733
25.5	7.6574	32.1111	25.0542	2.468E-01	0.3285	0.531	1478.01	61.04311	5.91267
26.0	7.6327	32.1297	25.0723	2.442E-01	0.3265	0.550	1477.94	61.30551	5.94071
26.5	7.5830	32.1428	25.0895	2.077E-01	0.3212	0.618	1477.78	60.75451	5.89348
27.0	7.5627	32.1561	25.1028	2.165E-01	0.3180	0.556	1477.72	59.80562	5.80361
27.5	7.5462	32.1716	25.1173	2.093E-01	0.3148	0.566	1477.69	59.14766	5.74134
28.0	7.5333	32.1768	25.1231	2.039E-01	0.3163	0.579	1477.65	59.30351	5.75798
28.5	7.5255	32.1777	25.1249	2.050E-01	0.3131	0.586	1477.63	60.08763	5.83511
29.0	7.5141	32.1874	25.1341	2.081E-01	0.3112	0.612	1477.61	60.89985	5.91514
29.5	7.5002	32.2494	25.1848	1.946E-01	0.3037	0.593	1477.64	61.44756	5.96782
30.0	7.5072	32.3315	25.2483	1.974E-01	0.2869	0.565	1477.78	61.70655	5.98879
30.5	7.4945	32.3534	25.2673	2.134E-01	0.2823	0.597	1477.77	61.81922	6.00060

Depth of measurement (m)	Temperature (°C)	Salinity (PSU)	Density (sigma-t, Kg/m³)	Fluorescence (Seapoint)	Fluorescence, WET Labs WETstar (mg/m³)	Turbidity, Seapoint (FTU)	Sound Velocity (Chen-Millero, m/s)	Oxygen, SBE 43 (% saturation)	Oxygen, SBE 43 (mg/L)
31.0	7.5001	32.3767	25.2849	1.902E-01	0.2788	0.567	1477.82	62.01518	6.01794
31.5	7.4836	32.4211	25.3221	1.895E-01	0.2674	0.596	1477.82	62.21902	6.03823
32.0	7.5406	32.4782	25.3590	1.837E-01	0.2608	0.528	1478.12	62.36580	6.04236
32.5	7.5747	32.4902	25.3637	2.123E-01	0.2560	0.511	1478.28	62.54188	6.05423
33.0	7.5854	32.4959	25.3667	2.082E-01	0.2515	0.515	1478.33	62.74587	6.07226
33.5	7.6110	32.5148	25.3779	1.978E-01	0.2490	0.484	1478.46	62.92373	6.08519
34.0	7.7551	32.5603	25.3934	1.922E-01	0.2324	0.453	1479.08	62.37250	6.01038
34.5	7.7859	32.6194	25.4354	1.890E-01	0.2100	0.425	1479.28	61.41612	5.91177
35.0	7.7679	32.6784	25.4843	2.054E-01	0.2054	0.420	1479.29	61.26950	5.89779
35.5	7.7643	32.6959	25.4985	1.769E-01	0.2027	0.434	1479.31	60.88403	5.86049
36.0	7.7120	32.7106	25.5175	2.012E-01	0.1976	0.425	1479.13	59.49142	5.73270
36.5	7.6872	32.7311	25.5372	1.880E-01	0.1963	0.419	1479.07	58.40696	5.63062
37.0	7.6727	32.7429	25.5484	2.004E-01	0.1958	0.435	1479.04	58.38429	5.62986
37.5	7.6650	32.7502	25.5553	1.816E-01	0.1958	0.440	1479.03	58.35623	5.62788
38.0	7.6395	32.7730	25.5768	1.896E-01	0.1906	0.450	1478.97	58.41490	5.63596
38.5	7.5988	32.8015	25.6049	1.755E-01	0.1835	0.423	1478.86	59.17217	5.71324
39.0	7.5792	32.8187	25.6211	2.020E-01	0.1814	0.440	1478.81	60.05410	5.80034
39.5	7.5726	32.8277	25.6292	2.174E-01	0.1793	0.432	1478.80	60.46705	5.84076
40.0	7.5500	32.8444	25.6455	1.931E-01	0.1743	0.442	1478.75	60.62990	5.85885
40.5	7.5065	32.8656	25.6682	1.859E-01	0.1722	0.434	1478.61	61.28902	5.92760
41.0	7.4918	32.8738	25.6767	1.916E-01	0.1692	0.443	1478.57	62.19839	6.01724
41.5	7.4777	32.8899	25.6914	1.795E-01	0.1706	0.438	1478.55	62.54715	6.05229
42.0	7.4555	32.9110	25.7110	2.040E-01	0.1679	0.448	1478.50	62.70553	6.06985
42.5	7.4042	32.9360	25.7379	1.915E-01	0.1613	0.444	1478.34	63.33230	6.13670
43.0	7.3648	32.9617	25.7635	1.734E-01	0.1589	0.454	1478.23	64.06669	6.21241
43.5	7.3308	32.9839	25.7857	1.860E-01	0.1575	0.448	1478.13	64.31379	6.24029
44.0	7.3206	32.9916	25.7932	1.805E-01	0.1572	0.449	1478.11	64.17083	6.22756
44.5	7.3043	33.0055	25.8064	1.741E-01	0.1558	0.466	1478.07	64.34006	6.24574
45.0	7.2794	33.0237	25.8241	1.821E-01	0.1503	0.483	1478.01	65.30701	6.34248
45.5	7.2515	33.0400	25.8408	1.813E-01	0.1468	0.477	1477.93	66.21774	6.43432
46.0	7.2237	33.0570	25.8580	1.721E-01	0.1493	0.474	1477.85	66.52030	6.46713
46.5	7.2191	33.0599	25.8609	1.745E-01	0.1461	0.482	1477.85	66.33096	6.44927
47.0	7.2004	33.0721	25.8731	1.737E-01	0.1449	0.478	1477.80	66.33167	6.45159
47.5	7.1872	33.0785	25.8799	1.798E-01	0.1443	0.473	1477.76	66.86430	6.50508
48.0	7.1676	33.0902	25.8918	1.708E-01	0.1417	0.479	1477.71	67.45721	6.56521
48.5	7.1562	33.0981	25.8996	1.709E-01	0.1409	0.500	1477.68	67.71947	6.59212
49.0	7.1490	33.1030	25.9044	1.728E-01	0.1425	0.497	1477.67	67.95074	6.61552
49.5	7.1476	33.1041	25.9054	1.750E-01	0.1386	0.500	1477.67	68.10011	6.63022
50.0	7.1430	33.1073	25.9086	1.864E-01	0.1374	0.491	1477.67	68.25827	6.64617
50.5	7.1349	33.1118	25.9133	1.710E-01	0.1393	0.504	1477.65	68.50896	6.67163

Depth of measurement (m)	Temperature (°C)	Salinity (PSU)	Density (sigma-t, Kg/m³)	Fluorescence (Seapoint)	Fluorescence, WET Labs WETstar (mg/m³)	Turbidity, Seapoint (FTU)	Sound Velocity (Chen-Millero, m/s)	Oxygen, SBE 43 (% saturation)	Oxygen, SBE 43 (mg/L)
51.0	7.1228	33.1200	25.9213	1.731E-01	0.1398	0.517	1477.62	68.52786	6.67496
51.5	7.1367	33.1111	25.9124	1.710E-01	0.1407	0.510	1477.67	68.50078	6.67059
52.0	7.1213	33.1210	25.9223	1.727E-01	0.1382	0.512	1477.64	68.57560	6.67979
52.5	7.1238	33.1188	25.9203	1.726E-01	0.1407	0.520	1477.65	68.74176	6.69569
53.0	7.1073	33.1296	25.9310	1.796E-01	0.1388	0.523	1477.61	68.70922	6.69458
53.5	7.0871	33.1430	25.9443	1.748E-01	0.1361	0.515	1477.55	68.35895	6.66295
54.0	7.0685	33.1544	25.9558	1.736E-01	0.1359	0.517	1477.50	68.18210	6.64806
54.5	7.0584	33.1610	25.9624	1.704E-01	0.1347	0.541	1477.48	68.17344	6.64847
55.0	7.0463	33.1688	25.9701	1.715E-01	0.1345	0.517	1477.45	68.30786	6.66308
55.5	7.0296	33.1802	25.9814	1.710E-01	0.1352	0.531	1477.41	68.54142	6.68793
56.0	7.0099	33.1936	25.9946	1.715E-01	0.1337	0.542	1477.36	68.86316	6.72177
56.5	7.0030	33.1978	25.9988	1.721E-01	0.1367	0.546	1477.35	68.92003	6.72821
57.0	6.9857	33.2099	26.0107	1.716E-01	0.1339	0.560	1477.30	69.05520	6.74355
57.5	6.9787	33.2151	26.0157	1.753E-01	0.1345	0.560	1477.29	69.45775	6.78372
58.0	6.9774	33.2156	26.0163	1.709E-01	0.1341	0.579	1477.29	69.65184	6.80286
58.5	6.9740	33.2178	26.0185	1.727E-01	0.1344	0.587	1477.29	69.50432	6.78888
59.0	6.9677	33.2224	26.0230	1.733E-01	0.1327	0.578	1477.28	69.36608	6.77615
59.5	6.9616	33.2266	26.0271	1.709E-01	0.1294	0.580	1477.27	69.29769	6.77023
60.0	6.9572	33.2295	26.0300	1.709E-01	0.1322	0.590	1477.26	69.25723	6.76684
60.5	6.9558	33.2304	26.0309	1.709E-01	0.1330	0.587	1477.27	69.03160	6.74497
61.0	6.9519	33.2333	26.0337	1.721E-01	0.1328	0.604	1477.27	68.80297	6.72311
61.5	6.9446	33.2387	26.0389	1.720E-01	0.1340	0.614	1477.25	68.88998	6.73250
62.0	6.9364	33.2440	26.0442	1.763E-01	0.1359	0.611	1477.23	69.07313	6.75143
62.5	6.9267	33.2508	26.0509	1.733E-01	0.1346	0.612	1477.21	69.19839	6.76488
63.0	6.9208	33.2551	26.0551	1.710E-01	0.1328	0.582	1477.20	69.16609	6.76245
63.5	6.9174	33.2578	26.0576	1.709E-01	0.1309	0.578	1477.20	68.96872	6.74356
64.0	6.9119	33.2619	26.0616	1.709E-01	0.1300	0.572	1477.19	68.70025	6.71799
64.5	6.9050	33.2669	26.0665	1.715E-01	0.1307	0.582	1477.18	68.40379	6.68984
65.0	6.9001	33.2701	26.0696	1.710E-01	0.1314	0.586	1477.17	68.08926	6.65969
65.5	6.8949	33.2735	26.0730	1.709E-01	0.1318	0.593	1477.17	68.17002	6.66823
66.0	6.8953	33.2733	26.0728	1.793E-01	0.1326	0.582	1477.18	68.47546	6.69807
66.5	6.8907	33.2768	26.0762	1.716E-01	0.1308	0.582	1477.17	68.76950	6.72738
67.0	6.8870	33.2797	26.0790	1.709E-01	0.1328	0.593	1477.17	68.97492	6.74793
67.5	6.8847	33.2811	26.0804	1.736E-01	0.1324	0.610	1477.17	68.93958	6.74477
68.0	6.8819	33.2830	26.0823	1.773E-01	0.1356	0.628	1477.17	68.79981	6.73143
68.5	6.8783	33.2858	26.0849	1.764E-01	0.1312	0.621	1477.17	68.83282	6.73510
69.0	6.8761	33.2875	26.0866	1.758E-01	0.1348	0.628	1477.17	69.02115	6.75379
69.5	6.8744	33.2889	26.0879	1.733E-01	0.1342	0.651	1477.17	69.15691	6.76729
70.0	6.8722	33.2906	26.0895	1.715E-01	0.1347	0.657	1477.18	68.95718	6.74800
70.5	6.8707	33.2917	26.0906	1.781E-01	0.1315	0.619	1477.18	68.49846	6.70329

Depth of measurement (m)	Temperature (°C)	Salinity (PSU)	Density (sigma-t, Kg/m³)	Fluorescence (Seapoint)	Fluorescence, WET Labs WETstar (mg/m³)	Turbidity, Seapoint (FTU)	Sound Velocity (Chen-Millero, m/s)	Oxygen, SBE 43 (% saturation)	Oxygen, SBE 43 (mg/L)
71.0	6.8681	33.2936	26.0924	1.720E-01	0.1326	0.590	1477.18	68.13850	6.66838
71.5	6.8645	33.2960	26.0948	1.739E-01	0.1313	0.594	1477.18	68.14580	6.66955
72.0	6.8620	33.2979	26.0966	1.710E-01	0.1296	0.589	1477.18	68.24848	6.67989
72.5	6.8600	33.2991	26.0979	1.720E-01	0.1330	0.615	1477.18	68.21659	6.67703
73.0	6.8570	33.3012	26.0999	1.709E-01	0.1322	0.608	1477.18	68.20745	6.67650
73.5	6.8543	33.3032	26.1018	1.741E-01	0.1295	0.599	1477.18	68.35538	6.69132
74.0	6.8508	33.3058	26.1044	1.722E-01	0.1298	0.596	1477.18	68.56654	6.71242
74.5	6.8471	33.3087	26.1071	1.733E-01	0.1284	0.621	1477.17	68.82141	6.73782
75.0	6.8445	33.3108	26.1091	1.709E-01	0.1302	0.588	1477.17	69.00434	6.75603
75.5	6.8431	33.3116	26.1099	1.709E-01	0.1293	0.587	1477.18	69.03392	6.75912
76.0	6.8411	33.3126	26.1110	1.727E-01	0.1253	0.588	1477.18	69.04334	6.76029
76.5	6.8388	33.3140	26.1125	1.704E-01	0.1262	0.587	1477.18	69.08737	6.76490
77.0	6.8376	33.3148	26.1132	1.704E-01	0.1295	0.581	1477.19	69.27866	6.78380
77.5	6.8348	33.3169	26.1152	1.698E-01	0.1299	0.595	1477.19	69.41929	6.79791
78.0	6.8335	33.3179	26.1162	1.715E-01	0.1286	0.606	1477.19	69.43009	6.79912
78.5	6.8334	33.3179	26.1162	1.703E-01	0.1280	0.592	1477.20	69.36858	6.79311
79.0	6.8337	33.3184	26.1166	1.709E-01	0.1259	0.599	1477.21	69.28373	6.78474
79.5	6.8333	33.3190	26.1171	1.721E-01	0.1257	0.604	1477.21	69.24911	6.78138
80.0	6.8324	33.3200	26.1180	1.799E-01	0.1259	0.594	1477.22	69.21930	6.77856
80.5	6.8306	33.3212	26.1192	1.732E-01	0.1257	0.612	1477.22	69.29268	6.78596
81.0	6.8297	33.3221	26.1200	1.709E-01	0.1254	0.591	1477.23	69.37783	6.79440
81.5	6.8290	33.3228	26.1206	1.735E-01	0.1253	0.591	1477.24	69.33999	6.79078
82.0	6.8284	33.3233	26.1211	1.709E-01	0.1254	0.599	1477.24	69.33001	6.78987
82.5	6.8278	33.3241	26.1218	1.726E-01	0.1242	0.592	1477.25	69.36163	6.79303
83.0	6.8273	33.3245	26.1222	1.721E-01	0.1249	0.593	1477.26	69.43400	6.80018
83.5	6.8272	33.3246	26.1223	1.704E-01	0.1278	0.585	1477.26	69.40583	6.79742
84.0	6.8271	33.3247	26.1224	1.716E-01	0.1268	0.587	1477.27	69.45040	6.80181
84.5	6.8267	33.3247	26.1225	1.746E-01	0.1271	0.594	1477.28	69.64485	6.82091
85.0	6.8266	33.3248	26.1226	1.726E-01	0.1271	0.650	1477.29	69.63595	6.82005
85.5	6.8261	33.3253	26.1230	1.710E-01	0.1282	0.596	1477.29	69.48448	6.80528
86.0	6.8256	33.3256	26.1233	1.768E-01	0.1281	0.608	1477.30	69.50376	6.80723
86.5	6.8253	33.3258	26.1235	1.727E-01	0.1264	0.614	1477.31	69.40929	6.79801
87.0	6.8251	33.3260	26.1237	1.752E-01	0.1247	0.596	1477.32	69.34728	6.79196
87.5	6.8248	33.3263	26.1240	1.740E-01	0.1267	0.612	1477.32	69.43707	6.80079
88.0	6.8249	33.3264	26.1241	1.810E-01	0.1273	0.601	1477.33	69.45562	6.80258
88.5	6.8249	33.3266	26.1242	1.788E-01	0.1254	0.598	1477.34	69.43724	6.80077
89.0	6.8246	33.3270	26.1245	1.757E-01	0.1286	0.607	1477.35	69.32006	6.78933
89.5	6.8242	33.3274	26.1249	1.802E-01	0.1287	0.618	1477.36	69.23485	6.78102
90.0	6.8240	33.3278	26.1253	1.915E-01	0.1274	0.618	1477.36	69.32028	6.78941
90.5	6.8244	33.3279	26.1253	1.760E-01	0.1280	0.609	1477.37	69.38375	6.79555

Depth of measurement (m)	Temperature (°C)	Salinity (PSU)	Density (sigma-t, Kg/m³)	Fluorescence (Seapoint)	Fluorescence, WET Labs WETstar (mg/m³)	Turbidity, Seapoint (FTU)	Sound Velocity (Chen-Millero, m/s)	Oxygen, SBE 43 (% saturation)	Oxygen, SBE 43 (mg/L)
91.0	6.8246	33.3278	26.1252	1.789E-01	0.1283	0.607	1477.38	69.33246	6.79050
91.5	6.8249	33.3279	26.1253	1.768E-01	0.1310	0.609	1477.39	69.12800	6.77043
92.0	6.8256	33.3281	26.1253	1.731E-01	0.1327	0.641	1477.40	68.86893	6.74494
92.5	6.8258	33.3279	26.1251	1.776E-01	0.1345	0.625	1477.41	68.52958	6.71168
93.0	6.8262	33.3284	26.1255	1.740E-01	0.1349	0.624	1477.42	68.16379	6.67577
93.5	6.8265	33.3285	26.1255	1.809E-01	0.1347	0.610	1477.43	68.02289	6.66192
94.0	6.8271	33.3285	26.1254	1.801E-01	0.1376	0.608	1477.44	67.82585	6.64253
94.5	6.8276	33.3285	26.1253	1.846E-01	0.1366	0.657	1477.45	67.53519	6.61399
95.0	6.8276	33.3286	26.1254	1.828E-01	0.1346	0.617	1477.46	67.19137	6.58032
95.5	6.8274	33.3286	26.1254	1.890E-01	0.1354	0.635	1477.47	66.92279	6.55405
96.0	6.8274	33.3287	26.1256	1.811E-01	0.1353	0.644	1477.48	67.02735	6.56429
96.5	6.8269	33.3291	26.1259	1.819E-01	0.1331	0.626	1477.48	66.98370	6.56006
97.0	6.8270	33.3296	26.1263	1.825E-01	0.1341	0.661	1477.49	66.80719	6.54274
97.5	6.8273	33.3292	26.1259	1.848E-01	0.1346	0.654	1477.50	66.75142	6.53725

Appendix C: Radiometric dating report

**** Note that this report reflects two cores sent for dating. Only information related to the V-60-A18 core (referred to as VP-60-AA in the report) is relevant.***

Radiometric dating of two marine sediment cores from inner Oslofjord, Norway

P.G.Appleby and G.T.Piliposian
Environmental Radioactivity Research Centre
University of Liverpool

Methods

Dating by ^{210}Pb and ^{137}Cs was carried out on two marine sediment cores from the inner Oslofjord, BL-A and VP-60-AA. Sub-samples from each core were analysed for ^{210}Pb, ^{226}Ra, and ^{137}Cs by direct gamma assay in the Liverpool University Environmental Radioactivity Laboratory, using Ortec HPGe GWL series well-type coaxial low background intrinsic germanium detectors (Appleby *et al*. 1986). ^{210}Pb was determined via its gamma emissions at 46.5 keV, and ^{226}Ra by the 295 keV and 352 keV γ-rays emitted by its daughter radionuclide ^{214}Pb following 3 weeks storage in sealed containers to allow radioactive equilibration. ^{137}Cs was measured by its emissions at 662 keV. The absolute efficiencies of the detectors were determined using calibrated sources and sediment samples of known activity. Corrections were made for the effect of self-absorption of low energy γ-rays within the sample (Appleby *et al.* 1992).

Results

The results of the radiometric analyses carried out on each core are given in Tables 1–2 and shown graphically in Figures 1.i–2.i. Supported ^{210}Pb activity was assumed to be equal to the measured ^{226}Ra activity, and unsupported ^{210}Pb activity calculated by subtracting supported ^{210}Pb from the measured total ^{210}Pb activity. ^{210}Pb dates were calculated using both the CRS and CIC models (Appleby & Oldfield 1978) where appropriate, and possible 1963 and 1986 depths determined from the ^{137}Cs record. Best chronologies for each core were determined following an assessment of all the data using the methods outlined in Appleby (2001). The results are shown in Figures 1.ii–2.ii and given in detail in Tables 3–4.

Core BL-A (Bekkelag basin)

Lead-210 Activity

This core has an unusual ^{210}Pb record in that although total ^{210}Pb activity (Figure 1.i(a)) in the upper half of the core declines in a fairly regular way to reach values close to equilibrium with the supporting ^{226}Ra at a depth of around 12 cm, there are large variations in the deeper layers. These are however largely driven by unusual variations in the supported activity, particularly in sediments between 12-17 cm. ^{226}Ra concentrations are relatively uniform in sediments below 17 cm and above 12 cm, with mean values of 44 Bq kg^{-1} and 61 Bq kg^{-1} respectively. Between these two values, in sediments immediately above 17 cm they initially fall steeply to a minimum value of just 14 Bq kg^{-1} in the 14-15 cm sample, but then rise abruptly to a peak value of 125 Bq kg^{-1} in the 12-13 cm slice. The latter result was confirmed by repeat analyses carried out on a second aliquot from that slice. Possible causes of these variations are deposition at this site of allochthonous material from two different sources, one of which was ^{226}Ra poor and the other ^{226}Ra rich. Sediments within this section, particularly between 11-16 cm, also have a higher dry bulk density.

Unsupported (total minus supported) ^{210}Pb activity declines more or less regularly with depth in the uppermost 12 cm of the core (Figure 1.i(b)), but is close to the limit of detection throughout the anomalous

12-17 cm section. Deeper in the core, a small but significant unsupported ^{210}Pb concentration in the 18-19 cm sample may indicate that sediments at this depth are relatively modern.

Artificial Fallout Radionuclides

^{137}Cs concentrations (Figure 1.i(c)) have a well-defined peak in the 5-6 cm. The proximity of this peak to the surface of the core suggests that it is more likely to be a record of fallout from the 1986 Chernobyl accident, though that is not certain. There are two smaller peaks, at 9-10 cm and 14-15 cm though it is not clear whether they are true records of atmospheric fallout. The latter feature may be associated with the events responsible for the ^{226}Ra anomalies between 12-17 cm.

Core Chronology

^{210}Pb dates calculated using the CRS model place 1986 at a depth of 6.5 cm and 1963 at a depth of 10 cm. These results suggest that the ^{137}Cs peaks at 5.5 cm and 9.5 cm may well be associated with the 1986 and 1963 fallout events. The calculations also suggest that the ^{210}Pb anomalies between 12-17 cm record an episode of rapid sedimentation in the 1940s. Although irregularities in the ^{210}Pb record preclude detailed use of the alternative CIC model, it can be used to help date individual samples that appear to have been unaffected by those events, such as that at 18-19 cm. Both ^{210}Pb models date this sample to around 1940. Revised ^{210}Pb dates calculated by applying the CRS model in a piecewise using the ^{137}Cs dates as reference points suggest that sedimentation rates were relatively constant from the late 1950s through to the end of the 20th century with a mean sedimentation rate during that time of 0.056 g cm^{-2} y^{-1} (0.17 cm y^{-1}). There may have been a small increase in the sedimentation rate in recent years. Dates for sediments below 12 cm are highly uncertain because of the very low ^{210}Pb concentrations in the anomalous section. The raw calculations suggest they record an episode of rapid sedimentation in the 1940s or early 1950s. The 12-13 cm sample with the unusually high ^{226}Ra concentration is dated 1951. The 14-15 cm sample with the unusually low value is dated 1946. All the results are shown in Figure 1.ii and given in detail in Table 3.

Core VP-60-AA

Lead-210 Activity

^{226}Ra concentrations are relatively uniform throughout this core with a mean value (41 Bq kg^{-1}) similar to that in sediments in BL-A below 17 cm. Total ^{210}Pb (Figure 2.i(a)) reaches values close to equilibrium the ^{226}Ra at a depth of around 10 cm though there does appear to be a small level of disequilibrium in sediments down to a depth around 20 cm. Unsupported ^{210}Pb concentrations initially increase with depth, reaching a maximum value in the 3-4 cm sample (Figure 2.i(b)). A more or less exponential decline in the deeper sections between 3-10 cm suggests relatively uniform sedimentation during the period of time spanned by this part of the core. Concentrations between 10-20 cm are all close to the limit of detection, though a slightly higher value in the 20-22 cm sample may indicate that sediments down to this depth are relatively modern.

Artificial Fallout Radionuclides

The ^{137}Cs activity versus depth record (Figure 2.i(c)) has no clear record either of the 1986 Chernobyl accident or of the early 1960s fallout maximum from the atmospheric testing of nuclear weapons. Concentrations are generally lower than in BL-A and have a maximum value in the surficial sample. A relative peak in the 3-4 cm sample coincides with the unsupported ^{210}Pb peak and is more likely to be caused by sedimentological processes.

Core Chronology

^{210}Pb dates calculated using the CRS model place 1986 and 1963 in the 5-6 cm and 8-9 cm samples. In the absence of supporting evidence from the ^{137}Cs record the chronology for this core has been based solely on the ^{210}Pb results. The post-1960 record appears to be similar to that in BL-A. The calculations indicate that sedimentation rates were relatively uniform from around 1960 through to the early 2000s, with a mean value during that time of 0.063 g cm^{-2} y^{-1} (0.12 cm y^{-1}). They also suggest that there may have been a small increase in recent years. Dates for pre-1960 sediments (below 10 cm) are more problematical. The raw

calculations again suggest an episode of rapid accumulation in the 1940s though because of the very low ^{210}Pb concentrations the results, shown in Figure 2.ii and given in detail in Table 4, have large uncertainties.

References

Appleby P.G., 2001. Chronostratigraphic techniques in recent sediments, in *Tracking Environmental Change Using Lake Sediments Volume 1: Basin Analysis, Coring, and Chronological Techniques*, (eds W M Last & J P Smol), Kluwer Academic, pp171-203.

Appleby,P.G., P.J.Nolan, D.W.Gifford, M.J.Godfrey, F.Oldfield, N.J.Anderson & R.W.Battarbee, 1986. ^{210}Pb dating by low background gamma counting. *Hydrobiologia*, **141**:21-27.

Appleby,P.G. & F.Oldfield, 1978. The calculation of ^{210}Pb dates assuming a constant rate of supply of unsupported ^{210}Pb to the sediment. *Catena*, **5**:1-8

Appleby,P.G., N.Richardson, & P.J.Nolan, 1992. Self-absorption corrections for well-type germaniun detectors. *Nucl. Inst.& Methods B*, **71**: 228-233.

Table 1. Fallout radionuclide concentrations in the Oslofjord sediment core BL-A

Depth		^{210}Pb Total		^{210}Pb Unsupported		^{210}Pb Supported		^{137}Cs	
cm	g cm^{-2}	Bq kg^{-1}	±	Bq kg^{-1}	±	Bq kg^{-1}	±	Bq kg^{-1}	±
0.5	0.13	178.9	10.8	126.0	11.0	52.9	2.2	25.5	1.6
2.5	0.74	197.4	9.5	138.1	9.8	59.3	2.2	21.8	1.6
3.5	1.13	180.0	14.5	108.1	14.9	71.9	3.2	24.3	2.0
4.5	1.56	152.9	10.3	88.4	10.6	64.5	2.5	34.4	1.9
5.5	1.98	150.6	14.0	88.5	14.4	62.2	3.4	52.3	3.0
6.5	2.36	160.2	10.2	95.3	10.5	64.8	2.5	31.9	1.9
7.5	2.72	143.4	9.6	87.2	9.9	56.1	2.4	22.5	1.7
8.5	3.01	140.1	9.2	79.5	9.4	60.7	2.2	19.5	1.7
9.5	3.26	107.9	10.9	54.1	11.2	53.8	2.5	21.3	1.9
10.5	3.51	73.7	5.6	33.6	5.8	40.1	1.4	12.6	1.0
11.5	3.77	86.3	7.1	39.0	7.3	47.3	1.6	6.0	1.0
12.5	4.09	133.5	13.5	8.1	13.9	125.4	3.5	3.2	1.4
13.5	4.48	45.6	7.5	9.8	7.8	35.9	1.9	3.5	0.7
14.5	4.98	19.7	3.4	5.5	3.5	14.1	0.8	12.6	0.7
15.5	5.44	33.4	7.8	7.7	8.0	25.7	1.8	5.4	1.2
16.5	5.74	33.2	6.1	7.8	6.3	25.3	1.4	1.2	0.7
17.5	6.02	47.5	5.7	8.1	5.9	39.4	1.4	3.3	0.8
18.5	6.30	59.5	5.7	15.6	5.9	44.0	1.5	0.0	0.0
19.5	6.60	45.0	5.7	1.3	5.9	43.7	1.5	0.7	0.8
21.0	7.08	51.8	7.1	8.6	7.3	43.2	1.8	0.2	1.0

Table 2. Fallout radionuclide concentrations in the Oslofjord sediment core VP-60-AA

Depth		^{210}Pb						^{137}Cs	
		Total		Unsupported		Supported			
cm	g cm^{-2}	Bq kg^{-1}	±	Bq kg^{-1}	±	Bq kg^{-1}	±	Bq kg^{-1}	±
0.5	0.14	109.4	8.7	73.0	8.9	36.4	1.9	15.7	1.4
1.5	0.45	118.2	8.9	85.6	9.1	32.6	1.8	8.4	1.0
2.5	0.81	129.3	8.3	91.6	8.5	37.7	1.7	10.0	1.2
3.5	1.23	133.9	9.7	93.0	9.9	40.9	2.1	13.7	1.3
4.5	1.68	112.6	8.6	73.2	8.8	39.4	1.9	11.4	1.2
5.5	2.17	92.3	7.7	45.3	7.8	47.0	1.7	7.8	1.0
6.5	2.69	79.8	8.2	41.1	8.3	38.6	1.7	8.9	1.2
7.5	3.24	64.8	6.8	29.4	7.0	35.3	1.6	8.2	1.1
8.5	3.84	63.5	6.1	25.2	6.3	38.3	1.5	6.7	0.8
9.5	4.46	51.9	6.2	13.7	6.4	38.2	1.5	5.8	0.9
10.5	5.08	40.4	5.4	2.6	5.6	37.8	1.4	4.6	0.8
12.5	6.38	46.2	5.3	4.0	5.4	42.3	1.2	5.4	0.8
14.5	7.69	50.9	5.5	7.2	5.7	43.7	1.4	4.2	0.8
16.5	8.95	47.2	5.8	2.7	6.0	44.5	1.4	2.8	0.7
18.5	10.26	43.1	5.1	0.4	5.2	42.6	1.2	3.6	0.8
19.5	10.92	45.4	5.3	7.0	5.4	38.5	1.3	2.0	0.7
21.0	11.90	53.5	5.5	11.2	5.6	42.4	1.2	2.0	0.8
23.0	13.20	36.1	5.1	-3.0	5.3	39.1	1.3	0.0	0.0
25.0	14.49	45.1	4.7	-4.8	4.8	49.9	1.1	0.8	0.6
29.0	17.53	39.1	4.8	-6.9	4.9	46.0	1.1	0.9	0.5

Table 3 ^{210}Pb chronology of the Oslofjord sediment core BL-A

Depth		Chronology			Sedimentation Rate		
		Date	Age				
cm	g cm^{-2}	AD	y	±	g cm^{-2} y^{-1}	cm y^{-1}	± (%)
0.0	0.00	2018	0	0			
0.5	0.13	2017	1	1	0.072	0.24	10.7
2.5	0.74	2008	10	2	0.065	0.20	10.5
3.5	1.13	2001	17	2	0.058	0.14	11.5
4.5	1.56	1994	24	3	0.056	0.13	11.5
5.5	1.98	1986	32	3	0.056	0.14	11.5
6.5	2.36	1979	39	4	0.056	0.15	11.5
7.5	2.72	1973	45	4	0.056	0.17	11.5
8.5	3.01	1968	50	5	0.056	0.21	11.5
9.5	3.26	1963	55	5	0.056	0.23	11.5
10.5	3.51	1959	59	6	0.056	0.22	11.5
11.5	3.77	1954	64	8	0.071	0.24	14.6
12.5	4.09	1951	67		0.128	0.36	
13.5	4.48	1949	69		0.205	0.46	
14.5	4.98	1946	72		0.223	0.47	
15.5	5.44	1944	74		0.209	0.54	
16.5	5.74	1943	75		0.176	0.61	
17.5	6.02	1941	77		0.134	0.48	
18.5	6.30	1939	79		0.070	0.46	

.

Table 4. ^{210}Pb chronology of the Oslofjord sediment core VP-60-AA

Depth		Chronology			Sedimentation Rate		
		Date	Age				
cm	g cm^{-2}	AD	y	±	g cm^{-2} y^{-1}	cm y^{-1}	± (%)
0.00	0.00	2018	0	0			
0.50	0.14	2017	1	1	0.105	0.35	16.9
1.50	0.45	2014	4	2	0.088	0.26	16.6
2.50	0.81	2009	9	2	0.071	0.18	17.4
3.50	1.23	2003	15	3	0.063	0.15	18.6
4.50	1.68	1995	23	3	0.063	0.13	18.6
5.50	2.17	1988	30	4	0.063	0.13	18.6
6.50	2.69	1979	39	5	0.063	0.12	18.6
7.50	3.24	1971	47	7	0.063	0.11	18.6
8.50	3.84	1961	57	8	0.063	0.11	18.6
9.50	4.46	1953	65		0.082	0.16	
10.50	5.08	1949	69		0.176	0.35	
12.50	6.38	1944	74		0.169	0.28	
14.50	7.69	1935	83		0.089	0.21	

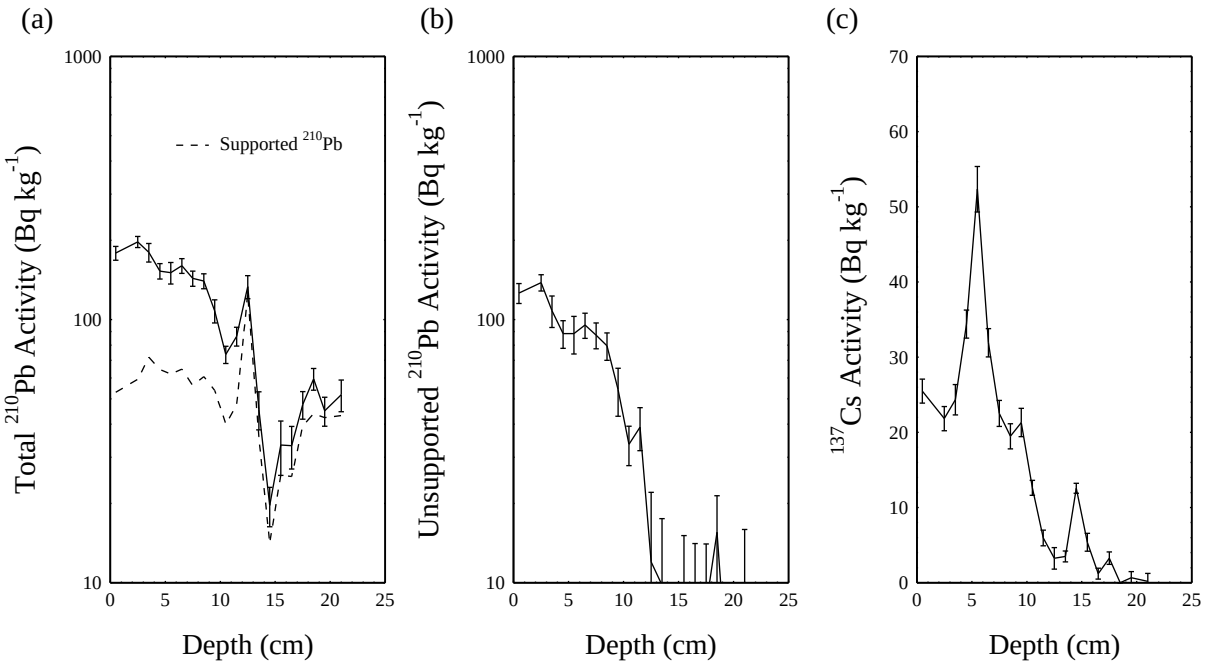

Figure 1.i. Fallout radionuclides in the Oslofjord sediment core BL-A showing (a) total and supported ^{210}Pb, (b) unsupported ^{210}Pb, (c) ^{137}Cs concentrations versus depth.

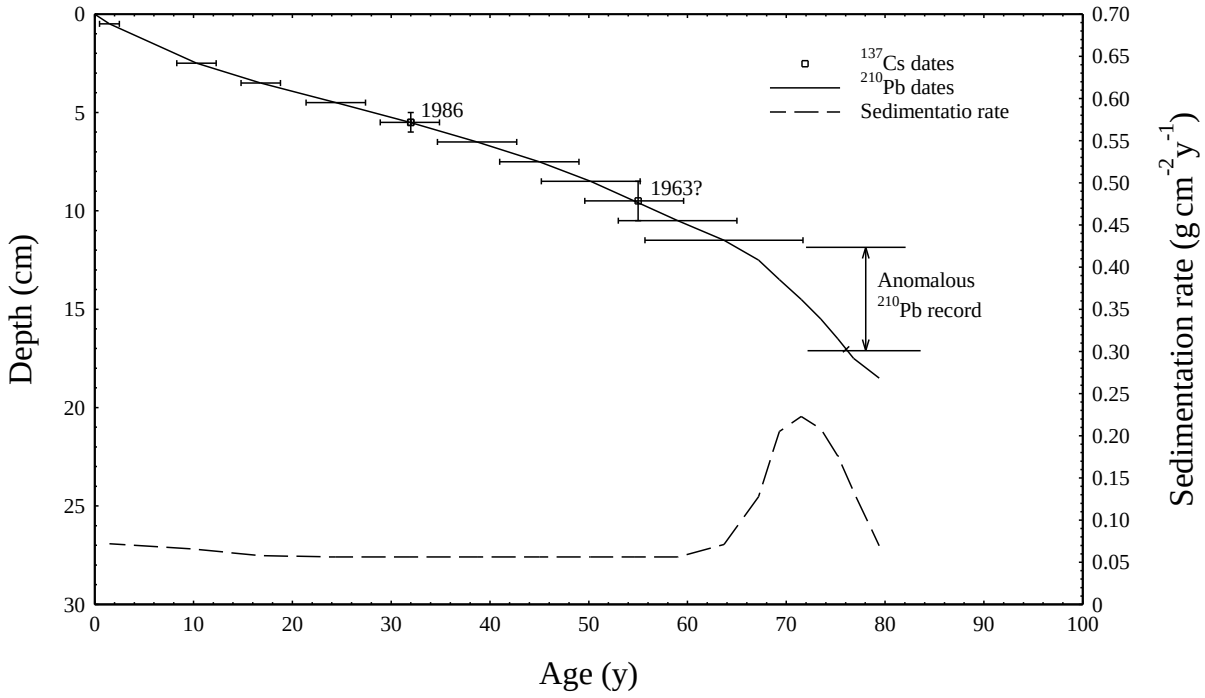

Figure 1.ii. Radiometric chronology of the Oslofjord sediment core BL-A showing the ^{210}Pb dates and sedimentation rates and the 1986 and 1963 depths suggested by the ^{137}Cs record. A small adjustment to the ^{210}Pb dates has been made using the ^{137}Cs dates as reference points.

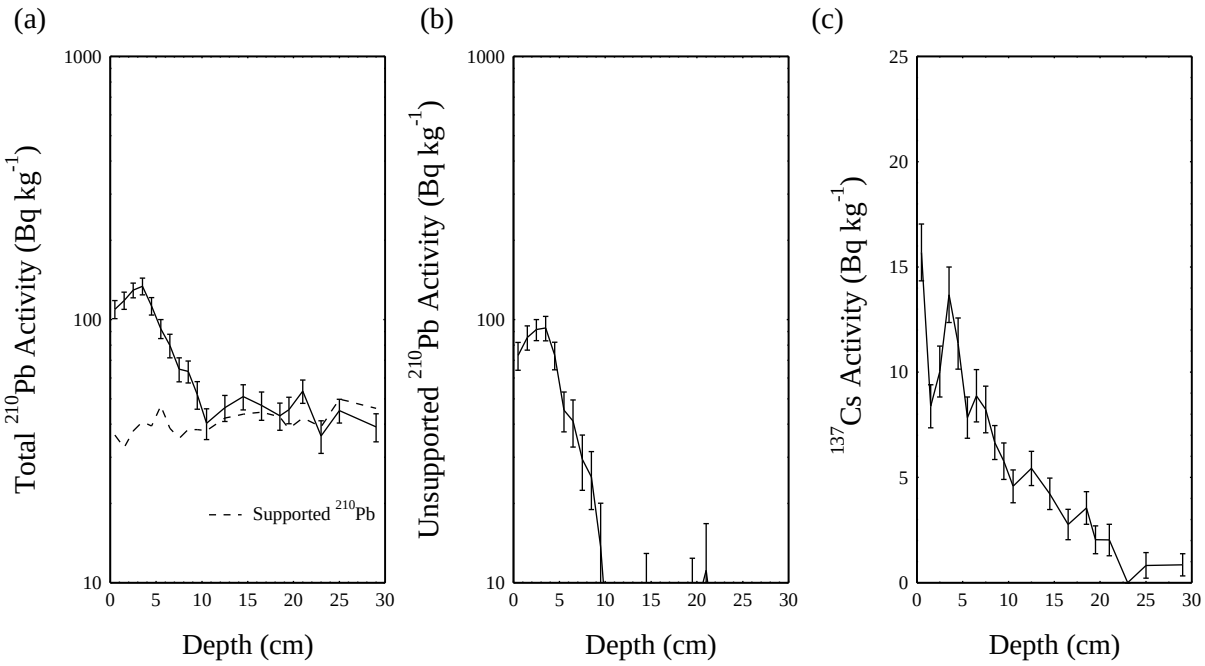

Figure 2.i. Fallout radionuclides in the Oslofjord sediment core VP-60-AA showing (a) total and supported ^{210}Pb, (b) unsupported ^{210}Pb, (c) ^{137}Cs concentrations versus depth.

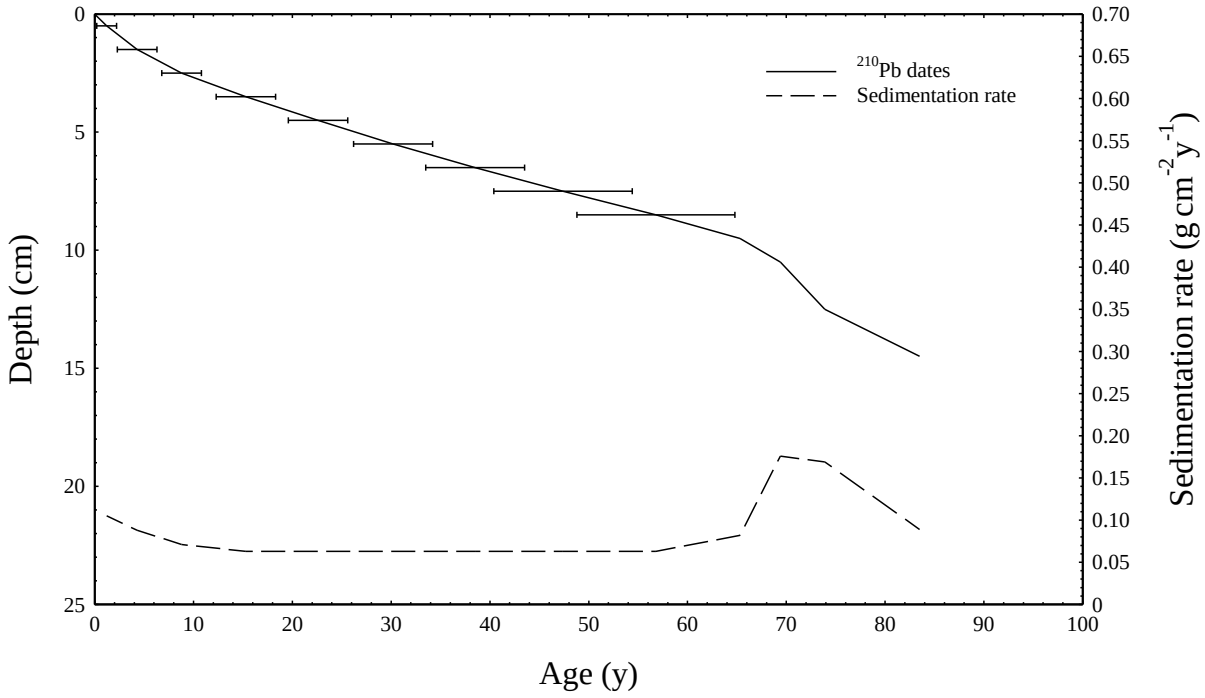

Figure 2.ii. Radiometric chronology of the Oslofjord sediment core VP-60-AA showing the ^{210}Pb dates and sedimentation rates.

Appendix D: Total organic carbon (TOC) and nitrogen (TN) raw and processed data

Table 13 *TOC and TN raw and processed data for the V-60-A18 sediment core collected on 03 May 2018 and processed by the UiO Biology Dept. Note that italicized data has been processed. Shaded areas indicate no values present.*

Sample No.	Core	Core interval (cm)	Core depth (cm)	*N (%)*	*C (%)*	Weight (mg)	*C/N ratio*	*N (%)*	*C (%)*	Weight (mg)	*C/N ratio*	*N (%)*	*C (%)*	Weight (mg)	*C/N ratio*	*Standard deviation of replicates (C%)*	*C(%) core (mean used if replicates available)*	*TOC_{63} (mg/g) based upon sand content from foram analysis*
1	**V-60-A18**	**0-1**	**0.5**	*0.55*	*4.81*	3.73	*8.77*	*0.51*	*4.94*	3.12	*9.68*	*0.55*	*4.61*	3.16	*8.45*	*0.14*	*4.79*	*51*
2	**V-60-A18**	**1-2**	**1.5**	*0.56*	*4.86*	3.64	*8.74*										*4.86*	*53*
3	**V-60-A18**	**2-3**	**2.5**	*0.52*	*4.03*	3.25	*7.79*										*4.03*	*45*
4	**V-60-A18**	**3-4**	**3.5**	*0.50*	*3.80*	3.21	*7.53*										*3.80*	*43*
5	**V-60-A18**	**4-5**	**4.5**	*0.45*	*3.60*	4.10	*7.97*										*3.60*	*41*
6	**V-60-A18**	**5-6**	**5.5**	*0.47*	*3.59*	3.38	*7.70*										*3.59*	
7	**V-60-A18**	**6-7**	**6.5**	*0.44*	*3.29*	3.01	*7.46*										*3.29*	
8	**V-60-A18**	**7-8**	**7.5**	*0.39*	*2.91*	3.82	*7.51*										*2.91*	
9	**V-60-A18**	**8-9**	**8.5**	*0.37*	*2.56*	3.39	*6.91*										*2.56*	
10	**V-60-A18**	**9-10**	**9.5**	*0.34*	*2.56*	4.40	*7.52*										*2.56*	*28*
11	**V-60-A18**	**10-11**	**10.5**	*0.32*	*2.19*	3.83	*6.91*	*0.33*	*2.21*	3.72	*6.69*	*0.36*	*2.13*	2.74	*5.87*	*0.03*	*2.18*	
12	**V-60-A18**	**11-12**	**11.5**	*0.27*	*1.74*	4.56	*6.38*										*1.74*	
13	**V-60-A18**	**12-13**	**12.5**	*0.29*	*1.78*	3.76	*6.03*										*1.78*	
14	**V-60-A18**	**13-14**	**13.5**	*0.29*	*1.84*	4.01	*6.39*										*1.84*	
15	**V-60-A18**	**14-15**	**14.5**	*0.33*	*1.93*	3.11	*5.84*										*1.93*	*21*
16	**V-60-A18**	**15-16**	**15.5**	*0.29*	*1.88*	4.35	*6.56*										*1.88*	
17	**V-60-A18**	**16-17**	**16.5**	*0.28*	*1.80*	4.21	*6.32*										*1.80*	
18	**V-60-A18**	**17-18**	**17.5**	*0.30*	*1.76*	3.92	*5.92*										*1.76*	
19	**V-60-A18**	**18-19**	**18.5**	*0.28*	*1.68*	4.17	*5.99*										*1.68*	
20	**V-60-A18**	**19-20**	**19.5**	*0.30*	*1.66*	3.26	*5.53*										*1.66*	*18*

Sample No.	Core	Core interval (cm)	Core depth (cm)	*N (%)*	*C (%)*	Weight (mg)	*C/N ratio*	*N (%)*	*C (%)*	Weight (mg)	*C/N ratio*	*N (%)*	*C (%)*	Weight (mg)	*C/N ratio*	*Standard deviation of replicates (C%)*	*C(%) core (mean used if replicates available)*	*TOC_{63} (mg/g) based upon sand content from foram analysis*
21	**V-60-A18**	**20-22**	**21**	*0.26*	*1.55*	4.25	*5.87*	*0.32*	*1.54*	2.86	*4.80*	*0.30*	*1.43*	2.82	*4.71*	*0.06*	*1.50*	
22	**V-60-A18**	**22-24**	**23**	*0.29*	*1.38*	3.25	*4.83*										*1.38*	
23	**V-60-A18**	**24-26**	**25**	*0.26*	*1.33*	3.88	*5.13*										*1.33*	*15*
24	**V-60-A18**	**26-28**	**27**	*0.24*	*1.20*	4.12	*5.01*										*1.20*	
25	**V-60-A18**	**28-30**	**29**	*0.24*	*1.03*	4.22	*4.30*										*1.03*	
26	**V-60-A18**	**30-32**	**31**	*0.24*	*1.07*	4.17	*4.51*	*0.26*	*1.06*	3.27	*4.05*	*0.29*	*1.07*	2.92	*3.73*	*0.00*	*1.07*	*12*

Table 14 *TOC and TN raw and processed data for the V-71-NW2 sediment core collected on 03 May 2018 and processed by the UiO Biology Dept. Note that italicized data has been processed. Shaded areas indicate no values present.*

Sample No.	Core	Core interval (cm)	Core depth (cm)	*N (%)*	*C (%)*	Weight (mg)	*C/N ratio*	*N (%)*	*C (%)*	Weight (mg)	*C/N ratio*	*N (%)*	*C (%)*	Weight (mg)	*C/N ratio*	*Standard deviation of replicates (C%)*
27	**V-71-NW2**	**0-1**	**0.5**	*0.65*	*6.21*	3.15	*9.63*	*0.79*	*6.23*	3.14	*7.90*	*0.79*	*6.15*	2.77	*7.82*	*0.03*
28	**V-71-NW2**	**1-2**	**1.5**	*0.67*	*5.65*	3.10	*8.41*									
29	**V-71-NW2**	**2-3**	**2.5**	*0.67*	*5.61*	3.19	*8.36*									
30	**V-71-NW2**	**3-4**	**3.5**	*0.61*	*5.26*	3.51	*8.61*									
31	**V-71-NW2**	**4-5**	**4.5**	*0.59*	*5.43*	3.95	*9.26*									
32	**V-71-NW2**	**5-6**	**5.5**	*0.56*	*4.72*	3.27	*8.43*									
33	**V-71-NW2**	**6-7**	**6.5**	*0.52*	*4.59*	3.34	*8.74*									
34	**V-71-NW2**	**7-8**	**7.5**	*0.49*	*4.09*	3.08	*8.30*									
35	**V-71-NW2**	**8-9**	**8.5**	*0.47*	*3.75*	3.30	*8.06*									
36	**V-71-NW2**	**9-10**	**9.5**	*0.40*	*3.37*	4.77	*8.46*									
37	**V-71-NW2**	**10-11**	**10.5**	*0.41*	*3.25*	3.50	*7.88*									
38	**V-71-NW2**	**11-12**	**11.5**	*0.38*	*2.54*	3.06	*6.62*									

Sample No.	Core	Core interval (cm)	Core depth (cm)	*N (%)*	*C (%)*	Weight (mg)	*C/N ratio*	*N (%)*	*C (%)*	Weight (mg)	*C/N ratio*	*N (%)*	*C (%)*	Weight (mg)	*C/N ratio*	*Standard deviation of replicates (C%)*
39	**V-71-NW2**	**12-13**	**12.5**	*0.37*	*2.75*	3.84	*7.50*									
40	**V-71-NW2**	**13-14**	**13.5**	*0.41*	*3.03*	3.58	*7.46*									
41	**V-71-NW2**	**14-15**	**14.5**	*0.37*	*2.72*	3.93	*7.44*	*0.36*	*2.75*	4.31	*7.54*	*0.36*	*2.66*	3.69	*7.30*	*0.03*
42	**V-71-NW2**	**15-16**	**15.5**	*0.36*	*2.62*	4.30	*7.28*									
43	**V-71-NW2**	**16-17**	**16.5**	*0.35*	*2.45*	4.16	*7.09*									
44	**V-71-NW2**	**17-18**	**17.5**	*0.34*	*2.33*	3.85	*6.76*									
45	**V-71-NW2**	**18-19**	**18.5**	*0.35*	*2.25*	3.61	*6.43*									
46	**V-71-NW2**	**19-20**	**19.5**	*0.32*	*2.11*	4.41	*6.60*									
47	**V-71-NW2**	**20-22**	**21**	*0.33*	*2.02*	4.03	*6.14*									
48	**V-71-NW2**	**22-24**	**23**	*0.32*	*1.86*	3.70	*5.83*									
49	**V-71-NW2**	**24-26**	**25**	*0.31*	*1.85*	4.48	*6.03*									
50	**V-71-NW2**	**26-28**	**27**	*0.33*	*1.75*	3.13	*5.31*									
51	**V-71-NW2**	**28-30**	**29**	*0.29*	*1.76*	4.24	*5.97*									
52	**V-71-NW2**	**30-32**	**31**	*0.31*	*1.74*	3.64	*5.58*									

Table 15 *TOC and TN raw and processed data for the surface core samples collected on 03 May 2018 and processed by the UiO Biology Dept. Note that italicized data has been processed. Shaded areas indicate no values present.*

Sample No.	Core	Core interval (cm)	Core depth (cm)	*N (%)*	*C (%)*	Weight (mg)	*C/N ratio*	*N (%)*	*C (%)*	Weight (mg)	*C/N ratio*	*N (%)*	*C (%)*	Weight (mg)	*C/N ratio*	*Standard deviation of replicates (C%)*
53	**V-75-SE1**	**0-1**	**0.5**	*0.60*	*4.46*	3.09	*7.47*									
54	**V-99-SE2**	**0-1**	**0.5**	*0.67*	*5.00*	3.49	*7.49*									
55	**V-87-NE1**	**0-1**	**0.5**	*0.62*	*4.67*	3.61	*7.49*									
56	**V-93-NE2**	**0-1**	**0.5**	*0.54*	*3.91*	3.90	*7.22*									
57	**V-66-NW1**	**0-1**	**0.5**	*0.71*	*5.79*	3.93	*8.19*	*0.71*	*5.72*	3.27	*8.06*	*0.72*	*5.88*	3.63	*8.17*	*0.06*

Appendix E: Trace metals raw and processed data

Table 16 *Metals analysis raw and processed data for sediment core V-60-A18 collected on 03 May 2018. Sample were processed on 07 November 2018. Note that values for Cd (highlighted in orange) were below the detection limit for the machine. Data for Hg (highlighted in yellow) is only analysized semi-quantitatively. Processed data appears in italics.*

Sample No.	Core interval (cm)	Core depth (cm)	Dry sample weight used for metal analyses (g)	Acid volume added to dry sample (mL)	Amount of sample added (dissolved in acid) (g)	Amount of sample and acid added for dilution (g)	*Dilution factor*	Cu (ppb)	% RSD	Zn (ppb)	% RSD	Cd (ppb)	% RSD	Hg (ppb)	% RSD	Pb (ppb)	% RSD	*Cu (mg/kg)*	*Zn (mg/kg)*	*Cd (mg/kg)*	*Pb (mg/kg)*	*Hg (mg/kg)*
1	0-1	0.5	1.0812	20	0.22	10.07	*46*	78.00	0.78	249.16	1.04	0.18	17.70	3.12	19.33	66.99	0.65	*66.05*	*210.96*	*0.15*	*56.72*	*2.64*
2	1-2	1.5	1.0826	20	0.22	10.05	*46*	79.75	1.30	262.55	2.30	0.26	24.16	3.22	12.36	67.45	0.58	*67.30*	*221.58*	*0.22*	*56.92*	*2.72*
3	2-3	2.5	1.0259	20	0.21	10.09	*48*	78.64	0.42	213.10	0.78	0.30	12.39	3.30	6.51	64.56	0.89	*73.67*	*199.61*	*0.29*	*60.47*	*3.09*
4	3-4	3.5	1.0394	20	0.23	10.05	*44*	80.57	0.81	219.84	1.46	0.35	12.26	3.23	11.60	65.14	0.40	*67.75*	*184.84*	*0.30*	*54.77*	*2.71*
5	4-5	4.5	1.0655	20	0.22	10.03	*46*	78.97	1.11	229.27	0.84	0.31	17.64	3.83	6.00	65.49	0.96	*67.58*	*196.20*	*0.27*	*56.05*	*3.28*
6	5-6	5.5	1.0605	20	0.22	10.06	*46*	70.84	1.06	222.94	1.27	0.34	18.21	3.10	7.93	64.26	0.83	*61.09*	*192.26*	*0.29*	*55.41*	*2.68*
7	6-7	6.5	1.0474	20	0.22	10.05	*46*	63.85	0.25	221.81	1.03	0.31	4.15	2.90	4.08	65.29	0.93	*55.70*	*193.48*	*0.27*	*56.95*	*2.53*
8	7-8	7.5	1.0343	20	0.22	10.04	*46*	59.59	0.78	217.63	0.85	0.29	21.02	2.96	6.60	64.31	0.80	*52.58*	*192.05*	*0.26*	*56.75*	*2.61*
9	8-9	8.5	1.0735	20	0.22	10.06	*46*	52.90	1.49	218.33	0.47	0.28	13.08	2.96	10.41	62.84	1.09	*45.06*	*186.00*	*0.24*	*53.54*	*2.52*
10	9-10	9.5	1.0901	20	0.22	10.08	*46*	49.33	0.53	220.74	0.59	0.26	27.13	2.87	5.31	64.16	1.19	*41.47*	*185.56*	*0.22*	*53.94*	*2.41*
11	10-11	10.5	1.0452	20	0.23	10.07	*44*	41.19	0.49	197.79	1.10	0.20	19.52	2.28	16.54	56.16	1.21	*34.50*	*165.71*	*0.17*	*47.05*	*1.91*
12	11-12	11.5	0.9993	20	0.22	10.06	*46*	31.63	1.24	173.32	0.90	0.16	21.91	1.81	3.48	46.28	0.56	*28.95*	*158.62*	*0.15*	*42.35*	*1.66*
13	12-13	12.5	1.0466	20	0.23	10.06	*44*	33.44	0.69	175.22	1.03	0.20	7.53	1.61	9.95	46.62	0.74	*27.95*	*146.46*	*0.17*	*38.97*	*1.34*
14	13-14	13.5	1.0636	20	0.22	10.05	*46*	35.27	0.44	217.08	0.28	0.20	21.94	2.22	8.37	53.45	0.53	*30.30*	*186.47*	*0.17*	*45.91*	*1.90*
15	14-15	14.5	1.0615	20	0.22	10.07	*46*	34.67	1.36	244.26	1.05	0.21	13.06	2.41	6.51	55.95	0.49	*29.90*	*210.65*	*0.18*	*48.26*	*2.08*
16	15-16	15.5	1.0235	20	0.23	10.07	*44*	31.55	0.48	228.49	1.04	0.17	15.59	1.91	8.37	52.95	1.02	*26.99*	*195.48*	*0.15*	*45.30*	*1.64*
17	16-17	16.5	1.0558	20	0.22	10.08	*46*	30.53	1.01	195.69	1.18	0.19	19.66	2.01	9.76	51.42	0.76	*26.50*	*169.84*	*0.16*	*44.63*	*1.75*
18	17-18	17.5	1.0195	20	0.22	10.05	*46*	28.38	0.62	179.08	0.61	0.16	17.43	1.57	5.39	45.45	0.45	*25.43*	*160.49*	*0.14*	*40.73*	*1.40*
19	18-19	18.5	1.0593	20	0.22	10.06	*46*	28.93	1.67	176.14	0.57	0.14	21.87	1.48	16.05	43.18	0.76	*24.98*	*152.07*	*0.12*	*37.28*	*1.28*
20	19-20	19.5	1.0785	20	0.22	10.07	*46*	30.38	0.82	176.37	0.65	0.14	26.79	1.38	10.00	42.83	0.59	*25.79*	*149.71*	*0.12*	*36.35*	*1.17*
21	20-22	21	1.0521	20	0.22	10.05	*46*	27.02	1.02	161.64	2.16	0.10	38.45	1.00	7.14	37.69	1.02	*23.46*	*140.37*	*0.09*	*32.73*	*0.87*
22	22-24	23	1.0479	20	0.23	10.06	*44*	22.91	1.70	143.62	1.06	0.11	8.26	0.75	21.84	31.14	1.49	*19.12*	*119.90*	*0.09*	*26.00*	*0.63*

Sample No.	Core interval (cm)	Core depth (cm)	Dry sample weight used for metal analyses (g)	Acid volume added to dry sample (mL)	Amount of sample added (dissolved in acid) (g)	Amount of sample and acid added for dilution (g)	*Dilution factor*	Cu (ppb)	% RSD	Zn (ppb)	% RSD	Cd (ppb)	% RSD	Hg (ppb)	% RSD	Pb (ppb)	% RSD	*Cu (mg/kg)*	*Zn (mg/kg)*	*Cd (mg/kg)*	*Pb (mg/kg)*	*Hg (mg/kg)*
23	**24-26**	**25**	**1.0894**	20	0.23	10.05	*44*	23.97	1.32	148.33	1.21	0.06	41.67	0.54	25.46	31.20	1.04	*19.23*	*118.99*	*0.05*	*25.03*	*0.43*
24	**26-28**	**27**	**1.0551**	20	0.23	10.09	*44*	21.59	0.78	124.95	1.54	0.08	40.01	0.27	70.51	23.14	0.80	*17.96*	*103.91*	*0.07*	*19.25*	*0.23*
25	**28-30**	**29**	**1.0575**	20	0.22	10.08	*46*	21.32	1.10	121.17	1.57	0.08	20.24	0.17	58.37	21.14	0.25	*18.48*	*105.00*	*0.07*	*18.32*	*0.15*
26	**30-32**	**31**	**1.0594**	20	0.23	10.08	*44*	21.37	1.14	119.28	1.11	0.06	53.74	0.24	31.54	20.86	0.61	*17.68*	*98.69*	*0.05*	*17.26*	*0.20*

Table 17 *Metals analysis raw and processed data for sediment core V-71-NW2 collected on 03 May 2018. Sample were processed on 07 November 2018. Note that values for Cd (highlighted in orange) were below the detection limit for the machine. Data for Hg (highlighted in yellow) is only analysized semi-quantitatively. Processed data appears in italics.*

Sample No.	Core interval (cm)	Core depth (cm)	Dry sample weight used for metal analyses (g)	Acid volume added to dry sample (ml)	Amount of sample added (dissolved in acid) (g)	Amount of acid added for dilution (g)	*Dilution factor*	Cu (ppb)	% RSD	Zn (ppb)	% RSD	Cd (ppb)	% RSD	Hg (ppb)	% RSD	Pb (ppb)	% RSD	*Cu (mg/kg)*	*Zn (mg/kg)*	*Cd (mg/kg)*	*Pb (mg/kg)*	*Hg (mg/kg)*
27	**0-1**	**0.5**	1.0459	20	0.22	10.10	*46*	84.79	0.52	241.39	0.88	0.16	23.39	2.90	4.20	72.14	1.24	*74.44*	*211.91*	*0.14*	*63.33*	*2.55*
28	**1-2**	**1.5**	1.0244	20	0.21	10.06	*48*	98.47	0.46	278.75	1.04	0.29	31.68	3.49	8.64	81.73	1.03	*92.10*	*260.71*	*0.27*	*76.44*	*3.26*
29	**2-3**	**2.5**	1.0533	20	0.21	10.07	*48*	105.20	1.26	303.63	0.79	0.32	15.55	4.15	4.40	88.78	0.65	*95.79*	*276.46*	*0.30*	*80.84*	*3.77*
30	**3-4**	**3.5**	1.0239	20	0.22	10.06	*46*	103.39	1.09	304.10	0.37	0.40	18.44	3.98	8.45	89.77	0.53	*92.34*	*271.62*	*0.36*	*80.18*	*3.55*
31	**4-5**	**4.5**	1.1107	20	0.22	10.06	*46*	111.39	1.27	342.98	0.99	0.43	14.55	5.89	6.18	105.33	0.45	*91.72*	*282.41*	*0.36*	*86.73*	*4.85*
32	**5-6**	**5.5**	1.0876	20	0.22	10.05	*46*	106.43	1.10	343.75	1.35	0.44	21.32	4.94	2.66	110.68	1.17	*89.40*	*288.76*	*0.37*	*92.97*	*4.15*
33	**6-7**	**6.5**	1.0464	20	0.22	10.06	*46*	91.29	1.26	326.43	1.41	0.41	18.51	4.65	4.48	104.26	0.46	*79.79*	*285.29*	*0.35*	*91.12*	*4.06*
34	**7-8**	**7.5**	1.0642	20	0.22	10.06	*46*	81.58	0.45	327.52	0.61	0.40	13.28	4.79	7.64	102.11	0.84	*70.11*	*281.46*	*0.34*	*87.75*	*4.12*
35	**8-9**	**8.5**	1.0155	20	0.22	10.05	*46*	71.18	0.65	312.57	0.77	0.41	20.89	4.31	4.42	94.16	0.79	*64.04*	*281.22*	*0.37*	*84.71*	*3.88*
36	**9-10**	**9.5**	1.0984	20	0.22	10.07	*46*	70.11	0.83	336.14	0.89	0.42	14.75	4.33	3.74	96.69	0.95	*58.43*	*280.15*	*0.35*	*80.58*	*3.61*
37	**10-11**	**10.5**	1.0498	20	0.21	10.07	*48*	56.76	0.76	282.78	1.29	0.35	10.10	3.70	6.92	81.08	0.77	*51.85*	*258.33*	*0.32*	*74.07*	*3.38*
38	**11-12**	**11.5**	1.0554	20	0.22	10.06	*46*	54.20	0.30	282.60	0.73	0.31	14.04	3.38	8.01	80.62	0.36	*46.96*	*244.88*	*0.27*	*69.86*	*2.93*
39	**12-13**	**12.5**	1.0435	20	0.22	10.06	*46*	49.99	0.55	285.56	0.79	0.33	24.83	3.07	4.33	81.25	0.74	*43.81*	*250.27*	*0.28*	*71.21*	*2.69*
40	**13-14**	**13.5**	1.0516	20	0.22	10.07	*46*	44.24	1.07	260.95	1.34	0.28	10.65	2.87	4.77	74.31	1.35	*38.51*	*227.17*	*0.25*	*64.69*	*2.50*
41	**14-15**	**14.5**	1.0705	20	0.22	10.09	*46*	44.51	0.60	272.71	1.25	0.26	20.91	2.68	10.21	75.94	0.51	*38.13*	*233.68*	*0.23*	*65.07*	*2.29*

Sample No.	Core interval (cm)	Core depth (cm)	Dry sample weight used for metal analyses (g)	Acid volume added to dry sample (ml)	Amount of sample added (dissolved in acid) (g)	Amount of acid added for dilution (g)	*Dilution factor*	Cu (ppb)	% RSD	Zn (ppb)	% RSD	Cd (ppb)	% RSD	Hg (ppb)	% RSD	Pb (ppb)	% RSD	*Cu (mg/kg)*	*Zn (mg/kg)*	*Cd (mg/kg)*	*Pb (mg/kg)*	*Hg (mg/kg)*
42	**15-16**	**15.5**	1.0259	20	0.23	10.05	*44*	41.54	0.86	256.15	0.51	0.26	18.47	2.21	7.13	69.97	0.57	*35.39*	*218.21*	*0.22*	*59.60*	*1.89*
43	**16-17**	**16.5**	1.0442	20	0.23	10.09	*44*	37.08	0.77	220.51	1.05	0.23	23.21	1.78	7.57	59.29	0.87	*31.15*	*185.29*	*0.19*	*49.82*	*1.49*
44	**17-18**	**17.5**	1.0675	20	0.22	10.08	*46*	34.95	0.43	211.06	1.00	0.17	12.67	1.44	8.56	55.32	0.81	*30.00*	*181.17*	*0.15*	*47.49*	*1.24*
45	**18-19**	**18.5**	1.0533	20	0.23	10.07	*44*	32.55	0.57	192.61	1.08	0.19	7.04	1.17	10.09	49.94	0.24	*27.06*	*160.13*	*0.15*	*41.52*	*0.97*
46	**19-20**	**19.5**	1.051	20	0.22	10.07	*46*	31.41	1.07	179.45	1.13	0.17	21.15	0.78	9.77	43.29	0.67	*27.36*	*156.30*	*0.15*	*37.71*	*0.68*
47	**20-22**	**21**	1.0403	20	0.22	10.10	*46*	29.40	0.83	160.41	1.09	0.13	15.04	0.41	39.65	35.53	0.37	*25.95*	*141.58*	*0.11*	*31.36*	*0.36*
48	**22-24**	**23**	1.058	20	0.22	10.08	*46*	28.55	1.57	153.18	0.84	0.11	15.51	0.34	13.79	32.00	0.19	*24.73*	*132.67*	*0.10*	*27.72*	*0.30*
49	**24-26**	**25**	1.1255	20	0.21	10.06	*48*	29.41	0.54	156.40	0.91	0.10	16.03	0.33	19.53	31.99	0.44	*25.03*	*133.14*	*0.08*	*27.23*	*0.28*
50	**26-28**	**27**	1.0558	20	0.21	10.08	*48*	27.00	1.28	144.43	1.24	0.10	27.52	0.18	36.55	27.97	0.44	*24.55*	*131.32*	*0.09*	*25.43*	*0.17*
51	**28-30**	**29**	1.1598	20	0.22	10.09	*46*	29.80	0.63	158.97	0.77	0.11	31.54	0.21	38.83	30.13	0.76	*23.57*	*125.72*	*0.08*	*23.83*	*0.17*
52	**30-32**	**31**	1.0769	20	0.22	10.09	*46*	27.52	0.98	145.98	0.67	0.09	20.59	0.17	16.31	27.31	0.81	*23.44*	*124.34*	*0.08*	*23.26*	*0.15*

Table 18 *Metals analysis raw and processed data for sediment surface samples collected on 03 May 2018. Sample were processed on 07 November 2018. Note that values for Cd (highlighted in orange) were below the detection limit for the machine. Data for Hg (highlighted in yellow) is only analysized semi-quantitatively. Processed data appears in italics.*

Sample No.	Core	Core interval (cm)	Core depth (cm)	Dry sample weight used for metal analyses (g)	Acid volume added (ml)	Amount of sample added (dissolved in acid) (g)	Amount of acid added for dilution (g)	*Dilution factor*	Cu (ppb)	%RSD	Zn (ppb)	%RSD	Cd (ppb)	%RSD	Hg (ppb)	%RSD	Pb (ppb)	%RSD	*Cu (mg/kg)*	*Zn (mg/kg)*	*Cd (mg/kg)*	*Pb (mg/kg)*	*Hg (mg/kg)*
53	**V-75-SE1**	**0-1**	**0.5**	1.0997	20	0.22	10.10	*46*	73.63	0.26	285.68	1.00	0.14	33.04	2.61	5.39	73.66	0.65	*61.48*	*238.52*	*0.11*	*61.50*	*2.18*
54	**V-99-SE2**	**0-1**	**0.5**	1.0757	20	0.22	10.09	*46*	73.26	0.75	341.56	0.70	0.15	20.15	2.63	7.43	78.68	0.59	*62.47*	*291.26*	*0.13*	*67.09*	*2.24*
55	**V-87-NE1**	**0-1**	**0.5**	1.0713	20	0.21	10.10	*48*	69.20	0.53	318.82	1.11	0.14	12.04	2.25	6.04	74.08	0.80	*62.13*	*286.26*	*0.13*	*66.52*	*2.02*
56	**V-93-NE2**	**0-1**	**0.5**	1.0965	20	0.22	10.08	*46*	57.12	0.80	319.45	0.64	0.12	23.20	1.71	5.40	57.11	0.67	*47.74*	*266.97*	*0.10*	*47.73*	*1.43*
57	**V-66-NW1**	**0-1**	**0.5**	1.0919	20	0.21	10.09	*48*	90.09	0.51	335.52	0.85	0.16	12.41	2.78	10.83	80.70	0.67	*79.28*	*295.29*	*0.14*	*71.02*	*2.44*

QICPMS test and instrument information report provided for metals analysis dated 07 November 2018 (tables 16, 17 and 18).

Solution ICPMS 071118

Instrument: Bruker Aurora Elite, equipped with a Cetac ASX-250 autosampler and an ESI oneFAST sample introduction system.

Acid used: 1% single distilled nitric acid (HNO_3).

Calibration standard: All elements, with the exception of Pb which does not use 1000 ppb, were calibrated using the 6020 Calibration Standard (Inorganic Ventures) at 1, 10, 100 and 1000 ppb.

Standard solutions run as unknown: CRM-TMDW-A (High-Purity Standards). See certified values below.

Isotopes analyzed: ^{63}Cu, ^{66}Zn, ^{111}Cd, ^{202}Hg, $^{206,207,208}Pb$ (analyzed in He collision gas mode). NB! Hg was analyzed semi-quantitatively.

Internal standards: Cu, Zn, Cd: ^{103}Rh. Hg, Pb: ^{209}Bi

Certified values for TMDW. All values in µg/L.

Cu	Zn	Cd	Hg	Pb
20	75	10	--	20

Standards run as part of metals analysis dated 07 November 2018. Orange highlighted values are below the detection limit for the testing machine. Note that Hg was analyzed semi-qualitatively.

Standards run as unknown	Cu (ppb)	%RSD	Zn (ppb)	%RSD	Cd (ppb)	%RSD	Hg (ppb)	%RSD	Pb (ppb)	%RSD
1%HNO3_blank	-0.0036	91.4	-0.0056	448.2	-0.005	0	-0.0323	94.73	0.0002	618.2
TMDW	20.326	0.8	75.263	1.7	9.855	5.37	-0.037	137.5	19.8361	0.6
TMDW	22.4689	0.63	81.8351	2.28	9.727	4.05	-0.0206	287.9	19.6399	0.72
6020-100ppb	114.7921	0.18	113.6276	0.97	101.9927	0.63	0.0113	75.66	98.9753	0.98
Detection limit of method	0.006045		0.03069		0.013037		0.052576		0.010346	

Appendix F: Reliability of analyses raw and processed data

Table 19 *TOC and TN raw and processed data for sediment core V-60-A17 retested in 2019 by the UiO Biology Dept. Note that shaded areas indicate no data present and processed data is italicized. Standard deviation calculations are for standard deviation of population (Excel). The abbreviation "Abd" is used to denote that these sample were collected using the Abdullah corer.*

Sample No.	Core	Core interval (cm)	Core depth (cm)	Sample weight (mg)	*N (%)*	*C (%)*	*C/N ratio*	Sample weight (mg)	*N (%)*	*C (%)*	*C/N ratio*	Sample weight (mg)	*N (%)*	*C (%)*	*C/N ratio*	*Mean C/N ratio - Bio processed samples*	*Standard deviation C/N ratio - Bio processed samples*	*Mean of C (%) for Bio. processed samples and replicates*	*Standard deviation of replicates (C%)*
1	V-60-A17	0-1	0.5	3.213	*0.48*	*6.26*	*13.14*	4.19	*0.56*	*6.59*	*11.85*	3.36	*0.55*	*6.54*	*11.87*	*12.29*	*0.60*	*6.46*	*0.15*
2	V-60-A17	1-2	1.5	3.859	*0.48*	*6.03*	*12.61*									*12.61*		*6.03*	
3	V-60-A17	2-3	2.5	4.396	*0.46*	*5.67*	*12.31*									*12.31*		*5.67*	
4	V-60-A17	3-4	3.5	4.373	*0.47*	*5.75*	*12.22*									*12.22*		*5.75*	
5	V-60-A17	4-5	4.5	3.835	*0.42*	*4.96*	*11.82*	4.39	*0.48*	*5.81*	*12.18*	4.49	*0.44*	*5.61*	*12.64*	*12.21*	*0.33*	*5.46*	*0.36*
6	V-60-A17	5-6	5.5	5.402	*0.45*	*5.51*	*12.10*									*12.10*		*5.51*	
7	V-60-A17	6-7	6.5	4.175	*0.46*	*5.72*	*12.31*									*12.31*		*5.72*	
8	V-60-A17	7-8	7.5	4.474	*0.42*	*5.12*	*12.27*									*12.27*		*5.12*	
9	V-60-A17	8-9	8.5	4.785	*0.39*	*4.66*	*12.03*	4.24	*0.37*	*4.46*	*11.98*	2.86	*0.44*	*4.87*	*11.10*	*11.70*	*0.43*	*4.66*	*0.17*
10	V-60-A17	9-10	9.5	3.218	*0.38*	*4.19*	*10.90*									*10.90*		*4.19*	
11	V-60-A17	10 - 12	11	4.889	*0.29*	*3.06*	*10.73*									*10.73*		*3.06*	
12	V-60-A17	12 - 14	13	4.955	*0.22*	*2.24*	*10.03*									*10.03*		*2.24*	
13	V-60-A17	14 - 16	15	5.094	*0.23*	*2.20*	*9.75*	3.82	*0.22*	*1.87*	*8.35*	5.77	*0.19*	*1.79*	*9.40*	*9.17*	*0.60*	*1.95*	*0.18*
14	V-60-A17	16 - 18	17	5.302	*0.19*	*1.67*	*8.74*									*8.74*		*1.67*	
15	V-60-A17	18 - 20	19	5.983	*0.18*	*1.56*	*8.80*									*8.80*		*1.56*	
16	V-60-A17	20 - 22	21	3.802	*0.20*	*1.40*	*7.06*									*7.06*		*1.40*	
17	V-60-A17	22 - 24	23	5.025	*0.20*	*1.81*	*9.00*	3.94	*0.21*	*1.73*	*8.26*	4.26	*0.21*	*1.76*	*8.41*	*8.56*	*0.32*	*1.77*	*0.03*
18	V-60-A17; Abd	40-45	42.5	6.038	*0.13*	*0.83*	*6.53*									*6.53*		*0.83*	
19	V-60-A17; Abd	50-55	52.5	6.214	*0.13*	*0.87*	*6.62*									*6.62*		*0.87*	

Table 20 *TOC and TN raw and processed data for sediment core V-60-A17 retested in 2019 by the UiO Geology Dept. (Sedimentology Lab). Note that processed data is italicized. Standard deviation calculations are for standard deviation of population (Excel). The abbreviation "Abd" is used to denote that these samples were collected using the Abdullah corer. Final column (shaded blue) reflects standard deviations for values presented in tables 19 and 20.*

Sample No.	Core	Core interval (cm)	Core depth (cm)	Sample weight (mg)	N (%)	C (%)	*C/N ratio*	Sample weight (mg)	N (%)	C (%)	*C/N ratio*	Mean C/N ratio - Sed. processed samples	Mean of C (%) for Sed. processed samples	*Standard deviation of replicates (C%)*	Standard deviation C/N ratio - Sed. processed samples	Standard deviation of C/N ration for second test (both labs)
1	V-60-A17	0-1	0.5	7.82	0.72	6.67	*9.29*	7.86	0.73	6.66	*9.08*	9.19	6.66	0.01	0.11	3.45
2	V-60-A17	1-2	1.5	7.95	0.67	6.31	*9.43*	8.11	0.64	6.09	*9.48*	9.45	6.20	0.11	0.03	4.15
3	V-60-A17	2-3	2.5	7.64	0.63	6.25	*9.96*	7.84	0.62	6.06	*9.81*	9.89	6.16	0.10	0.08	4.37
4	V-60-A17	3-4	3.5	8.05	0.58	5.87	*10.17*	8.06	0.59	5.90	*9.94*	10.05	5.88	0.01	0.12	4.46
5	V-60-A17	4-5	4.5	7.96	0.55	5.60	*10.13*	7.92	0.55	5.55	*10.11*	10.12	5.57	0.03	0.01	3.95
6	V-60-A17	5-6	5.5	8.55	0.52	5.31	*10.28*	8.72	0.50	5.22	*10.35*	10.32	5.26	0.04	0.03	4.63
7	V-60-A17	6-7	6.5	8.80	0.48	4.96	*10.33*	8.70	0.46	4.96	*10.69*	10.51	4.96	0.00	0.18	4.74
8	V-60-A17	7-8	7.5	7.78	0.41	4.67	*11.32*	7.68	0.43	4.76	*11.03*	11.18	4.71	0.05	0.15	5.07
9	V-60-A17	8-9	8.5	8.00	0.42	4.55	*10.94*	8.17	0.42	4.50	*10.77*	10.85	4.52	0.03	0.09	4.44
10	V-60-A17	9-10	9.5	8.88	0.42	4.35	*10.42*	8.52	0.42	4.26	*10.25*	10.34	4.30	0.04	0.09	4.68
11	V-60-A17	10 - 12	11	7.30	0.21	2.82	*13.45*	7.49	0.23	2.93	*12.58*	13.01	2.88	0.06	0.44	6.04
12	V-60-A17	12 - 14	13	7.70	0.14	2.10	*14.90*	7.39	0.14	2.15	*15.58*	15.24	2.13	0.02	0.34	7.12
13	V-60-A17	14 - 16	15	9.48	0.12	1.65	*14.29*	9.16	0.11	1.70	*14.89*	14.59	1.68	0.03	0.30	6.87
14	V-60-A17	16 - 18	17	7.19	0.07	1.64	*22.81*	6.86	0.06	1.64	*26.75*	24.78	1.64	0.00	1.97	11.76
15	V-60-A17	18 - 20	19	7.01	0.04	1.43	*35.06*	6.47	0.03	1.43	*45.66*	40.36	1.43	0.00	5.30	19.50
16	V-60-A17	20 - 22	21	8.28	0.08	1.45	*19.04*	8.28	0.08	1.49	*18.82*	18.93	1.47	0.02	0.11	8.89
17	V-60-A17	22 - 24	23	6.80	0.06	1.64	*29.09*	6.96	0.06	1.66	*26.31*	27.70	1.65	0.01	1.39	13.47
18	V-60-A17; Abd	40-45	42.5	7.86	0.00	0.84	*0.00*	7.24	0.00	0.87	*0.00*	0.00	0.85	0.01	0.00	0.00
19	V-60-A17; Abd	50-55	52.5	7.74	0.00	0.86	*0.00*	7.52	0.00	0.86	*0.00*	0.00	0.86	0.00	0.00	0.00

Table 21 *Metals analysis raw and processed data for retested sediment core V-60-A17 (discussed as V-60-A17_repeat in text). Samples were processed on 14 January 2019. Data for Hg (highlighted in yellow) is only analysized semi-quantitatively. Processed data appears in italics. The abbreviation "Abd" is used to denote that these samples were collected using the Abdullah corer.*

Sample No.	Core	Core interval (cm)	Core depth (cm)	Dry sample weight used for metal analyses (g)	Acid volume added to dry sample (mL)	Amount of sample added (dissolved in acid) (g)	Amount of sample and acid added for dilution (g)	*Dilution factor*	Cu (ppb)	% RSD	Zn (ppb)	% RSD	Cd (ppb)	% RSD	Hg (ppb)	% RSD	Pb (ppb)	% RSD	*Cu (mg/kg)*	*Zn (mg/kg)*	*Cd (mg/kg)*	*Pb (mg/kg)*	*Hg (mg/kg)*
1	V-60-A17	0-1	0.5	1.0026	21	0.22	10.05	*46*	113.40	0.49	209.89	0.67	0.32	4.09	4.42	6.69	64.78	1.20	108.50	200.83	0.31	61.98	4.23
2	V-60-A17	1-2	1.5	1.0060	21	0.22	10.07	*46*	139.29	0.60	260.81	0.95	0.49	3.53	5.53	2.28	78.49	0.55	133.09	249.21	0.47	75.00	5.28
3	V-60-A17	2-3	2.5	1.0254	21	0.21	10.06	*48*	134.37	0.26	258.46	0.99	0.55	2.57	5.44	5.07	74.79	0.79	131.83	253.57	0.54	73.37	5.34
4	V-60-A17	3-4	3.5	1.0348	21	0.21	10.07	*48*	140.43	0.80	275.97	0.85	0.59	1.06	5.58	2.22	76.95	1.39	136.65	268.56	0.58	74.88	5.43
5	V-60-A17	4-5	4.5	1.0294	21	0.21	10.06	*48*	141.30	0.41	290.24	0.43	0.66	2.18	5.89	2.08	79.38	0.95	138.08	283.64	0.65	77.57	5.76
6	V-60-A17	5-6	5.5	1.0208	21	0.22	10.06	*46*	128.70	0.57	271.97	0.65	0.64	3.89	5.06	2.91	74.61	0.97	121.08	255.86	0.60	70.19	4.76
7	V-60-A17	6-7	6.5	1.0382	21	0.21	10.05	*48*	129.99	0.91	283.27	0.45	0.71	3.35	5.57	4.56	79.67	0.39	125.83	274.21	0.69	77.12	5.40
8	V-60-A17	7-8	7.5	1.0074	21	0.22	10.06	*46*	125.23	0.61	288.98	0.71	0.71	2.18	5.15	2.98	79.15	0.87	119.37	275.47	0.67	75.44	4.91
9	V-60-A17	8-9	8.5	1.0283	21	0.21	10.05	*48*	137.24	0.36	319.06	0.50	0.76	2.60	5.55	5.90	85.59	0.81	134.13	311.84	0.75	83.65	5.42
10	V-60-A17	9-10	9.5	1.0100	21	0.22	10.05	*46*	141.46	0.59	335.75	0.87	0.79	0.85	5.64	2.09	88.96	0.97	134.36	318.91	0.75	84.49	5.35
11	V-60-A17	10 - 12	11	1.0003	21	0.22	10.05	*46*	86.10	1.01	261.36	0.56	0.55	3.36	3.72	7.09	69.88	0.55	82.57	250.64	0.53	67.01	3.56
12	V-60-A17	12 - 14	13	1.0304	21	0.22	10.06	*46*	52.52	0.45	187.87	1.07	0.32	2.24	2.14	8.46	48.14	0.61	48.94	175.08	0.29	44.86	2.00
13	V-60-A17	14 - 16	15	1.0130	21	0.22	10.07	*46*	35.41	0.28	157.12	1.17	0.21	3.59	1.44	10.50	36.69	0.77	33.60	149.09	0.20	34.82	1.36
14	V-60-A17	16 - 18	17	1.0379	21	0.22	10.04	*46*	31.80	0.44	145.06	0.37	0.18	4.73	1.26	9.38	33.97	0.36	29.36	133.94	0.17	31.37	1.16
15	V-60-A17	18 - 20	19	1.0329	21	0.21	10.05	*48*	26.34	0.56	128.65	0.34	0.14	4.88	0.72	11.75	27.64	0.53	25.62	125.18	0.13	26.89	0.70
16	V-60-A17	20 - 22	21	1.0140	21	0.21	10.04	*48*	28.53	0.91	166.41	0.92	0.14	2.02	1.01	8.42	36.07	1.42	28.25	164.78	0.14	35.71	1.00
17	V-60-A17	22 - 24	23	1.0375	21	0.22	10.03	*46*	27.51	0.95	167.12	1.08	0.14	2.42	1.60	4.68	41.55	1.22	25.38	154.23	0.13	38.34	1.47
18	V-60-A17; Abd	40-45	42.5	1.0343	21	0.22	10.05	*46*	21.81	0.82	122.24	0.92	0.07	4.30	0.19	28.75	18.16	0.39	20.23	113.37	0.07	16.84	0.18
19	V-60-A17; Abd	50-55	52.5	1.0276	21	0.21	10.04	*48*	22.33	0.68	120.52	0.92	0.07	8.09	0.21	13.37	18.00	0.82	21.81	117.76	0.07	17.58	0.20

QICPMS test and instrument information report provided for metals analysis dated 14 January 2019 (table 21).

Solution ICPMS 140119

Instrument: Bruker Aurora Elite, equipped with a Cetac ASX-250 autosampler and an ESI oneFAST sample introduction system.

Acid used: 1% single distilled nitric acid (HNO_3).

Calibration standard: All elements, with the exception of Cu and Pb which does not use 1000 ppb, were calibrated using the 6020 Calibration Standard (Inorganic Ventures), at 1, 10, 100 and 1000 ppb.

Standard solutions run as unknown: CRM-TMDW-A (High-Purity Standards). See values below.

Isotopes analyzed: ^{63}Cu, ^{66}Zn, ^{111}Cd, ^{202}Hg, $^{206,207,208}Pb$ (analyzed in He collision gas mode). NB! Hg was analyzed semi-quantitatively.

Internal standards: Cu, Zn, Cd, Hg, Pb: ^{159}Tb.

Certified values for TMDW. All values in µg/L.

Cu	Zn	Cd	Hg	Pb
20	75	10	--	20

Standards run as part of metals analysis dated 14 January 2019. Orange highlighted values are below the detection limit for the testing machine. Note that Hg was analyzed semi-qualitatively.

Standards run as unknown	Cu (ppb)	% RSD	Zn (ppb)	% RSD	Cd (ppb)	% RSD	Hg (ppb)	% RSD	Pb (ppb)	% RSD
Blank	0.01	33.52	-0.01	153.50	0.01	14.79	0.01	378.20	0.01	14.13
6020-100ppb	98.13	0.69	100.70	0.69	100.87	0.49	0.01	123.70	96.47	0.81
6020-10ppb	10.68	0.99	11.00	2.23	10.34	1.11	0.05	46.27	9.92	1.36
6020-1ppb	1.18	1.73	1.20	8.41	1.07	2.07	0.04	41.12	1.03	1.85
6020-0.5ppb	0.61	2.16	0.65	9.87	0.54	2.69	0.04	99.45	0.51	1.81
6020-0.1ppb	0.12	12.16	0.11	15.89	0.11	2.74	0.02	25.44	0.10	1.97
TMDW	20.98	1.19	79.41	2.20	10.23	1.22	0.05	97.27	19.39	1.31
Detection limit of method	0.02		0.04		0.01		0.05		0.01	

Table 22 *Metals analysis raw and processed data for retested sediment core V-60-A17 (labelled here and discussed in text as cores VA and VB). Core sections were reversed for blind testing (VA core represents standard downcore approach followed in all other sampling and VB core was same core sections only in reverse order). Samples were processed on 28 January 2019. Data for Hg (highlighted in yellow) is only analysized semi-quantitatively. Orange highlighted values represent those below the detection limit for the instrument. Processed data appears in italics. Sample number 39 was inserted as a blank.*

Sample No.	Core	Core interval (cm)	Core depth (cm)	Dry sample weight used for metal analyses (g)	Acid volume added to dry sample (mL)	Amount of sample added (dissolved in acid) (g)	Amount of sample and acid added for dilution (g)	*Dilution factor*	Cu (ppb)	% RSD	Zn (ppb)	% RSD	Cd (ppb)	% RSD	Hg (ppb)	% RSD	Pb (ppb)	% RSD	*Cu (mg/kg)*	*Zn (mg/kg)*	*Cd (mg/kg)*	*Pb (mg/kg)*	*Hg (mg/kg)*
1	VA	0-1	0.5	1.0026	21	0.23	10.12	44	125.46	0.78	225.87	1.14	0.35	7.23	4.82	5.53	71.89	0.43	115.63	208.16	0.32	66.26	4.44
2	VA	1-2	1.5	1.0060	21	0.22	10.09	46	125.14	0.79	226.70	0.70	0.42	4.03	4.85	5.69	70.27	0.85	119.81	217.04	0.40	67.27	4.64
3	VA	2-3	2.5	1.0254	21	0.23	10.10	44	135.82	0.62	253.19	0.24	0.55	2.14	5.31	7.18	74.64	0.62	122.15	227.70	0.49	67.12	4.77
4	VA	3-4	3.5	1.0348	21	0.22	10.09	46	136.53	0.79	261.98	1.12	0.56	1.85	5.59	3.13	76.40	1.00	127.08	243.84	0.52	71.11	5.20
5	VA	4-5	4.5	1.0294	21	0.22	10.09	46	142.00	0.80	285.20	1.35	0.64	2.69	6.15	6.61	82.21	0.95	132.86	266.85	0.60	76.92	5.75
6	VA	5-6	5.5	1.0208	21	0.23	10.08	44	133.35	1.14	275.27	1.06	0.66	2.27	5.62	6.75	80.18	0.53	120.23	248.19	0.59	72.29	5.07
7	VA	6-7	6.5	1.0382	21	0.22	10.07	46	130.66	0.44	278.29	0.79	0.68	3.37	5.28	7.12	81.25	0.68	120.97	257.66	0.63	75.23	4.89
8	VA	7-8	7.5	1.0074	21	0.22	10.05	46	120.87	0.44	270.89	0.69	0.69	2.07	4.93	7.55	78.63	0.37	115.11	257.97	0.66	74.88	4.70
9	VA	8-9	8.5	1.0283	21	0.22	10.05	46	114.51	0.92	257.23	1.06	0.62	2.73	4.67	5.38	74.89	0.96	106.83	239.98	0.58	69.86	4.36
10	VA	9-10	9.5	1.0100	21	0.22	10.07	46	116.85	0.52	271.54	0.50	0.65	1.19	4.95	3.35	77.05	0.62	111.22	258.44	0.62	73.33	4.71
11	VA	10 - 12	11	1.0003	21	0.22	10.06	46	71.98	0.69	213.86	0.36	0.47	3.42	3.21	11.68	60.29	0.44	69.10	205.29	0.45	57.87	3.08
12	VA	12 - 14	13	1.0304	21	0.23	10.05	44	53.61	0.74	186.80	0.67	0.32	5.72	2.09	9.55	51.15	0.54	47.74	166.35	0.28	45.55	1.86
13	VA	14 - 16	15	1.0130	21	0.22	10.04	46	32.39	1.01	139.79	1.05	0.18	6.30	1.50	8.87	35.85	0.33	30.64	132.24	0.17	33.91	1.42
14	VA	16 - 18	17	1.0379	21	0.22	10.04	46	31.71	0.66	139.39	1.26	0.17	9.17	1.22	10.62	35.27	1.63	29.28	128.71	0.16	32.57	1.13
15	VA	18 - 20	19	1.0329	21	0.22	10.02	46	26.16	0.71	124.76	0.82	0.14	6.04	0.69	25.54	28.53	0.63	24.23	115.53	0.13	26.42	0.64
16	VA	20 - 22	21	1.0140	21	0.22	10.03	46	22.50	0.77	127.20	0.98	0.12	10.74	0.84	8.62	30.88	0.36	21.24	120.10	0.11	29.16	0.79
17	VA	22 - 24	23	1.0375	21	0.22	10.05	46	26.06	0.84	155.26	0.91	0.13	6.85	1.63	14.71	42.35	0.88	24.09	143.57	0.12	39.16	1.50
18	VA	40-45	42.5	1.0343	21	0.22	10.04	46	19.46	1.11	105.88	0.87	0.06	13.68	0.17	77.53	17.41	0.97	18.03	98.10	0.06	16.13	0.16
19	VA	50-55	52.5	1.0276	21	0.22	10.04	46	20.60	0.75	108.53	1.05	0.07	13.66	0.15	31.78	17.83	0.85	19.21	101.22	0.06	16.63	0.14
20	VB	0-1	0.5	1.0276	21	0.22	10.03	46	19.23	0.95	100.78	0.53	0.06	7.46	0.19	31.99	16.94	0.70	17.92	93.90	0.06	15.79	0.18
21	VB	1-2	1.5	1.0343	21	0.22	10.04	46	19.80	0.45	108.88	0.40	0.05	5.93	0.20	24.75	18.09	0.76	18.35	100.88	0.05	16.76	0.19
22	VB	2-3	2.5	1.0375	21	0.23	10.05	44	25.36	0.53	149.77	0.53	0.12	4.55	1.35	13.49	41.48	0.86	22.43	132.47	0.11	36.69	1.20
23	VB	3-4	3.5	1.0140	21	0.23	10.03	44	23.08	0.75	130.84	0.46	0.11	5.88	0.91	9.90	31.12	0.93	20.85	118.18	0.10	28.11	0.82

Sample No.	Core	Core interval (cm)	Core depth (cm)	Dry sample weight used for metal analyses (g)	Acid volume added to dry sample (mL)	Amount of sample added (dissolved in acid) (g)	Amount of sample and acid added for dilution (g)	*Dilution factor*	Cu (ppb)	% RSD	Zn (ppb)	% RSD	Cd (ppb)	% RSD	Hg (ppb)	% RSD	Pb (ppb)	% RSD	*Cu (mg/kg)*	*Zn (mg/kg)*	*Cd (mg/kg)*	*Pb (mg/kg)*	*Hg (mg/kg)*
24	VB	4-5	4.5	1.0329	21	0.22	10.04	46	24.99	1.37	119.40	2.09	0.12	7.64	0.75	7.03	26.98	0.91	23.19	110.79	0.12	25.04	0.70
25	VB	5-6	5.5	1.0379	21	0.23	10.04	44	33.28	0.38	147.38	0.72	0.18	7.28	1.19	12.25	37.50	0.48	29.39	130.17	0.16	33.12	1.05
26	VB	6-7	6.5	1.0130	21	0.22	10.03	46	32.60	0.91	140.10	0.68	0.19	2.21	1.15	13.67	35.35	1.36	30.81	132.41	0.18	33.41	1.08
27	VB	7-8	7.5	1.0304	21	0.23	10.05	44	51.07	0.52	176.55	0.36	0.31	1.51	2.03	8.67	48.39	0.33	45.48	157.23	0.27	43.09	1.81
28	VB	8-9	8.5	1.0003	21	0.22	10.05	46	72.23	0.75	214.12	0.49	0.46	5.25	3.06	7.68	60.59	0.52	69.27	205.34	0.44	58.11	2.94
29	VB	9-10	9.5	1.0100	21	0.22	10.06	46	109.17	0.46	252.57	0.93	0.62	1.90	4.99	7.32	73.70	0.67	103.80	240.14	0.59	70.08	4.74
30	VB	10 - 12	11	1.0283	21	0.22	10.04	46	111.47	0.48	248.58	0.68	0.60	4.12	4.80	4.07	72.76	0.54	103.89	231.67	0.56	67.81	4.48
31	VB	12 - 14	13	1.0074	21	0.22	10.05	46	120.63	0.19	269.40	0.60	0.67	3.09	4.70	3.95	77.54	0.37	114.88	256.55	0.64	73.84	4.48
32	VB	14 - 16	15	1.0382	21	0.22	10.05	46	129.25	1.02	274.92	0.57	0.69	1.59	5.42	4.24	80.95	0.65	119.43	254.03	0.64	74.80	5.01
33	VB	16 - 18	17	1.0208	21	0.22	10.06	46	137.18	0.55	282.57	1.25	0.66	1.51	5.43	4.44	83.70	0.43	129.06	265.83	0.62	78.74	5.11
34	VB	18 - 20	19	1.0294	21	0.22	10.09	46	141.90	0.49	283.89	0.64	0.63	1.30	5.78	9.55	81.54	0.53	132.76	265.61	0.59	76.29	5.41
35	VB	20 - 22	21	1.0348	21	0.24	10.10	42	142.01	0.65	270.73	1.15	0.57	2.64	5.54	2.77	78.82	0.43	121.28	231.21	0.49	67.31	4.73
36	VB	22 - 24	23	1.0254	21	0.22	10.10	46	145.95	0.77	272.44	0.78	0.55	1.89	5.24	4.88	81.03	0.76	137.23	256.15	0.52	76.18	4.93
37	VB	40-45	42.5	1.0060	21	0.22	10.10	46	127.00	0.46	231.00	0.66	0.42	3.86	4.89	7.05	70.55	0.93	121.71	221.38	0.40	67.61	4.69
38	VB	50-55	52.5	1.0026	21	0.22	10.10	46	126.13	0.67	226.30	0.70	0.34	3.99	4.63	6.76	69.73	0.68	121.29	217.61	0.33	67.05	4.45
39	VB	60-65	62.5	1.0250	21	0.22	10.06	46	0.02	67.65	-1.05	3.68	0.00	93.90	0.06	105.40	0.01	23.20	0.01	-0.98	0.00	0.01	0.06

QICPMS test and instrument information report provided for metals analysis dated 28 January 2019 (table 22).

Solution ICPMS 140119

Instrument: Bruker Aurora Elite, equipped with a Cetac ASX-250 autosampler and an ESI oneFAST sample introduction system.

Acid used: 1% single distilled nitric acid (HNO_3).

Calibration standard: All elements, with the exception of Cu and Pb which does not use 1000 ppb, were calibrated using the 6020 Calibration Standard (Inorganic Ventures), at 1, 10, 100 and 1000 ppb.

Standard solutions run as unknown: CRM-TMDW-A (High-Purity Standards). See certified values below.

Isotopes analyzed: ^{63}Cu, ^{66}Zn, ^{111}Cd, ^{202}Hg, $^{206,207,208}Pb$ (analyzed in He collision gas mode). NB! Hg was analyzed semi-quantitatively.

Internal standards: Cu, Zn, Cd, Hg, Pb: ^{159}Tb.

Certified values for TMDW. All values in µg/L.

Cu	Zn	Cd	Hg	Pb
20	75	10	--	20

Standards run as part of metals analysis dated 28 January 2019. Orange highlighted values are below the detection limit for the testing machine. Note that Hg was analyzed semi-qualitatively.

Standards run as unknown	Cu (ppb)	% RSD	Zn (ppb)	% RSD	Cd (ppb)	% RSD	Hg (ppb)	% RSD	Pb (ppb)	% RSD
6020-100ppb	101.46	0.85	101.77	0.97	100.61	0.69	-0.02	97.87	98.57	0.51
6020-10ppb	10.76	1.36	9.60	3.61	10.30	0.78	0.01	192.90	9.82	1.43
6020 0.5ppb	0.5297	3.15	-0.632	5.23	0.5126	2.3	0.0204	128.5	0.5003	2.29
6020 0.1ppb	0.0728	6.89	-1.101	1.77	0.1065	4.31	0.0193	233.6	0.0983	8.27
TMDW	20.61	2.39	75.11	1.21	10.08	0.79	-0.02	120.30	19.61	0.90
blank	0.00	443.90	0.08	154.90	0.01	22.59	-0.01	294.40	0.01	23.43
Detection limit of method	0.02		0.06		0.00		0.08		0.02	

Appendix G: Micropaleontological raw and processed data

Table 23 *Micropaleontological raw and processed data for core V-60-A18 collected on 03 May 2018 in 60m water depth. Note that blank spaces indicate no data present for that interval and processed data has been italicized. Data for diversity indices (ES100, H'log2, NQI and nEQR) includes shading corresponding to EcoQS shown in table 1.*

Core interval (cm): Core depth (cm)	**0-1: 0.5**	**1-2: 1.5**	**2-3: 2.5**	**3-4: 3.5**	**4-5: 4.5**	**9-10: 9.5**	**14-15: 14.5**	**19-20: 19.5**	**24-26: 25**	**30-32: 31**
Agglutinated species										
Adercotryma glomerata/wrighti	21	13	16	10	10	10	14	10	2	1
Ammoscalaria tenuimargo									2	1
Cribrostomoides jeffreysii	3	1		1		1	6	4	8	5
Eggerella sp.	2	1	3	2	1	1			1	
Leptohalysis scottii	2	1	1							
Liebusella goësi	1		1	1						1
Recurvoides trochamminiforme			3		3	1				1
Reophax fusiformis			1							
Reophax spp.				3						2
Spiroplectammina biformis	15	3		3						
Textularia earlandi	3	6	13	5	8	5	1			
Textularia skagerakensis						1		2	2	3
Trochammina sp.	3	1	2		2	1		1		1
Trochamminopsis quadriloba							1		1	
Calcareous species										
Astrononion gallowayi		1		2	1		3		2	
Bolivinellina pseudopunctata	8	4	3	3	2		3	1	1	
Brizalina skagerrakensis			1							
Brizalina spathulata							1			
Buliminella elegantissima	3	1		1						
Bulimina marginata	81	88	83	106	112	114	92	79	40	37
Cassidulina obtusa										3
Cassidulina laevigata						14	23	27	42	56
Cibicides lobatulus						1		1		
Discorbinella bertheloti		1				1	4	4	1	
Elphidium albiumbilicatum	6	4	5	13	8	5	9	9	8	2
Elphidium excavatum		7	4	4	2	7	7	1		
Epistominella vitrea	6	2	4	3	2	3	3	2	5	7
Fissurina sp.								1		1
Gavelinopsis praegeri		1								

Core interval (cm): Core depth (cm)	0-1: 0.5	1-2: 1.5	2-3: 2.5	3-4: 3.5	4-5: 4.5	9-10: 9.5	14-15: 14.5	19-20: 19.5	24-26: 25	30-32: 31
Globobulimina turgida	1				2					
Hyalinea balthica							1	4	7	20
Lagena sp.		1	1							
Lenticulina sp.						1				
Nonionella iridea		1						13	46	39
Nonionella turgida										
Nonionellina labradorica	2	5	6	9	13	9	3	5	4	4
Nonionella stella	3		1							
Pyrgoella sphaera										1
Quinqueloculina seminula										1
Stainforthia fusiformis	54	69	55	49	47	49	34	24	35	24
Trifarina angulosa										5
Uvigerina peregrina										1

Sum counted tests	*214*	*211*	*203*	*215*	*213*	*224*	*205*	*188*	*207*	*216*
Sum only assigned species	***203***	***207***	***195***	***212***	***210***	***219***	***199***	***180***	***194***	***201***
No. tests/g dry sediment	*375.9*	*462.5*	*425.4*	*694.3*	*551.3*	*658.7*	*284.8*	*181.5*	*138.5*	*146.1*
% agglutinated tests	*23*	*12*	*20*	*12*	*11*	*9*	*11*	*9*	*8*	*7*
% calcareous tests	*77*	*88*	*80*	*88*	*89*	*91*	*89*	*91*	*92*	*93*
No. counted species	*17*	*20*	*18*	*16*	*14*	*17*	*16*	*17*	*17*	*22*
% sediment >63µm	*16.7*	*23.4*	*23.7*	*27.9*	*26.3*	*13.0*	*7.8*	*6.8*	*7.8*	*6.3*
% sediment<63µm	*83.3*	*76.6*	*76.3*	*72.1*	*73.7*	*87.0*	*92.2*	*93.2*	*92.2*	*93.7*

Dry weight (g) processed	3.06	3.077	3.032	3.015	3.005	3.069	3.085	3.075	3.087	3.037
Dry weight of the total of original material used for (g) sample	*0.5693*	*0.4562*	*0.4772*	*0.3096*	*0.3864*	*0.3401*	*0.7198*	*1.0358*	*1.4948*	*1.4780*
Dry weight (g) 63-500µm (picked)	0.080	0.086	0.096	0.076	0.090	0.041	0.049	0.064	0.092	0.073
Dry weight (g) 63-500µm (unpicked)	0.350	0.494	0.514	0.664	0.610	0.329	0.161	0.126	0.098	0.077
Dry weight (g) 63-500µm (total)	*0.430*	*0.580*	*0.610*	*0.740*	*0.700*	*0.370*	*0.210*	*0.190*	*0.190*	*0.150*
Dry weight (g) >500µm	0.08	0.14	0.11	0.1	0.09	0.03	0.03	0.02	0.05	0.04

Dominance (%)	*37.9*	*41.7*	*40.9*	*49.3*	*52.6*	*50.9*	*44.9*	*42.0*	*22.2*	*25.9*
Fisher alpha	*4.338*	*5.426*	*4.769*	*3.996*	*3.362*	*4.273*	*4.402*	*4.535*	*4.387*	*6.127*
H' log2 $_f$	*2.789*	*2.472*	*2.648*	*2.442*	*2.253*	*2.375*	*2.711*	*2.842*	*3.016*	*3.195*
ES100 $_f$	*14.29*	*14.1*	*14.14*	*13.09*	*11.38*	*12.28*	*13.69*	*14.06*	*13.75*	*16.11*
NQI $_f$	*0.463*	*0.442*	*0.454*	*0.442*	*0.415*	*0.447*	*0.503*	*0.516*	*0.506*	*0.582*
AMBI $_f$	*3.4*	*3.6*	*3.5*	*3.4*	*3.5*	*3.2*	*2.7*	*2.6*	*2.7*	*2.1*
nEQR (ES$_{100_f}$)	*0.65*	*0.64*	*0.65*	*0.60*	*0.44*	*0.53*	*0.63*	*0.64*	*0.63*	*0.72*
nEQR (H' $_{log2\_f}$)	*0.68*	*0.61*	*0.65*	*0.61*	*0.55*	*0.59*	*0.66*	*0.69*	*0.72*	*0.76*

Core interval (cm): Core depth (cm)	0-1: 0.5	1-2: 1.5	2-3: 2.5	3-4: 3.5	4-5: 4.5	9-10: 9.5	14-15: 14.5	19-20: 19.5	24-26: 25	30-32: 31
nEQR (NQI$_f$)	*0.63*	*0.59*	*0.61*	*0.59*	*0.55*	*0.60*	*0.72*	*0.75*	*0.73*	*0.82*
Mean nEQR$_f$	*0.653*	*0.616*	*0.634*	*0.600*	*0.513*	*0.572*	*0.669*	*0.692*	*0.693*	*0.767*

Taxonomic list of benthic foraminifera

Species are listed in alphabetical order. The list is based on the World Register of Marine Species (WoRMS Editorial Board, 2019)

Adercotryma glomerata (Brady) = *Lituola glomerata* Brady 1878.

Adercotryma wrighti Brönnimann & Whittaker 1987.

Ammoscalaria tenuimargo (Brady) = *Haplophragmium tenuimargo* Brady 1882.

Astrononion gallowayi Loeblich & Tappan 1953.

Bolivinellina pseudopunctata Höglund 1947.

Brizalina skagerrakensis Qvale & Nigam 1985.

Brizalina spathulata (Williamson) = *Textularia variabilis* var. *spathulata* Williamson 1858.

Bulimina marginata d'Orbigny 1826.

Buliminella elegantissima (d'Orbigny) = *Bulimina elegantissima* d'Orbigny 1839.

Cassidulina laevigata d'Orbigny 1826.

Cassidulina obtusa Williamson 1858.

Cibicides lobatulus (Walker & Jacob) = *Nautilus lobatulus* Walker & Jacob 1798.

Cribrostomoides jeffreysii (Williamson) = *Nonionina jeffreysii* Williamson 1858.

Discorbinella bertheloti (d'Orbigny) = *Rosalina bertheloti* d'Orbigny 1839.

Elphidium albiumbilicatum (Weiss) = *Nonion pauciloculum* (Cushman) subsp. *albiumbilicatum* Weiss 1954.

Elphidium excavatum (Terquem) = *Polystomella excavata* Terquem 1875

Epistominella vitrea Parker 1953.

Gavelinopsis praegeri (Heron-Allen & Earland) = *Discorbina praegeri* Heron-Allen & Earland 1913.

Globobulimina turgida (Bailey) = *Bulimina turgida* Bailey 1851.

Hyalinea balhica (Schröter) = *Nautilus balthicus* Schröter 1783.

Leptohalysis scottii Chaster 1892.

Liebusella goësi Höglund, 1947

Nonionella iridea Heron-Allen & Earland 1932.

Nonionella stella Cushman & Moyer 1930.

Nonionella turgida (Williamson) = *Rotalina turgida* Williamson 1858

Nonionellina labradorica (Dawson) = *Nonionina scapha* var. *labradorica* Dawson 1860.

Recurvoides trochamminiformis Höglund 1947.

Reophax fusiformis (Williamson) = *Proteonina fusiformis* Williamson 1858.

Pyrgoella sphaera (d'Orbigny) = *Biloculina sphaera* d'Orbigny 1839.

Quinqueloculina seminula (Linnaeus) = *Serpula seminulum* Linnaeus 1758.

Spiroplectammina biformis (Parker & Jones) = *Textularia agglutinans* var. *biformis* Parker & Jones 1865.

Stainforthia fusiformis (Williamson) = *Bulimina pupoides* d'Orbigny var. *fusiformis* Williamson 1858.

Textularia earlandi Parker 1952.

Textularia skagerakensis Höglund 1947.

Trifarina angulosa (Williamson) = *Uvigerina angulosa* Williamson 1858.

Trochamminopsis quadriloba Höglund 1948.

Uvigerina peregrina Cushman 1923.